

ROBUSTNESS ANALYSIS

**P. VANICEK
E. J. KRAKIWSKY
M. R. CRAYMER
YANG GAO
P. S. ONG**

September 1991



**TECHNICAL REPORT
NO. 156**

PREFACE

In order to make our extensive series of technical reports more readily available, we have scanned the old master copies and produced electronic versions in Portable Document Format. The quality of the images varies depending on the quality of the originals. The images have not been converted to searchable text.

ROBUSTNESS ANALYSIS

Petr Vaníček¹
Edward J. Krakiwsky²
Michael R. Craymer¹
Yang Gao²
Peng S. Ong¹

¹Department of Geodesy and Geomatics Engineering
University of New Brunswick
P.O. Box 4400
Fredericton, N.B.
Canada
E3B 5A3

²Department of Geomatics Engineering
The University of Calgary
2500 University Drive N.W.
Calgary, Alberta
T2N 1N4

November 1990
Corrected March 1991
Latest Reprinting April 1996

PREFACE

This technical report is a reproduction of a final contract report submitted to Geodetic Survey Division, Canada Centre for Surveying, Energy, Mines and Resources Canada, November 1990.

As with any copyrighted material, permission to reprint or quote extensively from this report must be received from the authors. The citation to this work should appear as follows:

Vaniček, P., E.J. Krakiwsky, M.R. Craymer, Y. Gao, and P.S. Ong (1990).
“Robustness analysis.” Final contract report, Department of Surveying
Engineering Technical Report No. 156, University of New Brunswick,
Fredericton, New Brunswick, Canada, 116 pp.

EXECUTIVE SUMMARY

Described in this report are the results of the investigations undertaken by two collaborating research groups at the University of New Brunswick and The University of Calgary under a DSS research contract #23244-9-4198/01-SS for the Geodetic Survey Division of the Canada Centre for Surveying. The investigations addressed the problem of geodetic network analysis techniques, and proposed alternatives to the standard statistical analysis techniques designed to analyse network sensitivity to gross errors and blunders.

The original aim of the investigations was to study the differences between and merits of two such alternative techniques: the reliability technique, introduced by Baarda and implemented by The University of Calgary group, and the geometrical strength analysis formulated by the University of New Brunswick group. It was discovered at the beginning of the investigation that these two techniques are very much complementary: that is, the weakness of each is in the area of the strength of the other. It was decided thus to combine the two techniques into one, which we call “robustness analysis.”

Experiments with both simulated and real networks have shown that robustness analysis works very well in depicting the strong and the weak points in the network, which have to be judged in three independent senses. The strength/weakness of a network must be studied in the sense of scale, shear, or local twist, each of which provides a different picture of strength. These three indicators (primitives) cannot be combined into a single scalar indicator.

It has been concluded that robustness analysis should be carried out side-by-side with the standard statistical analysis from which it differs fundamentally. It is recommended that the Canadian federal specifications for horizontal geodetic networks be amended to include pertinent prescriptions as far as desired robustness is concerned, i.e., specific robustness to be achieved through meeting robustness tolerance limits.

TABLE OF CONTENTS

	Page
Executive Summary	ii
Table of Contents	iii
List of Figures.....	v
List of Tables.....	v
1. Introduction.....	1
2. Covariance Analysis	3
2.1 Introduction	3
2.2 Statistical testing of observations.....	4
2.3 A posteriori testing of observation and/or model.....	5
2.4 Outlier detection in observations.....	6
2.5 Assessment of the estimated positions.....	9
3. Reliability Analysis	11
3.1 Baarda's reliability theory	11
3.2 Effect of blunders	12
3.3 Formulation of an alternative hypothesis	15
3.4 Redundancy measure	16
3.5 External reliability	21
4. Geometrical Strength Analysis	23
4.1 Concept of strain	23
4.2 Deformation primitives	25
4.3 Virtual deformation of geodetic networks	28
4.4 Strength analysis using strain.....	31
4.5 Datum independence of strength.....	32
5. Robustness Analysis.....	37
5.1 Merging reliability and geometrical strength analysis	37
5.2 Properties of robustness analysis.....	38
5.3 Comparison of robustness and geometrical strength analyses	40
5.4 Comparison of robustness and covariance analyses	43
6. NETAN Enhancements.....	50
6.1 Introduction	50
6.2 Update to user's guide.....	53
7. Numerical Examples.....	55
7.1 Introduction	55
7.2 Simulated network HOACS.....	55
7.3 Real 3D network.....	76

TABLE OF CONTENTS

	Page
8. Proposed Specifications for Analysis of Networks.....	109
8.1 Overall scheme.....	109
8.2 Preanalysis.....	109
8.3 Postanalysis.....	111
8.4 Other considerations	111
9. Conclusions, Recommendations, and Acknowledgements.....	112
References	115

LIST OF FIGURES

		Page
2.1	Detectability of blunders and their effect on a horizontal network.	8
3.1	The central and non-central normal distribution.	14
3.2	Probability distribution function of test statistic y under H_0 and H_1 .	17
3.3	$\sqrt{\lambda_0}$ shows the shift of the standard normal distribution of w when H_1 is true.	19
4.1	Examples of homogeneous and nonhomogeneous deformations.	23
4.2	Pure and simple shear.	27
5.1	Geometrical strength in scale (ppm).	41
5.2	Robustness in scale (ppm).	42
5.3	Geometrical strength in shear (ppm).	44
5.4	Robustness in shear (ppm).	45
5.5	Geometrical strength in twist (ppm).	46
5.6	Robustness in twist (ppm)	47
5.7	Relative confidence ellipses for the HOACS 3D network.	49
6.1	“Strength Analysis Options” menu.	53
7.1	Distance observations for simulated 3D HOACS network.	59
7.2	Direction observations for simulated 3D HOACS network.	60
7.3	Azimuth observations for simulated 3D HOACS network.	61
7.4	3D position observations for simulated 3D HOACS network.	62
7.5	3D position difference observations for simulated 3D HOACS network.	63
7.6	Robustness in rotation for simulated 3D HOACS network.	64
7.7	Robustness in shear for simulated 3D HOACS network.	65
7.8	Robustness in scale for simulated 3D HOACS network.	66
7.9	Distance observations for real 2D network.	80
7.10	Direction observations for real 2D network.	81
7.11	Azimuth observation for real 2D network.	82
7.12	Robustness in rotation for real 2D network.	83
7.13	Robustness in shear for real 2D network.	84
7.14	Robustness in scale for real 2D network.	85

LIST OF TABLES

3.1	Testing of a null hypothesis H_0 against an alternative hypothesis H_1	12
7.1	Summary of robustness results for the HOACS network.	57
7.2	GHOST input data file for simulated 3D HOACS network.	67
7.3	NETAN listing of reliability analysis results for simulated 3D HOACS network.	72
7.4	Summary of robustness results for the real network.	78
7.5	GHOST input data file for real 2D network.	86
7.6	NETAN listing of reliability analysis results for real 2D network.	98
8.1	Total analysis of a network.	110

1. INTRODUCTION

In Canada, as in most other countries, geodetic networks are designed and classified on the basis of the standard statistical approach. This approach, called in this report simply “covariance analysis,” assumes that only random, normally distributed errors are present in the observations. This analysis is oblivious to what may happen to the network if a sizeable error, called here an outlier or a blunder, fails to get intercepted by statistical testing performed during the covariance analysis.

About ten years ago, two groups — one at the University of New Brunswick (UNB) and the other at The University of Calgary (U of C) — independently started a quest for an alternative approach to network design and classification. The U of C group had taken Baarda’s [1968] statistically based reliability technique and implemented it for the case of horizontal geodetic networks [Mackenzie, 1985]. It was implemented in a program package called CANDSN [Mepham and Krakiwsky, 1984]. The UNB group took a completely geometrical approach to develop their “geometrical strength analysis” [Dare, 1983] based on using strain as the deformation descriptor. This technique was incorporated in the NETAN program developed for the Geodetic Survey Division of the Canada Centre for Surveying [Craymer et al., 1989].

The idea of looking at the response of geodetic networks to the presence of blunders in observations has been on many people’s minds for some time. It was responsible for the Geodetic Survey Division letting out a research contract on 24 August 1989, administered by DSS under SSC file #055SS.23244-9-4198 and #23244-9-4198/01-SS, to UNB with the U of C as a subcontractor. The aims of this contract can be summarized as follows:

- (i) to show that the network response to blunders in observations is different than its response to random errors;

- (ii) to show the differences between and relative merits of Baarda's reliability analysis and the geometrical strength analysis;
- (iii) to demonstrate how the two new techniques work with both a simulated and a real network;
- (iv) to present suggestions for updating the Canadian specifications for geodetic horizontal networks to include the reliability/strength aspects.

It became rather obvious at the earliest stages of the investigations that while the reliability analysis is based on rigorous statistical concepts, its treatment of the geometry of virtual (potential) network deformation, which is needed in studying the network response, is rather weak. Conversely, the geometrical strength analysis treats the virtual deformation quite rigorously, while its statistical foundations are weak. Thus, rather than dealing with the two techniques side-by-side, it was decided to combine the advantages of both into one technique called here the "network robustness analysis."

This report, being the final report on the above cited research contract, addresses the required issues in the following way: the three techniques that had to be studied and compared are described in Chapters 2, 3, and 4, respectively. Since the covariance analysis is a rather standard tool, it is presented in a more compact way than the other two techniques. Robustness analysis is discussed in Chapter 5, together with its comparison with geometrical strength and covariance analyses. Chapter 6 is devoted to describing how robustness analysis is implemented on the computer within the framework of the existing NETAN program. The required numerical examples are gathered together in Chapter 7, proposed specifications are in Chapter 8, and our conclusions and recommendations are brought forward in Chapter 9. Suggestions for new federal specifications are submitted as an external appendix to this report.

2. COVARIANCE ANALYSIS

2.1 Introduction

Throughout the discussion in this chapter, we will consider only distance, angle, and azimuth observations. This will simplify our discussion, but some generalizations for the benefit of the reader are thus necessary. We first consider the mathematical model shown below:

$$\mathbf{Ax} = \boldsymbol{\ell} + \mathbf{v}, \mathbf{C}\boldsymbol{\ell} \quad , \quad (2.1)$$

where \mathbf{A} = the design matrix,
 \mathbf{x} = vector of unknown parameters,
 $\boldsymbol{\ell}$ = vector of observations,
 \mathbf{v} = vector of residuals, and
 $\mathbf{C}\boldsymbol{\ell}$ = covariance matrix of the observation.

Equation (2.1) is merely the differential form of a non-linear mathematical model. The equation is formed by linearizing around the Taylor point $\mathbf{x}^{(0)}$ with $\mathbf{x} = \boldsymbol{\delta}$ (correction to initial approximate parameter vector) and $\boldsymbol{\ell} = \mathbf{w}$ (misclosure vector). \mathbf{x} can be solved using the well-known least-squares estimation technique utilizing the normal equations shown below:

$$\mathbf{N} \hat{\mathbf{x}} = \mathbf{A}^t \mathbf{P} \boldsymbol{\ell} \quad , \quad (2.2)$$

where $\mathbf{N} = \mathbf{A}^t \mathbf{P} \mathbf{A} + \mathbf{C}_{\mathbf{x}^0}^{-1}$ ($\mathbf{C}_{\mathbf{x}^0}$ is the a priori covariance matrix for the unknown parameters; it is optional and is not considered further in our discussion), and
 $\mathbf{P} \boldsymbol{\ell} = \sigma_0^2 \mathbf{C}_{\boldsymbol{\ell}}^{-1}$ (σ_0^2 is the a priori variance factor).

Before we can use the results from our estimation, we need to assess our observations and mathematical model. This allows us to determine if we can rely on the results that we have obtained. The assessment is made using statistical testing. The most important tests that usually are carried out are briefly discussed below.

2.2 Statistical Testing of Observations

Testing of observations is done before they are used to estimate unknown parameters. The reason for testing observations is quality control. We want to know whether the observations that have been collected contain any gross errors. Screening the observations for gross errors before they are used is supposed to ensure that the estimated unknown parameters will not be biased.

The quantities used for testing the observations are either the observations themselves or their residuals. In the latter case, we assume that the observations ℓ are composed of two parts,

$$\ell = \hat{\ell} - \hat{v} , \quad (2.3)$$

where $\hat{\ell}$ = the estimated value of the observations,

\hat{v} = the estimated value of the residual of the observations.

Since we are testing only one observation at a time here, univariate testing is used in this context.

There are three types of tests that can be carried out on the observations: namely, :

- (a) χ^2 goodness of fit test,
- (b) test on the variance, and
- (c) test on the mean.

The first test determines whether the histogram of the residuals is compatible with a postulated probability density function (PDF). The PDF that is used here is the normal distribution. This test is important as all the other statistical tests assume that the residuals are normally distributed. (There are, however, statistical tests that do not rely on the normality assumption, known as the non-parametric test [Rao, 1973]. These are seldom used in network analysis and will not be discussed here.)

The second test determines whether the hypothesized population variance σ^2 is compatible with the assessed variance s^2 and can be used only when several values have been collected for one observable. σ^2 can sometimes be viewed as the design variance. If this test fails, then

there is a reason to believe that the observations were not collected according to the design. The third test is designed to examine the mean of the data collected for one observable. The comparison between the population mean (μ) and the sample mean (\bar{I}) tells us of the presence of possible biases in the observed sample. The last two tests cannot be performed on residuals.

For the three tests described above, there are six situations under which the tests can be carried out. These situations reflect whether the population mean μ and the population variance σ^2 are known or unknown. If μ and/or σ^2 are unknown, they are estimated from the sample mean \bar{I} and the sample variance s^2 . It is important to know whether we are treating the population parameters as known or unknown as this will determine the PDF that we should use to carry out the tests. Vaníček and Krakiwsky [1986] explain the tests described above in greater details.

2.3 A Posteriori Testing of Observation and/or Model

The tests use the estimated residuals \hat{v} or the misclosure vector w' (when w' is a function of the observation and not due to the linearization process). The residuals \hat{v} are indicative of the behaviour of both the observation and the mathematical model. It is generally impossible to separate the two, therefore, the observations and the model are tested simultaneously.

There are two tests that can be conducted on \hat{v} and w' depending on whether the variance factor σ_0^2 used for scaling the covariance matrix of observations is known or unknown. When carrying out the test to detect outliers, the covariances between the residuals have to be taken into consideration. In such a situation, the Baarda test statistic should be used or Bonferroni's inequality employed. Both approaches take covariances into account in quite different ways.

The assumption behind the standard testing is that the observations ℓ are normally distributed with expected value of $A\hat{x}$, i.e.,

$$H_0 : \ell \in n(\xi; A\hat{x}, C\ell) \quad (2.4)$$

(Any symmetrical probability distribution function with mean $\hat{\mathbf{A}}\hat{\mathbf{x}}$ will suffice to satisfy conditions for unbiasedness and maximum likelihood of $\hat{\mathbf{x}}$ but not for testing.)

This hypothesis is tested by the “test on the variance factor.” The a posteriori variance factor $\hat{\sigma}_0^2$ is computed from

$$\hat{\sigma}_0^2 = \frac{\hat{\mathbf{v}} \mathbf{P} \hat{\boldsymbol{\ell}} \hat{\mathbf{v}}}{v}, \quad (2.5)$$

where v is the number of degrees of freedom. If the a priori variance factor σ_0^2 is known, then the null hypothesis for testing is

$$H_0: \frac{v\hat{\sigma}_0^2}{\sigma_0^2} \in \chi^2(\xi; v). \quad (2.6)$$

One of the necessary conditions for this null hypothesis to be satisfied is that the expected value of v equals to $\mathbf{0}$, i.e., that the observations $\boldsymbol{\ell}$ are burdened only with random errors (with zero-mean). Thus observations are usually again screened against gross errors/biases using tests for outliers.

2.4 Outlier Detection in Observations

Outliers are observations that are considered statistically incompatible with the rest of the series [Vaníček and Krakiwsky, 1986]. This incompatibility is thought to be caused by a blunder made in the measurement or by some sort of disturbance affecting the performance of the measuring system. Outliers can be detected by examining the residuals of the observations after the estimation process.

Because the residuals are mathematically correlated to each other, we would have to work with a multivariate distribution function. This would make the testing procedure quite complex. It is easier and more efficient to work with a univariate distribution. To do this we have to standardize the residuals. Since it is assumed that all the residuals are coming from the same population with different normal density, the standardization process is straightforward. The standardization process is accomplished by the transformation :

$$\tilde{r}_i = \frac{\hat{r}_i}{\sigma_{\hat{r}_i}} \quad (2.7)$$

where $\hat{r}_i = \ell_i - \hat{\ell}_i$ and $\sigma_{\hat{r}_i} = \sigma_{(\ell_i - \hat{\ell}_i)}$.

The univariate tests that are available for outlier detection are shown in Table 13.5 in Vaníček and Krakiwsky [1986]. The table shows the tests when each ℓ_i has been taken out of context, i.e., the question as to whether the other members of the series may also be outliers is deliberately ignored. The tests are thus called the out-of-context tests. An in-context test examines the ℓ_i in light of their existence as one of the members of the series. In this case, the significance level for the test is different from that used in the out-of-context tests. The significance level for the in-context and the out-of-context tests is related by the equation:

$$\alpha \doteq \frac{a}{N} , \quad (2.8)$$

where α = out-of-context significance level,
 a = in-context significance level, and
 N = the number of observations.

A more detailed description of the out-of-context and the in-context testing can be found in Vaníček and Krakiwsky [1986].

The outlier detection process plays a very important role in our robustness analysis technique as will be shown later. As a matter of fact, there may exist observations in a network that cannot be tested for outliers and the level of detectability varies with network geometry. What happens if ℓ_i burdened with blunders $\Delta\ell_i$, e.g., gross error of bias, are used in the computation? The effect of the blunder and whether it is detectable will depend on the geometry of the network. Figure 2.1 illustrates this point.

Figure 2.1 (a) shows a closed network of points. All the points in the network are determined employing redundant observations. If observation ℓ_3 is burdened with a blunder, it either can be detected from the residual of that observation or has only a small effect on point A as other observations are also used to compute coordinates of the point. In Figure 2.1 (b), the

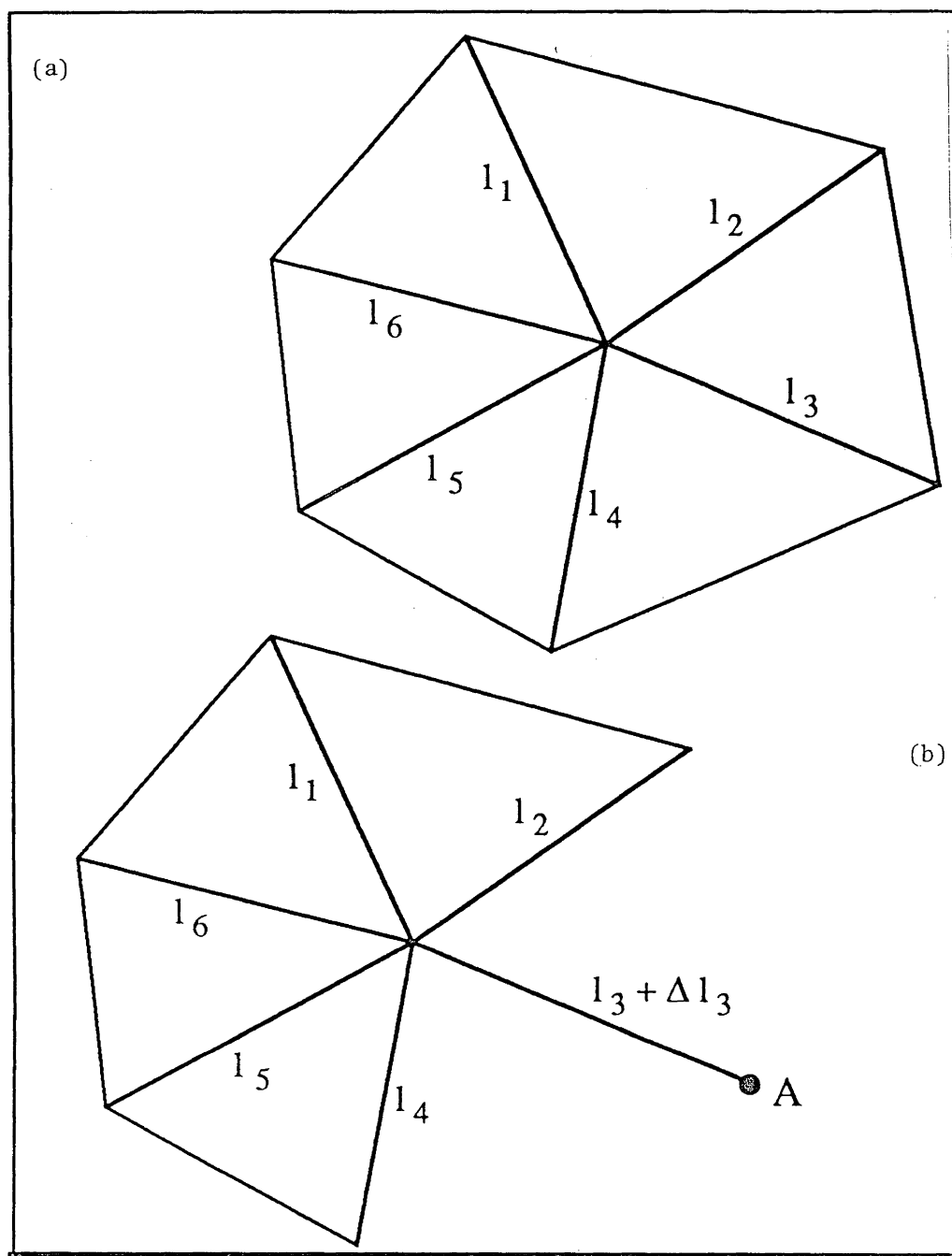


Figure 2.1. Detectability of blunders and their effect on a horizontal network.

(a) A blunder either can be detected or has a small effect on the network.

(b) Blunder Δl_3 cannot be detected and has a large effect on the network (only on point A).

blunder in the observation cannot be detected as there are no redundant measurements made to point A. The effect of the blunder will be large as only the observation burdened with the blunder was used to compute the position of A.

The effect of a blunder on the network depends on the following two circumstances:

- (a) if $\Delta\ell_i$ can be detected by statistical testing, and
- (b) how the network reacts to the presence of $\Delta\ell_i$.

Both are functions of network geometry, the observation accuracy, and the magnitude of $\Delta\ell_i$. When can a blunder be detected? The answer lies in Baarda's reliability theory explained in Chapter 3.

2.5 Assessment of the Estimated Positions

Once the observations have been screened and the mathematical model examined, the estimated parameters (positions) should be assessed. The assessment consists of the determination of confidence regions (sometimes known as error ellipses for 2D positions or error ellipsoids for 3D positions) for the positions. These represent the amount of trust that one can place on the estimated positions.

The confidence region determined for the estimated position depends on the test statistic y shown below. There are two different cases where y can be determined, i.e., when σ_0^2 is either known or unknown. If σ_0^2 is known then the test statistic used is:

$$y = (x - \hat{x})^t C_{\hat{x}}^{-1} (x - \hat{x}) \quad , \quad (2.9)$$

where x = the unknown parameters (coordinates),
 \hat{x} = estimate of the unknown parameters, and
 $C_{\hat{x}}$ = covariance matrix of the estimated parameters.

The test statistic y shown above has a χ^2 distribution with u degrees of freedom, where u is also the number of unknown parameters in the estimation process. If σ_0^2 is unknown, then the test y is given by:

$$y = \frac{(\mathbf{x} - \hat{\mathbf{x}})^t \mathbf{C}_{\hat{\mathbf{x}}}^{-1} (\mathbf{x} - \hat{\mathbf{x}})}{u} \quad (2.10)$$

The test statistic shown in equation (2.10) has an $F_{(u,v,\infty)}$ distribution ($v =$ number of observations minus the number of unknown parameters).

For a given significance level α , the critical value of y can be looked up from the χ^2 of the F tables depending on whether σ_0^2 is known or unknown. If we substitute this value for y in equations (2.9) or (2.10), we will get a u -dimensional hyperellipsoid. This hyperellipsoid can be understood as a u -dimensional confidence region centred at $\hat{\mathbf{x}}$. Any tested value \mathbf{x} that falls within the hyperellipsoid must then be considered compatible with $\hat{\mathbf{x}}$ on the level of probability $(1-\alpha)$. Two-dimensional subvectors of \mathbf{x} similarly fall into 2D confidence regions centred on corresponding 2D subvectors of $\hat{\mathbf{x}}$, i.e., the points of the network. The axes and orientation of the confidence regions can be computed by solving the eigenvalue problem for each confidence ellipse. The equations for computing the axes and orientation of the confidence ellipse can be found in Steeves and Fraser [1983].

There are two types of confidence regions: point confidence and relative confidence region. The point confidence region reflects how accurately the station has been positioned with respect to the ‘datum’ of the network: point confidence regions thus depend on the datum defining the network. The relative confidence region represents the relative accuracy between the two stations. It is not datum dependent and is most often used to define the accuracy of a network.

The confidence regions are usually computed for a probability level of 39%. Such confidence regions are called the standard confidence regions. This probability level can be increased by multiplying it with an expansion factor. The expansion factor is given by:

$$C_{\alpha}(u) = \sqrt{\xi_{(y, 1-\alpha)}}. \quad (2.11)$$

where $\xi_{(y, 1-\alpha)}$ is the absence of the appropriate PDF corresponding to the $1-\alpha$ probability. This expansion factor is multiplied with the axes of the standard confidence region to obtain the $1-\alpha$ in-context confidence interval.

3. RELIABILITY ANALYSIS

3.1 Baarda's Reliability Theory

Before we go into detail on the theory, the concept of hypothesis testing should be explained first. The role of hypothesis testing is to allow us to make a statistical decision concerning postulated population parameters, e.g., mean μ or variance σ^2 , etc., to have some particular value. This is called the null hypothesis (H_0). For every null hypothesis, there exists an infinite number of alternative hypotheses (H_1), each of which states that the population parameters have some other particular values.

When we perform hypothesis testing, there are only two possible outcomes, i.e., to accept H_0 or to reject H_0 . Similarly, there are two possible outcomes for the test of the alternative hypothesis H_1 . None of the hypotheses may be true, in which case the test at least should tell us which hypothesis is better. To make a definite decision concerning H_0 , we need to have an infinite sample to work with. Since this is never available, a decision made on a finite sample should be trusted only to a certain degree. Such a decision has attached to it only a limited confidence.

The probability α of rejecting H_0 when in fact H_0 is true (Type I error) is called the significance level. The complementary probability $(1-\alpha)$ is called the confidence level, and it is the measure of confidence we have in the decision (Type I error). Likewise, a situation might arise that H_0 is false and we accept it. This is called the Type II error. The probability of making this decision is β . $(1-\beta)$ is called the power of the test, and it expresses the confidence we have in the decision made. The situation described above can be summarized in Table 3.1.

When Baarda first developed his reliability theory, he treated the blunders as unknown parameters to be estimated, i.e., the blunders are treated as deterministic quantities. Most of the research work and literature dealing with outliers or blunders treat them as deterministic quantities that have to be estimated.

Table 3.1. Testing of a null hypothesis H_0 against an alternative hypothesis H_1 (after Vaniček and Krakiwsky [1986]).

Situation	Decision	Test tells us to accept H_0	Test tells us to reject H_0
H_0 true		Correct decision Probability = $1-\alpha$ (confidence level)	Type I error Probability = α (significance level)
H_0 false (H_1 true)		Type II error Probability = β	Correct decision Probability = $1-\beta$ (power of test)

The blunders can be estimated from the residuals obtained after a least-squares adjustment. The relationship between the observational errors and the residuals is shown below [Stefanovic, 1978; Kavouras, 1982]:

$$\hat{\mathbf{v}} = \mathbf{Q}_{\hat{\mathbf{v}}} \mathbf{C}_{\ell}^{-1} \boldsymbol{\varepsilon} \quad (3.1)$$

where $\hat{\mathbf{v}}$ = the estimated residuals,
 $\boldsymbol{\varepsilon}$ = the true observational errors,
 $\mathbf{Q}_{\hat{\mathbf{v}}}$ = the cofactor matrix of the estimated residuals, and
 \mathbf{C}_{ℓ} = the covariance matrix of the observations.

The cofactor matrix and the covariance matrix of the residuals is related by σ_0^2 [Mikhail, 1976]. Therefore, if σ_0^2 is assumed known, then equation (3.1) can be rewritten as:

$$\hat{\mathbf{v}} = \mathbf{C}_{\hat{\mathbf{v}}} \mathbf{C}_{\ell}^{-1} \boldsymbol{\varepsilon} \quad (3.2)$$

where $\mathbf{C}_{\hat{\mathbf{v}}}$ is the covariance matrix of the residuals.

3.2 Effect of Blunders

Now, if we assume $\boldsymbol{\varepsilon}$ to be made up of two parts consisting of a random part $\boldsymbol{\varepsilon}_r$ and a gross error part (blunder) $\nabla \boldsymbol{\ell}$, we have:

$$\boldsymbol{\varepsilon} = \boldsymbol{\varepsilon}_r + \nabla \boldsymbol{\ell} \quad (3.3)$$

Substituting equation (3.3) into equation (3.2), we have:

$$\begin{aligned}
\hat{\mathbf{v}} &= \mathbf{C}_{\hat{\mathbf{v}}} \mathbf{C}_{\ell}^{-1} (\boldsymbol{\varepsilon}_v + \nabla \ell) \\
&= \mathbf{C}_{\hat{\mathbf{v}}} \mathbf{C}_{\ell}^{-1} \boldsymbol{\varepsilon}_r + \mathbf{C}_{\hat{\mathbf{v}}} \mathbf{C}_{\ell}^{-1} \nabla \ell \\
\hat{\mathbf{v}} &= \mathbf{v}_r + \nabla \mathbf{v} \quad , \tag{3.4}
\end{aligned}$$

where \mathbf{v}_r = influence of the random error on the residual,

$\nabla \mathbf{v}$ = influence of the blunder on the residual.

If an observation ℓ_i is not burdened with a blunder, then $\nabla \ell_i$ will be zero. On the other hand, if observation ℓ_i is burdened with a blunder, then $\nabla \ell_i$ will be non-zero. Therefore, through testing of the residuals $\hat{\mathbf{v}}$, an observation containing a blunder could be detected.

In carrying out the statistical test on our observations, we always assume that the observations are normally distributed with mean μ and variance σ^2 . If an observation is burdened with a blunder, then it will have a distribution with mean, say, $\mu + \sqrt{\lambda}$, and variance of σ^2 . This method of modelling the blunder is called the mean shift model [Chen et al., 1987] where the (unknown) mean shift is given by $\sqrt{\lambda}$. The PDF of the observation containing a blunder is shifted by $\sqrt{\lambda}$ from its own PDF not burdened by a blunder. This situation is depicted in Figure 3.1.

One of the statistical tests carried out after a least-squares adjustment is to test the estimated reference variance $\hat{\sigma}_0^2$ against a hypothesized reference variance σ_0^2 , as described in the previous chapter.

There are many reasons why the test can fail and H_0 be rejected. Some of these reasons can be found in Uotila [1976], or Vaníček and Krakiwsky [1986]. For our purpose, however, we shall assume that the reason why the test fails is that blunders exist in our observations. This is a valid assumption because blunders have an influence on $\hat{\mathbf{v}}$. Since $\hat{\sigma}_0^2$ is estimated using $\hat{\mathbf{v}}$, the presence of blunders will cause the distribution of test statistic y to be shifted by λ . The shift λ is also known as the non-centrality parameter [Mackenzie, 1985]. The amount of shift can be computed from the blunders themselves, through their influence $\nabla \mathbf{v}$. The derivation of λ using $\nabla \mathbf{v}$ is discussed below.

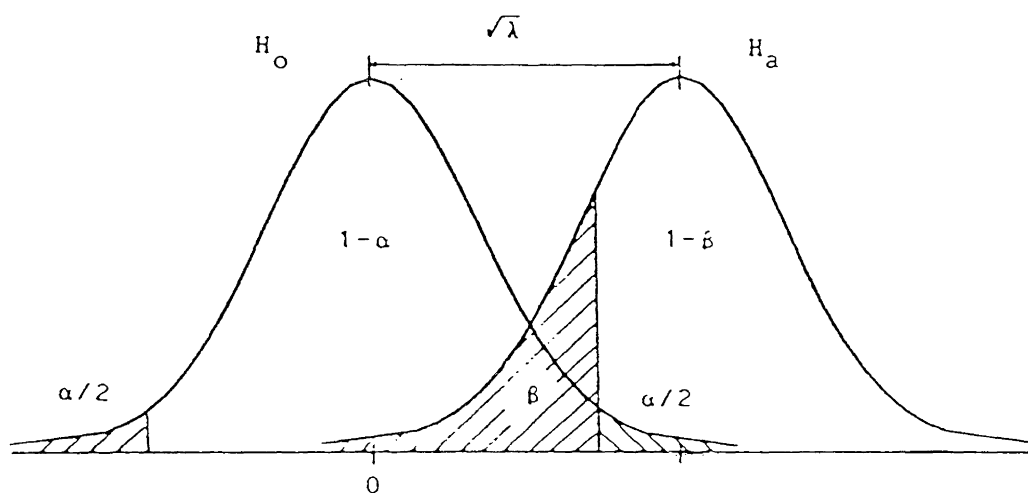


Figure 3.1 The central and non-central normal distribution (after Mackenzie [1985]).

3.3 Formulation of an Alternative Hypothesis

Under the null hypothesis, the expectation of $y' = y/v$ is 1, as seen from equation (2.6). In an alternative hypothesis, the expected value of y' is not equal to 1. We can write the expected value of y' under H_1 in two parts as shown below:

$$E[y'|H_1] = E[y'|H_0] + \nabla[y'] \quad (3.5)$$

where $\nabla y'$ is the amount by which the χ^2 distribution has shifted due to the presence of blunders. Therefore,

$$E[y'|H_1] = 1 + \nabla[y'] \quad (3.6)$$

But $y' = \hat{\sigma}_0^2 / \sigma_0^2$ and substituting y into equation (3.6) we get:

$$\begin{aligned} \nabla[y'] &= \nabla(\hat{\sigma}_0^2 / \sigma_0^2) \\ &= \nabla \hat{\sigma}_0^2 / \sigma_0^2 \end{aligned}$$

where $\nabla \hat{\sigma}_0^2$ is the amount of shift of $\hat{\sigma}_0^2$ due to the presence of blunders

$$\nabla[y'] = \frac{1}{\sigma_0^2} (\nabla \mathbf{v}^t \mathbf{C}_\ell^{-1} \nabla \mathbf{v}) / v \quad (3.7)$$

Equation (3.6) can be rewritten as:

$$\begin{aligned} E[y'|H_1] &= 1 + \frac{1}{\sigma_0^2} (\nabla \mathbf{v}^t \mathbf{C}_\ell^{-1} \nabla \mathbf{v}) / v \\ &= 1 + \lambda / v \end{aligned}$$

where

$$\lambda = \frac{1}{\sigma_0^2} \nabla \mathbf{v}^t \mathbf{C}_\ell^{-1} \nabla \mathbf{v} \quad (3.8)$$

Since $\nabla \mathbf{v} = \mathbf{C}_\ell \hat{\nabla} \mathbf{C}_\ell^{-1} \nabla \boldsymbol{\ell}$ (equation (3.4)), we can write equation (3.8) as

$$\lambda = \frac{1}{\sigma_0^2} (\mathbf{C}_\ell \hat{\nabla} \mathbf{C}_\ell^{-1} \nabla \boldsymbol{\ell})^t \mathbf{C}_\ell^{-1} \mathbf{C}_\ell \hat{\nabla} \mathbf{C}_\ell^{-1} \nabla \boldsymbol{\ell} \quad (3.9a)$$

$$= \frac{1}{\sigma_0^2} \nabla \boldsymbol{\ell}^t \mathbf{C}_\ell^{-1} \mathbf{C}_\ell \hat{\nabla} \mathbf{C}_\ell^{-1} \mathbf{C}_\ell \hat{\nabla} \mathbf{C}_\ell^{-1} \nabla \boldsymbol{\ell} \quad (3.9b)$$

Using the idempotence property of $\mathbf{C}_\ell \hat{\nabla} \mathbf{C}_\ell^{-1}$ [Mikhail, 1976], we can write,

$$\lambda = \frac{1}{\sigma_0^2} \nabla \ell^t C_\ell^{-1} C_\ell^\wedge C_\ell^{-1} \nabla \ell . \quad (3.9c)$$

If $\sigma_0^2 = 1$, then equation (3.9c) is reduced to:

$$\lambda = \nabla \ell^t C_\ell^{-1} C_\ell^\wedge C_\ell^{-1} \nabla \ell . \quad (3.9d)$$

Figure 3.2 shows the shift of the probability distribution function of H_0 due to blunders $\nabla \ell$ in the observations.

When formulating the reliability technique, we are not interested in the magnitude of $\nabla \ell$ itself. What is important is to know the magnitude of the blunder that cannot be detected. To be able to determine this we need to know λ . Since $\nabla \ell$ is unknown, however, λ cannot be computed using equation (3.9d). Instead, we can select a critical value λ_0 (based upon selected α_0 and β_0 , as shown later) to determine the magnitude of $\nabla \ell$ that cannot be detected. Equation (3.9d) can then be rewritten as

$$\lambda_0 = \nabla_0 \ell^t C_\ell^{-1} C_\ell^\wedge C_\ell^{-1} \nabla_0 \ell . \quad (3.10)$$

In carrying out the test for detecting blunders in our observations, we have assumed that only one blunder at a time was present: each observation is tested in turn to see if it is burdened with a blunder. The hypothesis set up for each observation is

$$\forall i = 1, n : \begin{cases} H_{0i} : \nabla \ell_i = 0 \\ H_{1i} : \nabla \ell_i \neq 0 \end{cases} .$$

Baarda called the consecutive testing of the alternative hypotheses H_{1i} “a data snooping strategy” [Baarda, 1968; Kok, 1984].

3.4 Redundancy Measure

Since we are testing one observation at a time, the test hypothesis will be one dimensional [Kok, 1984]. Therefore, we only have to deal with a univariate probability distribution. Baarda [1968] has ascertained that in testing the residuals to detect the presence of blunders,

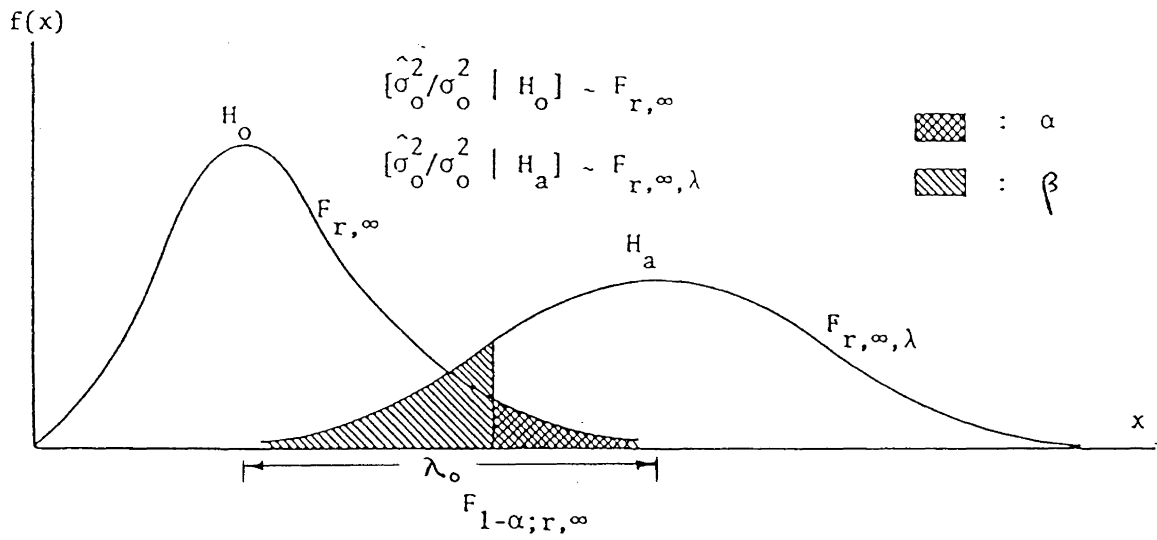


Figure 3.2 Probability distribution function of test statistic y under H_0 and H_1 (after Kavouras [1982]).

the most sensitive test quantity is the weighted residual. If we test one observation at a time, the weighted residual of observation ℓ_i is given by

$$\forall i : v_i^* = (C_\ell^{-1} \hat{v})_i . \quad (3.11)$$

The variance of the weighted residual in equation (3.11) is given by:

$$\forall i : (\sigma_{v_i}^*)^2 = (C_\ell^{-1} C_\ell^* C_\ell^{-1})_{ii} . \quad (3.12)$$

The test statistic that is used to test the hypothesis above is the standardized residual having a standard normal distribution with $\mu = 0$ and $\sigma^2 = 1$. The test statistic is thus

$$\forall i : w_i = \frac{v_i^*}{\sigma_{v_i}^*} . \quad (3.13)$$

If $|w_i| > n_{(1-\alpha)}$ then H_{0i} is rejected. If H_{1i} is true, then observation ℓ_i is burdened with a blunder. Under H_{1i} , w_i will have a non-central standard normal distribution. The amount of shift with respect to the central distribution is given by $\sqrt{\lambda_0}$. This situation is depicted in Figure 3.3. Under the null hypothesis, the expectation of w_i is zero

$$E[w_i|H_0] = 0 , \quad (3.14)$$

and under the alternative hypothesis, the expectation of w_i is $\sqrt{\lambda_0}$

$$E[w_i|H_1] = \sqrt{\lambda_0} . \quad (3.15)$$

The practical application of Baarda's reliability theory is to determine the magnitude of blunders that cannot be detected on a given probability level α_0 when accepting a level of risk β_0 of committing a Type II error (accepting that there is no blunder present when there is one present). If we assume that all our observations are burdened with blunders, then we are interested in the minimum size of blunder in each observation that can still be detected. Therefore, having preselected α_0 and β_0 (the selection of these two quantities will be discussed later), $\sqrt{\lambda_0}$ can be determined. Figure 3.3 shows how $\sqrt{\lambda_0}$ can be computed using the formula shown below:

$$\sqrt{\lambda_0} = \xi_{n(0,1),1-\alpha/2} + \xi_{n(0,1),1-\beta} . \quad (3.16)$$

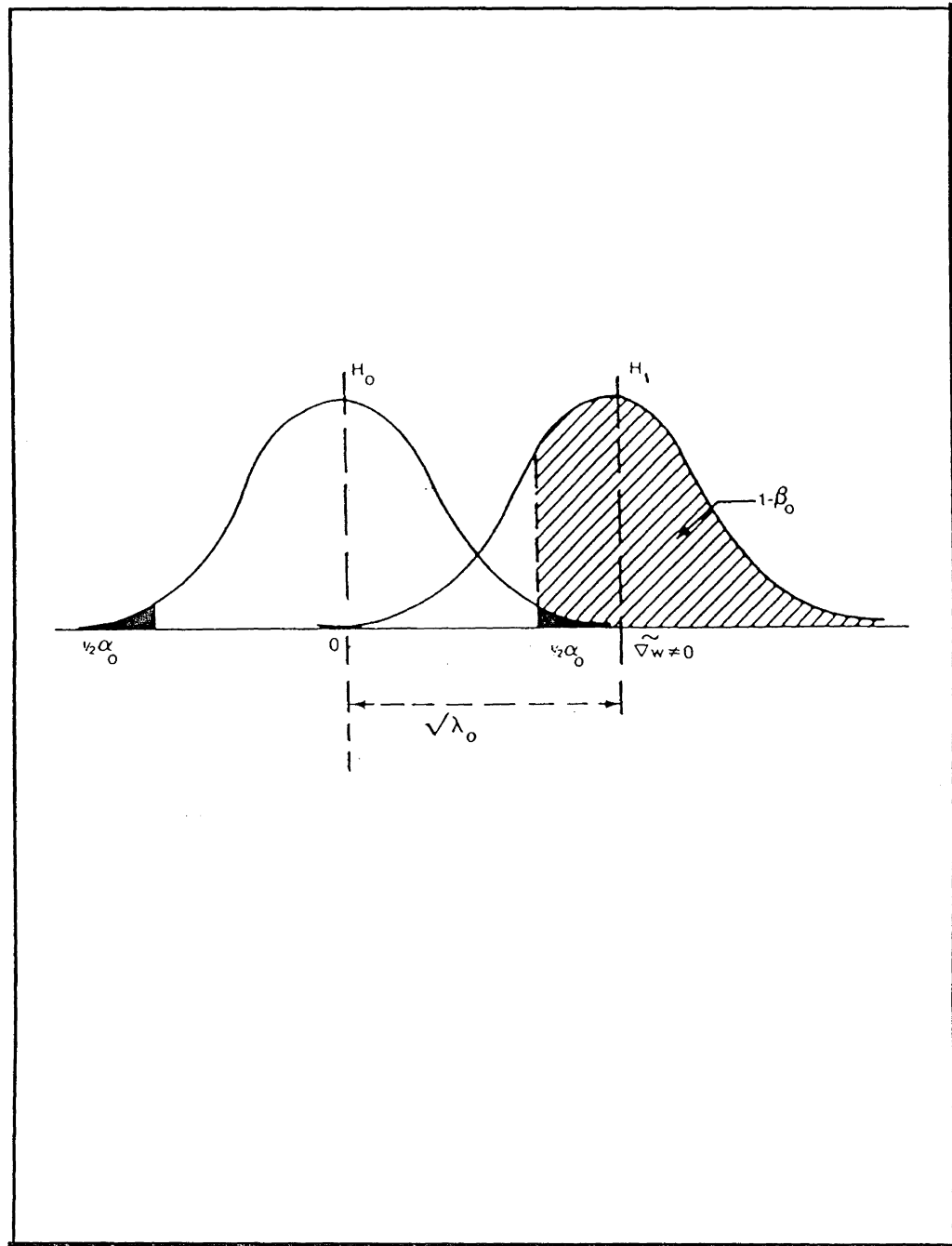


Figure 3.3 $\sqrt{\lambda_0}$ shows the shift of the standard normal distribution of w when H_1 is true (after Kok [1984]).

The maximum undetectable blunder (or minimum detectable blunder) can be computed using equation (3.10). Since we are testing one observation ℓ_i at a time, equation (3.10) can be rewritten as:

$$\forall i : \lambda_0 = \nabla_0 \ell_i^2 (C_\ell^{-1})_{ii} (C_\Delta) (C_\ell^{-1})_{ii} . \quad (3.17)$$

In equation (3.17), the product $(C_\Delta)(C_\ell^{-1})_{ii}$ is called the redundancy number r_i [Forstner, 1979; Mackenzie, 1985]. The r_i gives an insight into the ‘controllability’ of the observations. An observation is said to be ‘fully controlled’ if all of the observational errors (random and non-random) show up in the estimated residual [Mackenzie, 1985]. This is obvious from equation (3.2) which can be rewritten as

$$\hat{\mathbf{v}} = \mathbf{r} \boldsymbol{\varepsilon} \quad (3.18)$$

where $\mathbf{r} = C_\Delta C_\ell^{-1}$. Rewriting now equation (3.17), we get

$$\forall i : \lambda_0 = \nabla_0 \ell_i^2 (C_\ell^{-1})_{ii} r_i . \quad (3.19)$$

Rearranging equation (3.19), we arrive at

$$\forall i : \nabla_0 \ell_i^2 = \frac{\lambda_0}{r_i (C_\ell^{-1})_{ii}}$$

or

$$\forall i : \nabla_0 \ell_i = \frac{\sqrt{\lambda_0}}{\sqrt{r_i} \sqrt{(C_\ell^{-1})_{ii}}} . \quad (3.20a)$$

Since $(C_\ell)_{ii} = \sigma_{\ell_i}^2$, we have

$$\forall i : \nabla_0 \ell_i = \sigma_{\ell_i} \frac{\sqrt{\lambda_0}}{\sqrt{r_i}} . \quad (3.20b)$$

$\nabla_0 \ell_i$ is called the internal reliability measure [Baarda, 1968]. It represents the maximum blunder in an observation undetectable with selected α_0 and β_0 . We note that if $r_i = 0$, no error can be detected by the outlier test (case requiring only the minimal number of observations linking the point to the rest of the network). The $r_i = 1$ case represents the other extreme when any $\sqrt{\lambda_0}$ multiple of σ_{ℓ_i} could be recognized as an outlier.

3.5 External Reliability

Another reliability measure that Baarda developed in 1968 is called the external reliability. External reliability tells us about the effect of $\nabla_0 \ell_i$ on the positions obtained through the least-squares adjustment. External reliability, however, is not used in our method; the effect of $\nabla_0 \ell_i$ on the result is handled in a different way. To make our discussion more complete and to make a comparison between our method and Baarda's method in assessing the effect of $\nabla_0 \ell_i$, a brief discussion on the external reliability is still given below.

In the least-squares adjustment, the unknown parameters are estimated using equation (1.2). If we pre-multiply equation (1.2) by N^{-1} , we get:

$$\hat{\mathbf{x}} = N^{-1} A^t P_{\ell} \ell , \quad (3.21a)$$

or

$$\hat{\mathbf{x}} = (A^t P_{\ell} A)^{-1} A^t P_{\ell} \ell . \quad (3.21b)$$

Supposing that the observation vector ℓ is burdened by blunders $\nabla \ell$, i.e., $\ell' = \ell + \nabla \ell$ and substituting ℓ' into equation (3.21b), we get

$$\hat{\mathbf{x}}' = (A^t P_{\ell} A)^{-1} A^t P_{\ell} \ell' , \quad (3.22)$$

where $\hat{\mathbf{x}}'$ are the shifted unknown parameters affected by blunders $\nabla \ell$. Substituting for ℓ' into equation (3.22), we get

$$\begin{aligned} \hat{\mathbf{x}}' &= (A^t P_{\ell} A)^{-1} A^t P_{\ell} (\ell + \nabla \ell) \\ &= (A^t P_{\ell} A)^{-1} A^t P_{\ell} \ell + (A^t P_{\ell} A)^{-1} A^t P_{\ell} \nabla \ell . \end{aligned} \quad (3.23)$$

and denoting by $\nabla \hat{\mathbf{x}}$ the shift of $\hat{\mathbf{x}}$ due to $\nabla \ell$ yields

$$\nabla \hat{\mathbf{x}} = (A^t P_{\ell} A)^{-1} A^t P_{\ell} \nabla \ell . \quad (3.24)$$

The effect of the maximum undetectable blunder $\nabla_0 \ell_i$ on the estimated parameters can be determined by substituting $\nabla_0 \ell_i$ for $\nabla \ell$:

$$\forall i : \nabla_0 \hat{\mathbf{x}}_i = (A^t P_{\ell} A)^{-1} A^t P_{\ell} \nabla_0 \ell_i . \quad (3.25)$$

Here, $\nabla_0 \hat{\mathbf{x}}_i$ is dependent on the coordinate definition, i.e., it is datum dependent. Baarda [1976; 1979] proposed another kind of external reliability measure:

$$\lambda_{0i} = (\nabla_0 \hat{x}_i)^t C_{\hat{x}}^{-1} (\nabla_0 \hat{x}_i) . \quad (3.26)$$

known as the relative external reliability measure.

As we shall see in the next chapter, the effect of blunders on the network is better handled as a virtual deformation and thus depicted by a more appropriate technique than the ‘external reliability.’

4. GEOMETRICAL STRENGTH ANALYSIS

In this chapter, the use of strain for the strength analysis of geodetic networks is described. The basic concepts of strain are given followed by its application to geodetic networks, and specifically its use as a tool for analysing the geometrical strength of networks. We also show that changes in the network datum have only a second-order effect on strength.

4.1 Concept of Strain

Strain is a purely geometric approach to the analysis of the deformation of a physical body. It is based on the theory of elasticity in mechanics where it is applied to the description of the relative deformation of a body with respect to some initial state. Here deformation is taken to mean the change in shape or configuration of the body.

Deformation can be classified as either homogeneous or nonhomogeneous. If the deformation is homogeneous, straight or parallel lines will remain as straight or parallel lines after deformation. If, on the other hand, the deformation is nonhomogeneous, initially straight or parallel lines become curved or nonparallel after deformation. These deformations are illustrated in Figure 4.1.

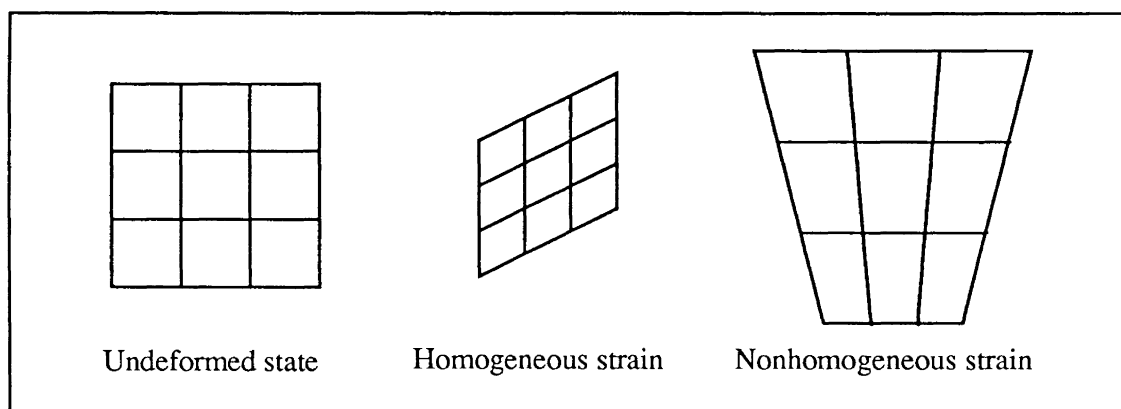


Figure 4.1 Examples of homogeneous and nonhomogeneous deformations.

Strain induced by homogeneous deformation is called homogeneous strain and is constant over all parts of the region of deformation. Nonhomogeneous deformation, on the other hand, produces a more complicated nonhomogeneous strain field.

Deformation and strain can also be classified as finite or infinitesimal. Finite strain usually describes an instantaneous deformation of a continually deforming body with respect to its original undeformed state, i.e., cumulative strain. On the other hand, infinitesimal or incremental strain describes the instantaneous deformation of the current deformed state with respect to some earlier, not necessarily undeformed, instantaneous state.

Only nonhomogeneous and infinitesimal deformation is needed in strength analysis due to the following considerations:

- (a) the deformation of a geodetic network is generally nonhomogeneous, and
- (b) in the strength analysis of a geodetic network, the deformation is much smaller compared to the size of the network and we can thus use infinitesimal strain theory.

The latter allows us to take advantage of the fact that infinitesimal deformation is differentially small in order to simplify the mathematical description of strain.

Mathematically, infinitesimal strain is defined as the rate of change (i.e., gradient or slope) of an object's displacement field with respect to position. Given a three-dimensional (3D) displacement field $\mathbf{u}(x,y,z)=(u,v,w)^T$, as a function of position $\mathbf{x}=(x,y,z)^T$, the strain matrix \mathbf{E} consists of 9 linear displacement gradients given by

$$\mathbf{E} = \text{grad}(\mathbf{u}) = \frac{\partial \mathbf{u}(x,y,z)}{\partial \mathbf{x}} = \begin{bmatrix} \frac{\partial u}{\partial x} & \frac{\partial u}{\partial y} & \frac{\partial u}{\partial z} \\ \frac{\partial v}{\partial x} & \frac{\partial v}{\partial y} & \frac{\partial v}{\partial z} \\ \frac{\partial w}{\partial x} & \frac{\partial w}{\partial y} & \frac{\partial w}{\partial z} \end{bmatrix} = \begin{bmatrix} e_{ux} & e_{uy} & e_{uz} \\ e_{vx} & e_{vy} & e_{vz} \\ e_{wx} & e_{wy} & e_{wz} \end{bmatrix}, \quad (4.1)$$

where the derivatives are evaluated at the point of concern. These linear strains e correspond to the rate of change of displacement in each of the three coordinate components along the three coordinate axes. For example, e_{uy} is the rate of change or gradient of displacement in the x -direction with respect to position in the y -direction.

Note that the mechanical properties of the material are not involved in strain. Strain is applicable, whatever the mechanical behaviour of the material. Note also that strains describe only the relative displacement of points so that rigid body translations do not affect strain. This will be discussed in more detail later in this chapter.

4.2 Deformation Primitives

The strain matrix contains all of the strain information about the displacement field. It is not easily interpreted, however. Various scalar parameters can be derived from the strain matrix in order to make the interpretation of strain more convenient and illustrative. We call these parameters deformation primitives.

The strain matrix \mathbf{E} can be decomposed into its symmetric \mathbf{S} and anti-symmetric \mathbf{A} parts; i.e.,

$$\mathbf{E} = \mathbf{S} + \mathbf{A} \quad , \quad (4.2)$$

where

$$\mathbf{S} = \begin{bmatrix} \epsilon_{ux} & \epsilon_{uy} & \epsilon_{uz} \\ \epsilon_{vx} & \epsilon_{vy} & \epsilon_{vz} \\ \epsilon_{wx} & \epsilon_{wy} & \epsilon_{wz} \end{bmatrix} = \begin{bmatrix} \epsilon_{ux} & \frac{1}{2}(\epsilon_{uy} + \epsilon_{vx}) & \frac{1}{2}(\epsilon_{uz} + \epsilon_{wx}) \\ \frac{1}{2}(\epsilon_{uy} + \epsilon_{vx}) & \epsilon_{vy} & \frac{1}{2}(\epsilon_{vz} + \epsilon_{wy}) \\ \frac{1}{2}(\epsilon_{uz} + \epsilon_{wx}) & \frac{1}{2}(\epsilon_{vz} + \epsilon_{wy}) & \epsilon_{wz} \end{bmatrix}, \quad (4.3)$$

$$\mathbf{A} = \begin{bmatrix} 0 & -\omega_z & \omega_y \\ \omega_z & 0 & -\omega_x \\ -\omega_y & \omega_x & 0 \end{bmatrix} = \begin{bmatrix} 0 & -\frac{1}{2}(\epsilon_{uy} - \epsilon_{vx}) & \frac{1}{2}(\epsilon_{uz} - \epsilon_{wx}) \\ \frac{1}{2}(\epsilon_{uy} - \epsilon_{vx}) & 0 & -\frac{1}{2}(\epsilon_{vz} - \epsilon_{wy}) \\ -\frac{1}{2}(\epsilon_{uz} - \epsilon_{wx}) & \frac{1}{2}(\epsilon_{vz} - \epsilon_{wy}) & 0 \end{bmatrix}. \quad (4.4)$$

The symmetric part is often referred to as the symmetric strain tensor.

The symmetric strain tensor \mathbf{S} describes the expansion and contraction as well as the shearing deformation at a point. The strain tensor is usually parameterized in terms of the so-called strain ellipse or ellipsoid in the same manner that error ellipses and ellipsoids are computed from covariance matrices, except that no square roots of the semi-axis lengths are taken. The principal strains ($\lambda_1, \lambda_2, \lambda_3$) are the eigenvalues of the strain tensor and the

eigenvectors are the directions of the principal axes. Negative principal strains indicate contraction and positive principal strains expansion.

The anti-symmetric strain matrix \mathbf{A} describes the twisting deformation at a point. The quantities ω are called average differential rotations and describe the twisting about each of the three coordinate axes at a point. Note that in the two-dimensional case there is only a twist ω_z about the local z-axis (i.e., in the x-y horizontal plane).

More convenient scalar deformation primitives for strength analysis can also be derived from the strain matrix (see Schneider [1982]). Dilation σ describes the average extension or contraction at a point and is defined as the average of the principal strains; e.g., for 3D

$$\sigma = \frac{\lambda_1 + \lambda_2 + \lambda_3}{3} = \frac{\epsilon_{ux} + \epsilon_{vy} + \epsilon_{wz}}{3} = \frac{e_{ux} + e_{vy} + e_{wz}}{3}. \quad (4.5)$$

Note that the sum of principal strains is equivalent to the trace of the symmetric strain tensor which is equal to the trace of the strain matrix. Total strain λ is a similar quantity, defined as the geometric mean of the principal strains [Dare, 1983]; i.e.,

$$\lambda = \sqrt{\lambda_1^2 + \lambda_2^2 + \lambda_3^2}. \quad (4.6)$$

Shear strain can be classified as either pure shear or simple shear. Pure shear τ deforms a square into a rectangle so that separation between lines changes. It is defined by [Schneider, 1982]

$$\tau_{xy} = -\tau_{yx} = \frac{1}{2} (e_{ux} - e_{vy}) = \frac{1}{2} \left(\frac{\partial u}{\partial x} - \frac{\partial v}{\partial y} \right), \quad (4.7)$$

$$\tau_{xz} = -\tau_{zx} = \frac{1}{2} (e_{ux} - e_{wz}) = \frac{1}{2} \left(\frac{\partial u}{\partial x} - \frac{\partial w}{\partial z} \right), \quad (4.8)$$

$$\tau_{yz} = -\tau_{zy} = \frac{1}{2} (e_{vy} - e_{wy}) = \frac{1}{2} \left(\frac{\partial v}{\partial z} - \frac{\partial w}{\partial y} \right). \quad (4.9)$$

Simple shear ν deforms a rectangle into a rhombus so that angles between lines change. It is defined as [Schneider, 1982]

$$v_{xy} = -v_{yx} = \frac{1}{2} (e_{uy} + e_{vx}) = \frac{1}{2} \left(\frac{\partial u}{\partial y} + \frac{\partial v}{\partial x} \right), \quad (4.10)$$

$$v_{xz} = -v_{zx} = \frac{1}{2} (e_{uz} + e_{wx}) = \frac{1}{2} \left(\frac{\partial u}{\partial z} + \frac{\partial w}{\partial x} \right), \quad (4.11)$$

$$v_{yz} = -v_{zy} = \frac{1}{2} (e_{vy} + e_{wz}) = \frac{1}{2} \left(\frac{\partial v}{\partial y} + \frac{\partial w}{\partial z} \right). \quad (4.12)$$

Neither type of shear produces any rotation. These two types of shear are illustrated in Figure 4.2. Another type of shear, total shear γ , is the geometric mean of the components of pure and simple shear; i.e.,

$$\gamma_{xy} = \sqrt{\tau_{xy}^2 + v_{xy}^2}, \quad (4.13)$$

$$\gamma_{xz} = \sqrt{\tau_{xz}^2 + v_{xz}^2}, \quad (4.14)$$

$$\gamma_{yz} = \sqrt{\tau_{yz}^2 + v_{yz}^2}. \quad (4.15)$$

The principal axes of the strain tensor define the directions in which no shear takes place. The directions of maximum shear are at 45° to the principal axes of the strain ellipse/ellipsoid. The magnitude of shear can also be determined indirectly from the difference of the principal strains (lengths of the principal axes of the strain ellipse/ellipsoid) [Schneider, 1982].

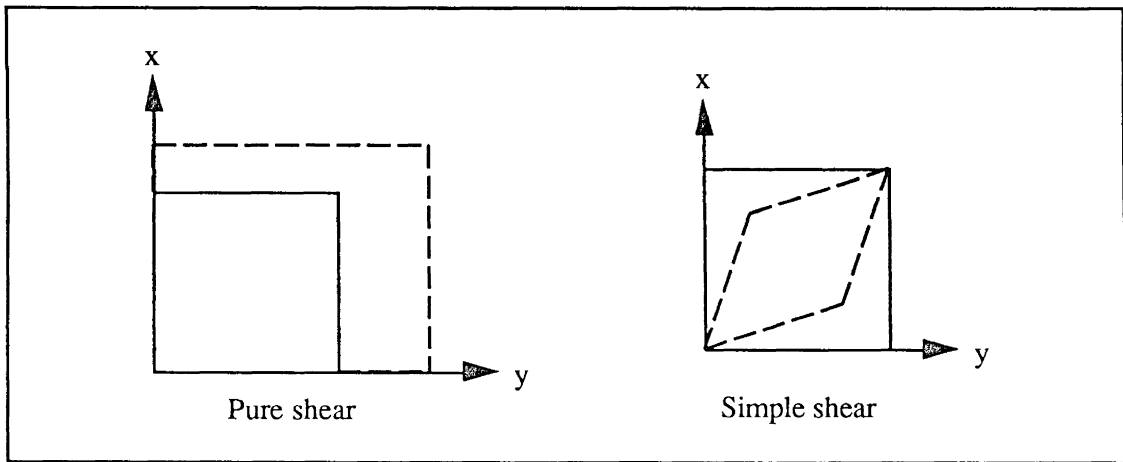


Figure 4.2 Pure and simple shear. Solid lines are the undeformed state and broken lines are the deformed state.

Note that the symmetric strain tensor \mathbf{S} can be represented in terms of dilation, pure shear, and simple shear. Using the above definitions, we find that

$$\mathbf{S} = \begin{bmatrix} \sigma + \tau_{xy} + \tau_{xz} & \upsilon_{xy} & \upsilon_{xz} \\ \upsilon_{yx} & \sigma + \tau_{xy} + \tau_{xz} & \upsilon_{yz} \\ \upsilon_{zx} & \upsilon_{zy} & \sigma + \tau_{xy} + \tau_{xz} \end{bmatrix}. \quad (4.16)$$

Although the expressions for the various deformation primitives have been developed in 3D, previous investigations by Craymer et al. [1987] have found that only 2D primitives have any practical meaning in the context of geodetic networks. The problem is that geodetic networks are inherently only 2D in nature since they lie on the surface of the Earth whose variations in height are much smaller than those in the horizontal dimension. When two points have very nearly the same height (a common occurrence), the displacement field gradients with respect to height can become extremely large or even discontinuous, resulting in artificially large and misleading results.

The deformation can be displayed in a variety of ways (see Thapa [1980], Schneider [1982], Dare [1983], and Craymer [1987]). In network strength applications, the only scalar primitives needed are differential rotation, dilation, and total shear. These scalar deformation primitives are most conveniently displayed using either 3D surfaces or contour plots. Only the latter is currently supported in the NETAN software which implements this analysis.

4.3 Virtual Deformation of Geodetic Networks

The concept of strain can be readily applied to the analysis of geodetic networks by considering the network to be a structure in itself. That is, stations are held together by the interconnecting observations as a building is held together by its beams. In this analogy, stations are considered to be the joints and observations are the beams and brackets. Distance observations can be thought of as beams of rigid length whose orientation in space is not fixed. Angles can be considered as brackets which fix the relative orientation (angles) between beams of arbitrary length. Azimuths can be thought of as brackets that fix the orientation of a beam of

arbitrary length with respect to the foundation (which acts as the datum definition). We have found that using such an analogy helps in the interpretation of the strain parameters.

In practice, the displacement field over a structure is never known as a continuous function of the position of points on the body. The displacements are known only for a discrete set of points describing the structure. Only a discrete displacement field can therefore be obtained which approximates the actual continuous displacement field.

For the strain analysis of geodetic networks, the displacements are of a virtual nature. They represent changes to the coordinates of the points in the network that may result from a variety of changes (perturbations) of the network. Some of these are:

- changes in observation values,
- changes in observation weights,
- deletion or addition of observations,
- deletion or addition of points,
- changes in network constraints.

The virtual displacement field is the set of coordinate changes for all points in the network. Only virtual displacements due to changes of observation values are needed in strength analysis.

Given a local displacement field δ around a point, the strain can be easily determined from the displacement gradient evaluated at the point. For geodetic networks, we can define the “local displacement field” at a point to consist of displacements of either all interconnected points (i.e., all points connected by observations to the point of interest) or all stations within a specified radius of the point of interest. The virtual displacements (i.e., changes in coordinates) of all points within the local displacement field can then be approximated by a simple surface such as a plane or low-degree algebraic surface (surface described by a low-degree algebraic polynomial). In our experience, we have found a plane to be the most robust approximation of the local displacement field at each point. Higher-order algebraic polynomials are not suitable for such applications since they tend to produce spurious gradients

when the points are not regularly distributed in space (i.e., they tend to ‘fall through’ areas without stations).

The gradients of the local displacement field are evaluated separately for each of the coordinate components. A separate local displacement field is determined for each coordinate component and the gradients along each of the coordinate axes are evaluated to give the components of the strain matrix. Fitting a plane surface to each displacement field results in a very simple determination of the strain; the strain components are just the slopes of the planes along each of the coordinate axes.

For the 2D case, the local displacement field components u and v are approximated by

$$u = a_0 + a_1 x + a_2 y , \quad (4.17)$$

$$v = b_0 + b_1 x + b_2 y , \quad (4.18)$$

where x and y are the coordinate components of the points in the local displacement field, and the a 's and b 's are the coefficients defining the planes. For numerical stability, these coordinates are expressed relative to the point of interest. Solving for the coefficients in both sets of equations results in

$$\begin{bmatrix} a_0 \\ a_1 \\ a_2 \end{bmatrix} = N^{-1} A^T u , \quad (4.19)$$

$$\begin{bmatrix} b_0 \\ b_1 \\ b_2 \end{bmatrix} = N^{-1} A^T v , \quad (4.20)$$

where $N=A^T A$ and $A=[\mathbf{1} \ x \ y]$ with $\mathbf{1}$ being a column of ones. The strain elements are then

$$e_{ux} = a_1 , \quad e_{uy} = a_2 , \quad (4.21)$$

$$e_{vx} = b_1 , \quad e_{vy} = b_2 . \quad (4.22)$$

Letting \tilde{N} denote the reduced normal equation matrix with a_0 or b_0 eliminated, the elements of the strain matrix can be expressed together in vector form as

$$\mathbf{e} = \begin{bmatrix} e_{ux} \\ e_{uy} \\ e_{vx} \\ e_{vy} \end{bmatrix} = \begin{bmatrix} \tilde{\mathbf{N}}^{-1} \mathbf{A}^T \mathbf{u} \\ \tilde{\mathbf{N}}^{-1} \mathbf{A}^T \mathbf{v} \end{bmatrix} = \mathbf{Q} \boldsymbol{\delta}, \quad (4.23)$$

where the local displacement field vector is ordered as $\boldsymbol{\delta}^T = (\mathbf{u}^T, \mathbf{v}^T)$.

4.4 Strength Analysis Using Strain

The use of strain to analyse the strength of a geodetic network was first proposed by Vaníček et al. [1981] and later developed by Dare [1983]. Rather than describing the ability of a network to resist the propagation and accumulation of random errors, the strain approach is based on the ability to resist the propagation and accumulation of systematic errors or blunders (i.e., changes of a non-random nature).

The basic approach is to perform a series of separate strain analyses by individually changing the observation values. Each such perturbation produces a new displacement field and thus strain at each point. The most realistic results were obtained when changing each observation by its standard deviation [Dare, 1983]. A measure of strength is obtained by assuming the network is only as strong as its weakest link. The weakest link corresponds to the largest strain parameter at each station from the entire series of strain solutions for all observation perturbations.

With this technique, a virtual displacement field must be generated for every observation in the network. Although this may seem like a daunting task, sequential estimation methods can be used to advantage here (see Craymer et al. [1989]). The displacement field $\boldsymbol{\delta}$ in response to a change of an observation can then be given directly in terms of the perturbed observation vector $\Delta \mathbf{l}$, which contains only one non-zero element equal to the standard deviation of the observation; i.e.,

$$\boldsymbol{\delta} = -\mathbf{N}^{-1} \mathbf{A}^T \mathbf{P} \Delta \mathbf{l} = \mathbf{T} \Delta \mathbf{l}, \quad (4.24)$$

where \mathbf{A} is the design matrix, \mathbf{P} is the weight matrix of the observations and $\mathbf{N} = \mathbf{A}^T \mathbf{P} \mathbf{A}$ is the normal equation matrix. Because only one observation is changed at a time, only one

column of the normal equation matrix is needed to evaluate the displacement field if the observations are independently weighted. Since the strain elements are linear functions of the displacements (see eqn. (4.23)), we can write the following system of linear equations for each change to an observation:

$$\mathbf{e} = \mathbf{Q} \boldsymbol{\delta} = \mathbf{Q} \mathbf{T} \Delta \mathbf{l} = \mathbf{R} \Delta \mathbf{l} . \quad (4.25)$$

We are now interested only in the largest deformations at each point as measured by the deformation primitives: dilation σ , total shear γ , and differential rotation ω (cf. eqns. (4.5), (4.13) to (4.15) and (4.4)). New deformation primitives are computed one at a time for a change in each observation by its standard deviation. Only the largest primitives (in absolute value) at each point are retained as a measure of the weakest link. These maximum values (denoted by σ_{\max} , γ_{\max} , and ω_{\max}) at each point in the network describe the network strength and are referred to as strength in scale, strength in shear, and strength in rotation (twist), respectively. They can be displayed as contour plots or 3D surface plots. Only the former is currently supported in the NETAN program [Craymer et al., 1988; 1989].

4.5 Datum Independence of Strength

The effect of the coordinate system or datum definition on the computed strain parameters is an important issue in the strength analysis of networks. Datum is taken here to mean the definition of the origin and orientation of the coordinate system as well as the scale. The origin is usually defined by specifying fixed or heavily weighted coordinates for one or several points in the network. The orientation is often defined using weighted observations such as azimuths or observed position differences between points. The scale is generally defined using weighted distances or, again, position difference observations. Two or more weighted position observations can also be used to define datum orientation and scale.

Ideally the strength of a network should not depend on the choice of a datum so that different people analysing the same network, but using different datums, will get the same strength parameters. It is shown here that rotations and scale changes have only a very small

and negligible effect on the strength parameters and that translations of the datum origin have no effect at all. The effects of translations, rotations, and scale changes on strength parameters will be evaluated in terms of strain parameters only, strength being just the largest strain parameter at each station resulting from a series of virtual displacement fields.

It is important to bear in mind that only one datum definition is used in a single strength analysis. The virtual displacement fields generated for the strength analysis are due only to changes in the network observations ('blunders') and not to changes in the datum. The question is whether a displacement field generated by such a 'blunder' gives the same strain as another displacement field also generated by the same 'blunder' but using a different datum. In practice, the differences in datums are likely to be very small; say, less than a degree in the orientation of the coordinate axes, and a few hundred parts per million in scale.

Translations of Datum Origin

Differences in the datum origin between different strain (or strength) solutions completely cancel in the determination of the displacement field. That is, the displacement fields for both solutions are identical even though they may be based on datums with different origins.

This can be proven very easily by considering one strain solution where x_1 are the original coordinates of points in the local displacement field and x_2 are the coordinates after the network has been perturbed by a single blunder. The local displacement field δ is then

$$\delta = x_2 - x_1 . \quad (4.26)$$

Consider now a second strain solution using a different datum origin which is offset from that for the first solution by a translation Δx . For this solution, the original coordinates x_1^* and those x_2^* after perturbation by the same blunder can be expressed in terms of the coordinates for the first solution as

$$x_1^* = x_1 + \Delta x , \quad (4.27)$$

$$x_2^* = x_2 + \Delta x . \quad (4.28)$$

The displacement field δ^* for this second solution is then

$$\delta^* = x_2^* - x_1^* = x_2 - x_1 = \delta, \quad (4.29)$$

which is identical to that for the first solution. Any translation of the datum origin therefore cancels in the virtual displacement field. Since the virtual displacement fields are identical in both strain solutions, the strain and strength parameters also will be identical. Strain and strength parameters are therefore invariant to translations of the datum origin.

It is important to point out here that strain is also invariant to displacements resulting from the translation of all points in a network. The 2D displacement fields in this case will have constant values for both the u and v components at all stations (i.e., they will be horizontal planes). The gradients (strain) of these displacement fields will be zero since a horizontal plane will have zero slope. This is the reason that strain is preferred in studies of crustal motion where it is not known whether the point fixed in a previous adjustment has moved.

Rotations of Datum Coordinate Axes

A change in the orientation of the coordinate axes defining the datum in a strain (or strength) analysis results in only a very small and negligible effect on the resulting strain and strength parameters. Given the same displacement field δ for the first strain solution as above (generated by a blunder), the strain matrix E is defined by

$$E = \text{grad}(\delta). \quad (4.30)$$

Consider a second solution where the coordinate system has been rotated by an arbitrary rotation matrix R . The new coordinates before and after perturbation by the same blunder are, respectively,

$$x_1^* = R x_1, \quad (4.31)$$

$$x_2^* = R x_2. \quad (4.32)$$

The displacement field δ^* for this second solution is then

$$\delta^* = x_2^* - x_1^* = R x_2 - R x_1 = R \delta. \quad (4.33)$$

Note that for a small angle of rotation, the term $R \delta$ is only a second-order effect. The corresponding strain matrix E^* is

$$\mathbf{E}^* = \text{grad}(\boldsymbol{\delta}^*) = \mathbf{R} \text{grad}(\boldsymbol{\delta}) = \mathbf{R} \mathbf{E} . \quad (4.34)$$

If the rotation angle $\Delta\alpha$ is small, the rotation matrix for a single rotation about, e.g., the z-axis can be simplified to

$$\mathbf{R} \approx \begin{bmatrix} 1 & \Delta\alpha & 0 \\ -\Delta\alpha & 1 & 0 \\ 0 & 0 & 1 \end{bmatrix} = \mathbf{I} + \begin{bmatrix} 0 & \Delta\alpha & 0 \\ -\Delta\alpha & 0 & 0 \\ 0 & 0 & 0 \end{bmatrix} = \mathbf{I} + \Delta\mathbf{R} . \quad (4.35)$$

The strain matrix in this new datum is then

$$\mathbf{E}^* = \mathbf{R} \mathbf{E} \approx \mathbf{E} + \Delta\mathbf{R} \mathbf{E} = \mathbf{E} + \Delta\mathbf{E} . \quad (4.36)$$

The effect of a change in datum orientation is therefore $\Delta\mathbf{E}=\Delta\mathbf{R} \mathbf{E}$. For strength analyses of geodetic networks, the changes to this will result in only a very small effect which will be negligible in all practical cases.

A worst case effect can be estimated by considering a solution with very large strains of about $e=1 \times 10^{-4}$ (100 ppm). If the datum is changed by a rotation of the coordinate system by a large amount, say $\Delta a=1 \times 10^{-2}$ radians (over half a degree), the change in the strain matrix from the first solution is only $\Delta a \cdot e=1 \times 10^{-6}$ (1 ppm). In a strength analysis, the strain elements are unlikely to exceed 50 ppm in which case a rotation of over 1° will be required to produce a 1 ppm effect on strain. In practice, the orientation of the network datum will generally be known to much better than 1 degree accuracy. These estimates have been verified using numerical tests.

Changes of Datum Scale

The effect on strain (and strength) parameters due to changes in datum scale can be determined in a similar manner. In this case, the strain solutions before and after a change in scale of Δs results in the following coordinates

$$\mathbf{x}_1^* = (1 + \Delta s) \mathbf{x}_1 , \quad (4.37)$$

$$\mathbf{x}_2^* = (1 + \Delta s) \mathbf{x}_2 . \quad (4.38)$$

The displacement field $\boldsymbol{\delta}^*$ for this second solution is then

$$\boldsymbol{\delta}^* = \mathbf{x}_2^* - \mathbf{x}_1^* = (1 + \Delta s) \boldsymbol{\delta} . \quad (4.39)$$

and the corresponding strain matrix \mathbf{E}^* is

$$\mathbf{E}^* = \text{grad}(\boldsymbol{\delta}^*) = (1+\Delta s) \text{grad}(\boldsymbol{\delta}) = (1+\Delta s) \mathbf{E} = \mathbf{E} + \Delta s \mathbf{E} . \quad (4.40)$$

Note that $\Delta s \boldsymbol{\delta}$, and thus $\Delta s \mathbf{E}$, is again only a second-order effect.

A worst case effect can also be estimated by again considering a solution with very large strains of about $\epsilon=1 \times 10^{-4}$ (100 ppm). If the datum is changed in scale by an extremely large amount, say $\Delta s=1 \times 10^{-2}$ (10 000 ppm), the change in the strain matrix from the first solution is only $\Delta s \cdot \epsilon=1 \times 10^{-6}$ (1 ppm). In a strength analysis, the strain elements are unlikely to exceed 50 ppm in which case a scale change of over 20 000 ppm will be required to produce a 1 ppm effect on strain. In practice, the orientation of the network datum will generally be known to much better than 10 ppm accuracy which would result in scale effects of only 0.001 ppm for this example. These estimates have been verified using numerical tests.

5. ROBUSTNESS ANALYSIS

5.1 Merging Reliability and Geometrical Strength Analysis

In the 20 plus years since Baarda [1968] proposed the concept of reliability analysis, the technique has found, albeit quite slowly, many proponents and followers. Based on a rigorous statistical foundation, the technique offers an alternative tool for analysing networks of various kinds, e.g., geodetic, photogrammetric, and those for engineering surveys. The only problem with reliability analysis is that the interpretation of its results, particularly those pertaining to positions as opposed to observations, is rather difficult. We can quantify the maximum expected observation residual that can escape purging as an outlier (blunder) by the standard statistical test for outliers. What we cannot learn from the analysis is just how much damage (distortion) such an undetected error (possible blunder) can cause to the network. On the other hand, there is a global indicator of ‘external reliability’ (equation (3.26)) provided in Baarda’s technique, but this is far too coarse a measure to be of much real use. What is really needed is a much finer measure, commensurate in its fineness with the distinguishing power of the internal reliability, that would pinpoint areas, or even better, points, where one can expect the damage to be significant and other points where the damage should be expected to be insignificant. The individual indicators of ‘external reliability’ (equation (3.25)) associated with individual points provide a fine enough measure but they are datum dependent and there are far too many of them to be practical.

Some 10 years ago, work on one such measure started at UNB and culminated in 1983 with Dare’s [1983] formulation of ‘geometrical strength analysis’ (GSA). This technique approaches the problem of network deformability or lack of it, i.e., strength, from a purely geometrical point of view. The question GSA answers is: How could a geodetic network deform in the worst case if the observations were burdened with some undetected non-random errors? The answer includes a somewhat unexpected complication — there does not exist one

single scalar measure of such a deformation, but three independent measures. In Chapter 4, these three measures are called the ‘deformation primitives.’ They are the pure strain (scale), the total shear (shape), and the differential rotation (twist). Every one of these primitives shows one independent aspect of network deformation.

In Dare’s formulation of GSA and the later application program NETAN [Craymer et al., 1988], little attention was paid to possible values of observation errors that could cause the virtual deformation analysed by GSA. Values equal to the standard deviations of individual observations were used to generate the studied deformation. GSA thus starts where Baarda’s reliability analysis ends. This became obvious to us at the outset of this contract, and we decided to put these two techniques together to obtain a full image of the strength of a geodetic network. All that is required to ‘marry’ the two techniques is to take the maximum errors (blunder) undetectable by the standard statistical tests for outliers as estimated by the reliability analysis and use them as values that can cause the virtual deformation of the network in GSA. The result is that equation (4.25), which generates the vector of displacement gradients (strains), changes to

$$\mathbf{e} = \sqrt{\lambda_0} \mathbf{R} \boldsymbol{\sigma}^* , \quad (5.1)$$

where

$$\sigma_i^* = \frac{\sigma_i}{\sqrt{r_i}} . \quad (5.2)$$

In other words, this equation is created by substituting $\nabla \ell_i$ from equation (3.20b) for σ_i in equation (4.25). The subsequent treatment of \mathbf{e} remains the same as in GSA.

5.2 Properties of Robustness Analysis

The resulting analysis, which combines the statistical aspects of Baarda’s theory with the geometrical aspects of GSA, gives an answer to the proper question that one must ask if analysing the strength of a network; namely, What would be the worst possible deformation of a network whose observations had been tested for outliers (and detected outliers purged) on a

specific confidence level $1-\alpha_0$? The analysis — we call it ‘network robustness analysis,’ to reflect contemporary statistical terminology where robustness means insensitivity to blunders — gives a picture of the network’s potential worst deformation in terms of the three independent deformation primitives. Clearly, a high value of one of the primitives associated with a point, or a region, shows a weakness (in resistance to deformation) of the network at that point, or region, in the sense of that particular primitive (aspect). Low values, on the other hand, are indicative of good resistance to deformation, i.e., indicative of strength.

For the purpose of designing a network that would meet specific strength criteria, it would be necessary to formulate meaningful tolerance limits for admissible weaknesses in the three independent primitives: scale, shear, and twist. In other words, for specifications dealing with a design of desirably strong networks, it will be necessary to come up with a specific value of λ_0 , which scales the three indicators of strength. (As we see from equation (5.1), $\sqrt{\lambda_0}$ is a common scale factor to all the results obtained from the robustness analysis.) In Chapter 3, it was shown that λ_0 is a function of α_0 , the significance level selected for testing adjusted observations for outliers, and β_0 , the probability of Type II error in the testing. While α_0 is selected beforehand, prior to the outlier testing, β_0 is free but should be specified for the purpose of choosing tolerance limits in the robustness specifications.

Two types of singularities can appear in a network subjected to robustness analysis: a geometrical singularity, and a singularity due to no redundancy. The first singularity is caused by specific geometrical configurations when the point to be analysed is either connected only to one other point, or when it is colinear with all the connected points. This type of singularity does not have anything to do with the strength of the network at that point; strength simply cannot be (reliably or at all) determined at that point. In the enhanced NETAN (see Chapter 6), strength indicators at these singular points are simply not plotted at all.

The other type of singularity occurs at points attached to the network by observation(s) whose redundancy number equals zero, i.e., at points whose position is derived from the minimal number of observations with no redundancy (e.g., two intersecting directions).

Because such observations are not checked at all by the test for outliers, there is no guarantee that such observations are not burdened with huge blunders and the point in question represents a point of infinite weakness — zero strength — in the network. The strength indicators at these points show very large values.

Finally, we wish to note here that robustness analysis is datum independent. The proof for the independence was shown in the previous chapter for the geometrical strength analysis and it fully applies here as well. The consequence of this property is that any choice of a minimally constrained adjustment model will yield the same results as far as network strength is concerned. It must be emphasized, however, that a network adjusted with some weighted constraints, e.g., a network for which positions of some points, together with their errors, are known a priori, cannot be viewed in the same light. Weighted constraints become an indivisible part of the network itself as much as the observations are, and the strength of such a network is as much affected by the constraints (and their weights) as it is by the observations (and their weights). The fact that the weighted constraints may also supply a datum for the adjustment is only incidental.

5.3 Comparison of Robustness and Geometrical Strength Analyses

To demonstrate the difference between the GSA and the robustness analysis, results of both analyses applied to the HOACS 3D synthetic network, are shown here. For a full discussion of the HOACS 3D network and its robustness, the reader is referred to Chapter 7.

Figures 5.1 and 5.2 show strength in scale as estimated by both techniques. The results are somewhat similar insofar as the extreme values are concerned: the maxima (in absolute value) are located at the same points, the northeast and the southwest corners, i.e., the weaknesses of the network have been pinpointed by both techniques the same way. On the other hand, the details are quite different and so are the magnitudes, as one should expect.

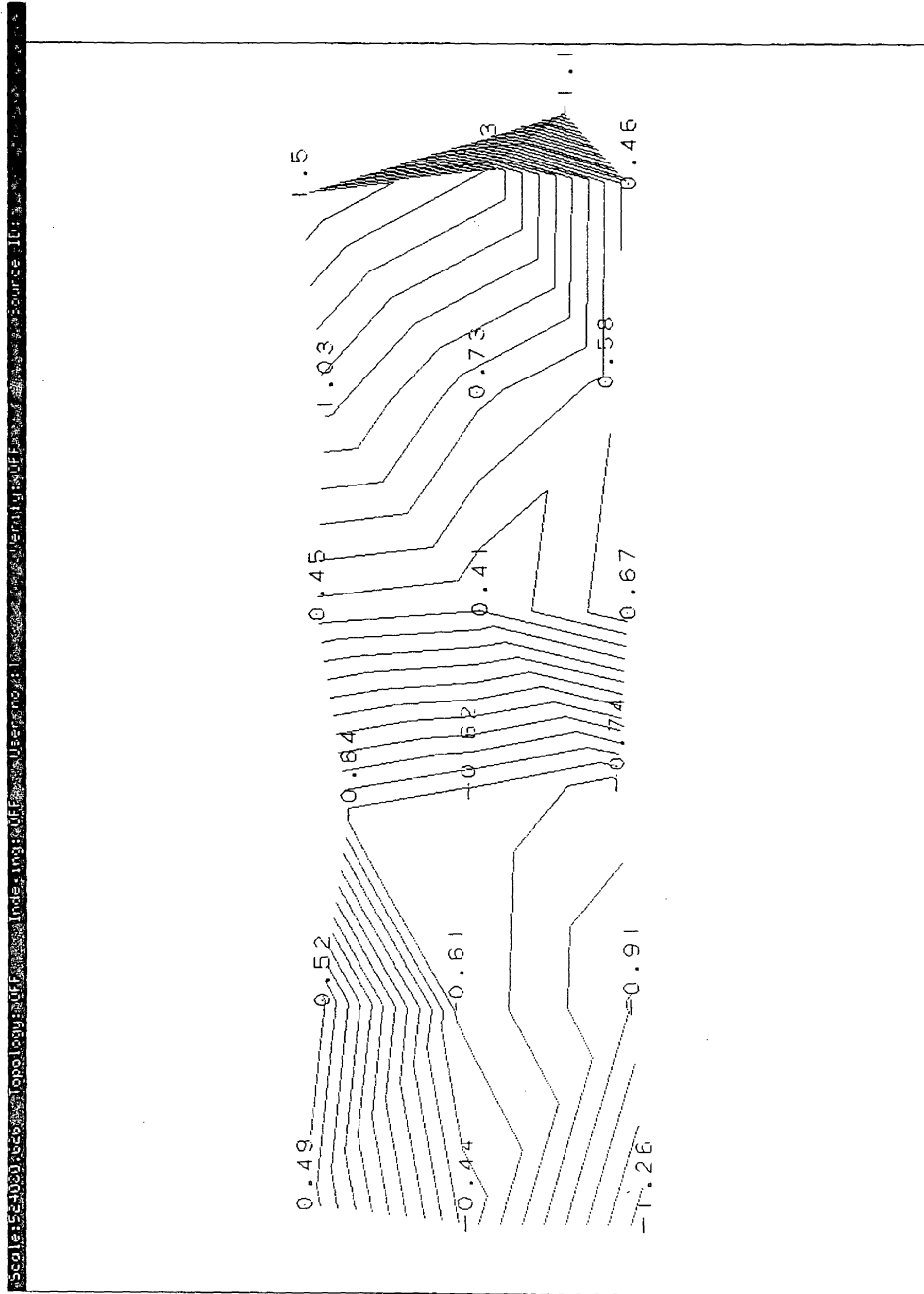


Figure 5.1 Geometrical strength in scale (ppm).

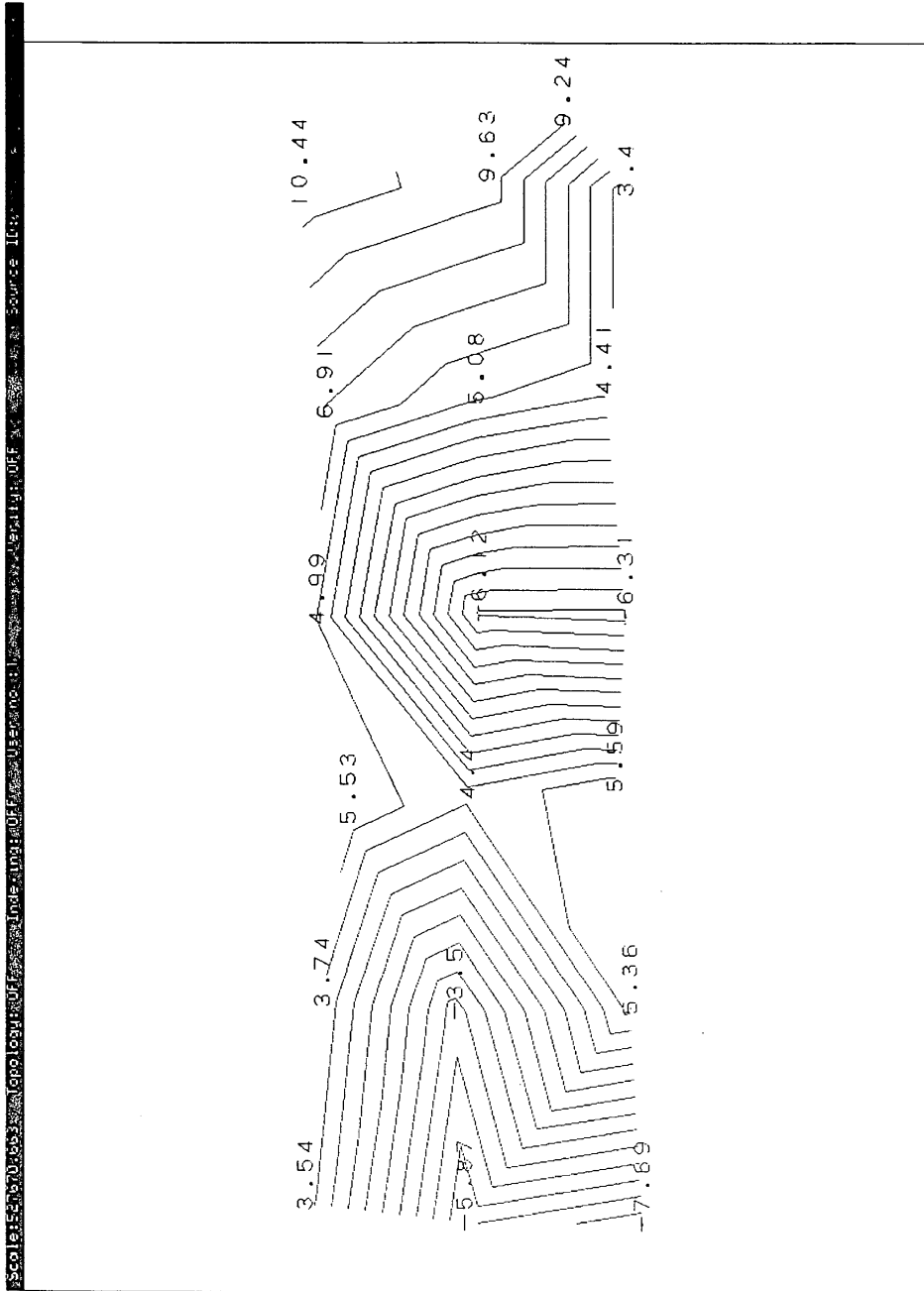


Figure 5.2 Robustness in scale (ppm).

Figures 5.3 and 5.4 show strength in shear. Once again, the point of extreme weakness is placed at the easternmost part of the network equally by both techniques. In the other aspects, the two plots are different.

Figures 5.5 and 5.6 display strength in twist. This time even the locations of extreme weaknesses are different; so much so that the point at the westernmost end of the network is at once identified as being the geometrically strongest, yet showing the least robustness. Interestingly, all the values of robustness in twist are negative, while geometrical strength shows both positive and negative values.

5.4 Comparison of Robustness and Covariance Analyses

In Chapter 2, we described what is generally understood by covariance analysis: the conglomerate of statistical tests based on the covariance matrices of the observations and of the adjusted positions (coordinates). This traditional analysis is based solely on statistical considerations and is concerned only with Type I error, random errors and their effect on the network. The effect is normally quantified by absolute and relative confidence regions and various derived quantities such as relative accuracies, whose purpose is to show just how much the network may be distorted (deformed) by the presence of errors presumed random.

In many countries, including Canada, this kind of analysis is the only one ever applied to geodetic networks. It forms the basis for Canadian federal specifications for horizontal control networks. The information contained in the covariance matrix of estimated positions is the only information about the 'strength of the network.' The effect of possible blunders that may escape detection by appropriate statistical tests is not considered and neither is the effect of geometrical weaknesses, at least not directly. The test that comes closest to a consideration of a blunder (but not its effect) is the one for outlier detection, where the result is assumed to be a set of blunderless observations. In brief, the covariance analysis deals with the second moments of the PDFs of observations and estimated parameters.

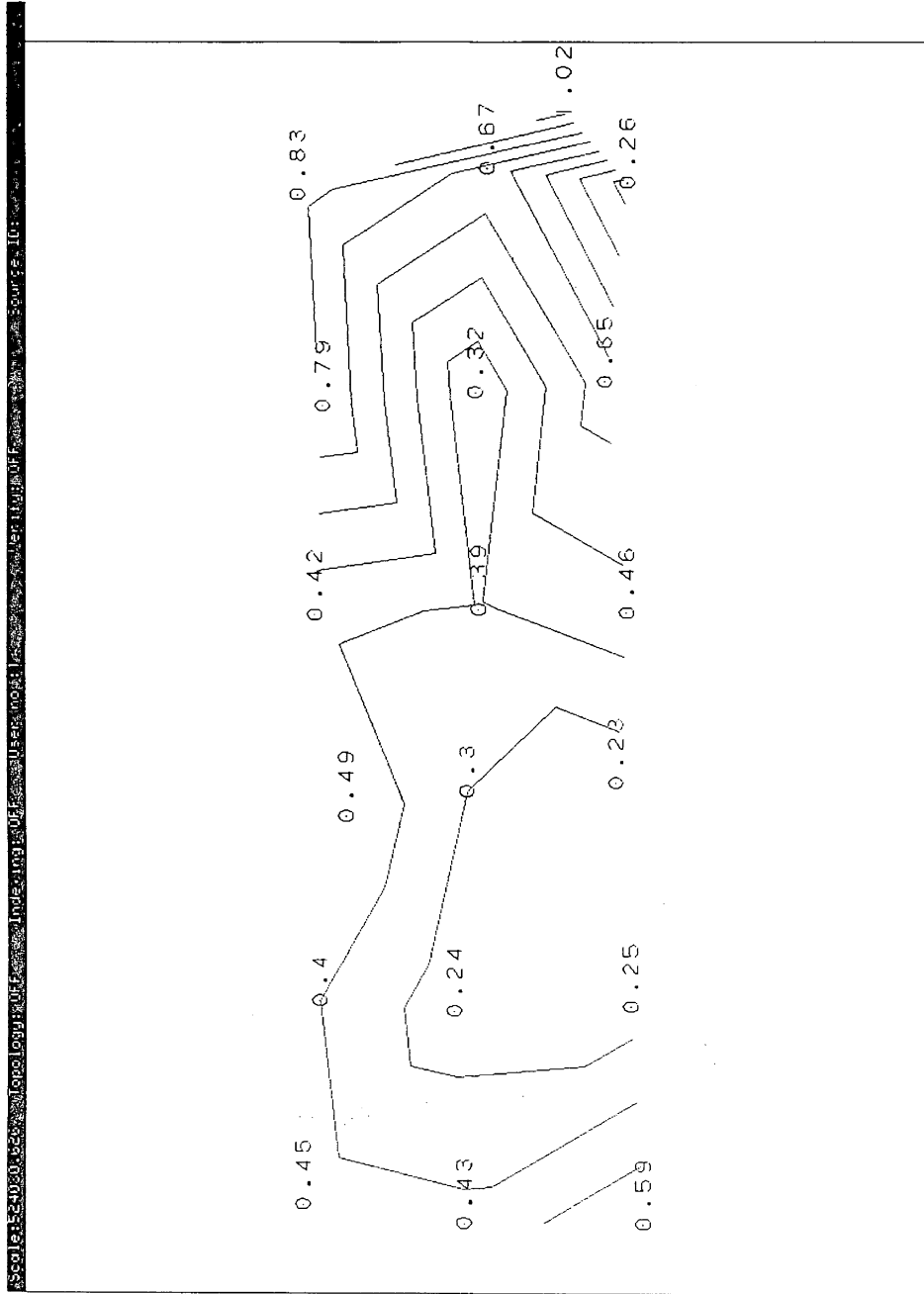


Figure 5.3 Geometrical strength in shear (ppm).

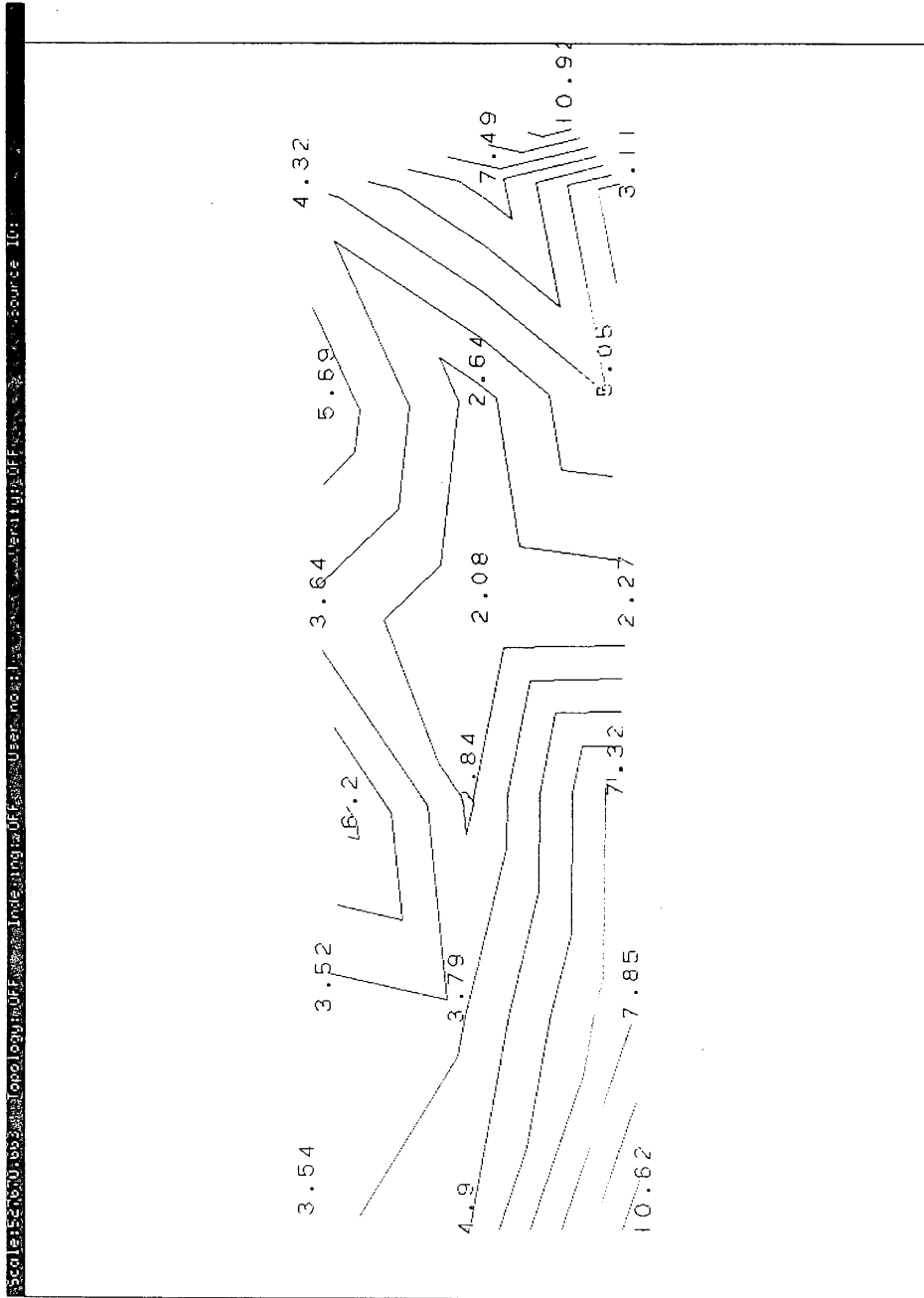


Figure 5.4 Robustness in shear (ppm).

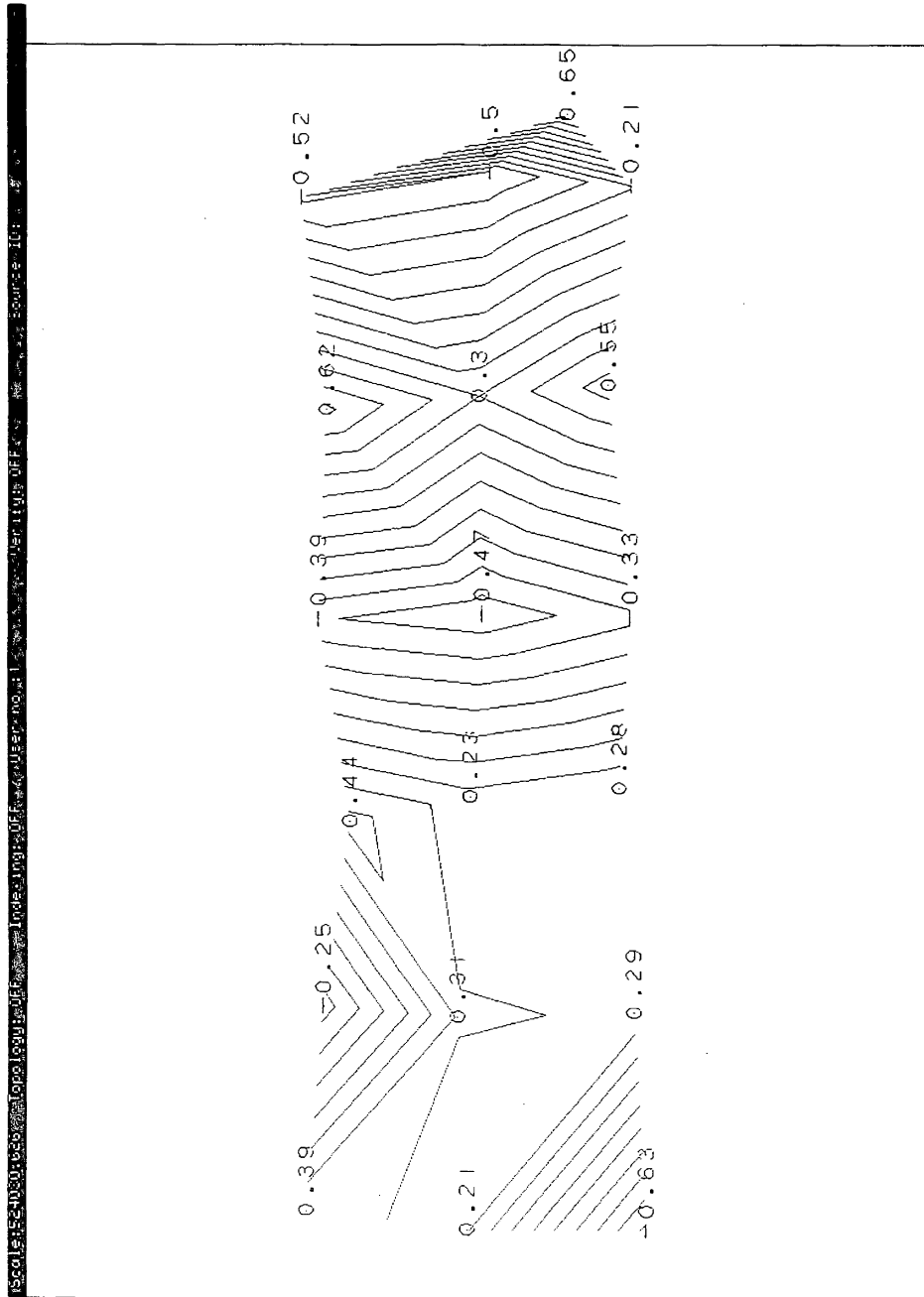


Figure 5.5 Geometrical strength in twist (ppm).

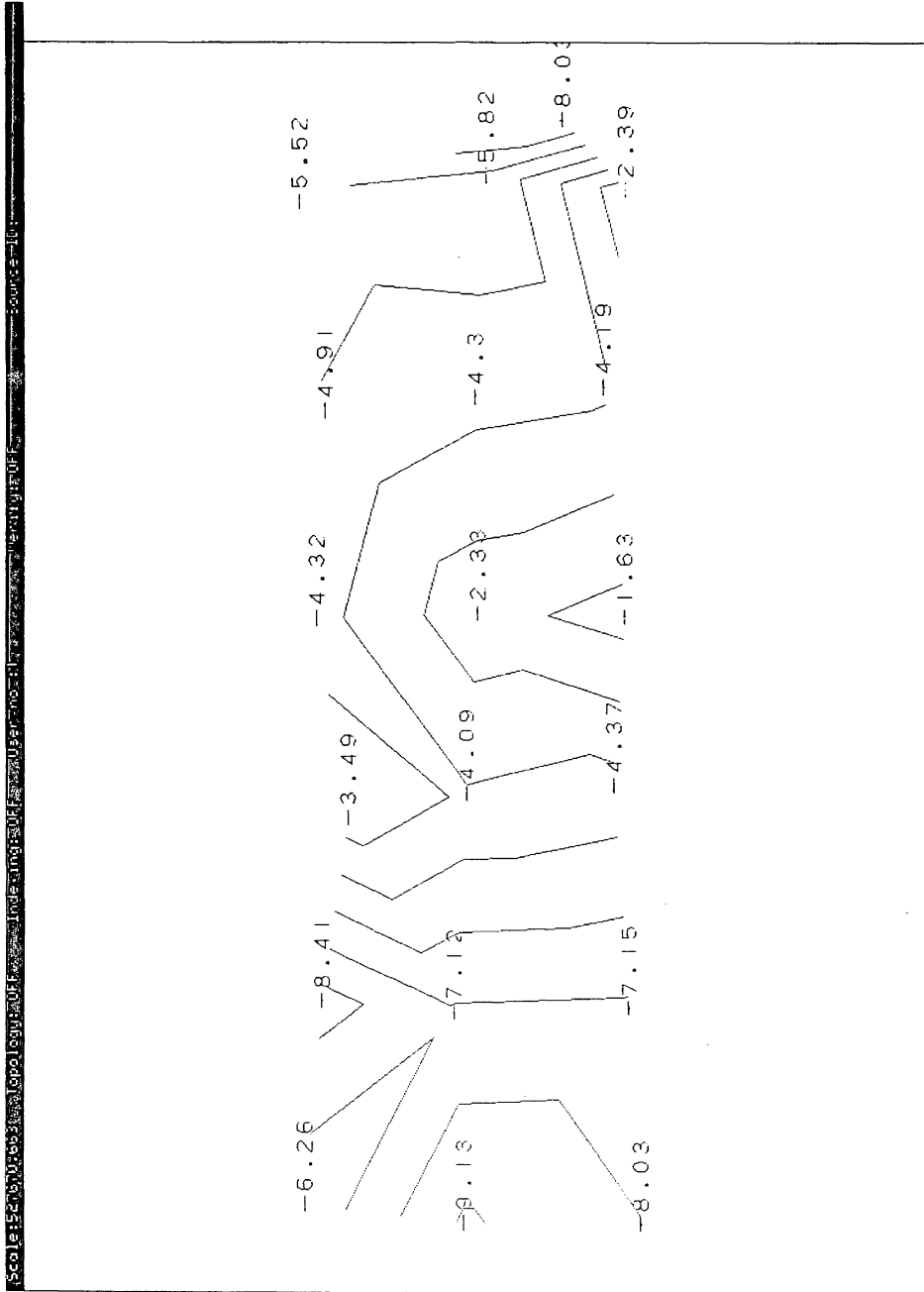


Figure 5.6 Robustness in twist (ppm).

Robustness analysis looks at the network from a different point of view, assuming that some blunders inevitably escape detection and make their presence felt by deforming the network. Hence it uses statistical tools also but only to estimate the magnitudes of potential undetectable blunders, i.e., it deals with first-order moments of the PDFs of observations. The rest of the analysis is purely deterministic (geometrical) and has no statistical connotation whatever. The picture of the network presented by the robustness analysis is what one should expect the strength to be: the ability to resist deformation, and should be understood as such; the robustness analysis is a strength analysis.

Clearly, the two analyses present quite different pictures of the analysed network. In some parts of the network, the messages from both analyses may be similar; in other parts, they may be very different, even contradictory. As an example, let us take the strength singularity caused by the lack of redundancy. In this case, the point in question will have zero strength while both absolute and relative confidence regions may not show any irregularity at all. Quite the contrary; if the single observation has a very low standard deviation, the pertinent relative confidence region will be very small, indicating a good network design.

To show the difference between the information contained in the results of either analysis, Figure 5.7 is included here. This figure is a plot of some relative confidence ellipses for the HOACS 3D network (for a full discussion of this network, see Chapter 7). This plot should be compared with Figures 5.2, 5.4, and 5.6 to see that the information content is quite different. One would be hard pressed to find any similarities between Figure 5.7 and any of the other three figures.

In some countries, e.g., Switzerland and Germany, Baarda's reliability analysis is used side-by-side with the standard covariance analysis. Robustness analysis should replace (complete) the reliability approach as a tool for analysing networks, side-by-side with the standard covariance analysis. As such, robustness analysis should make its way into network specifications to be used as a tool for network design, classification, and analysis.

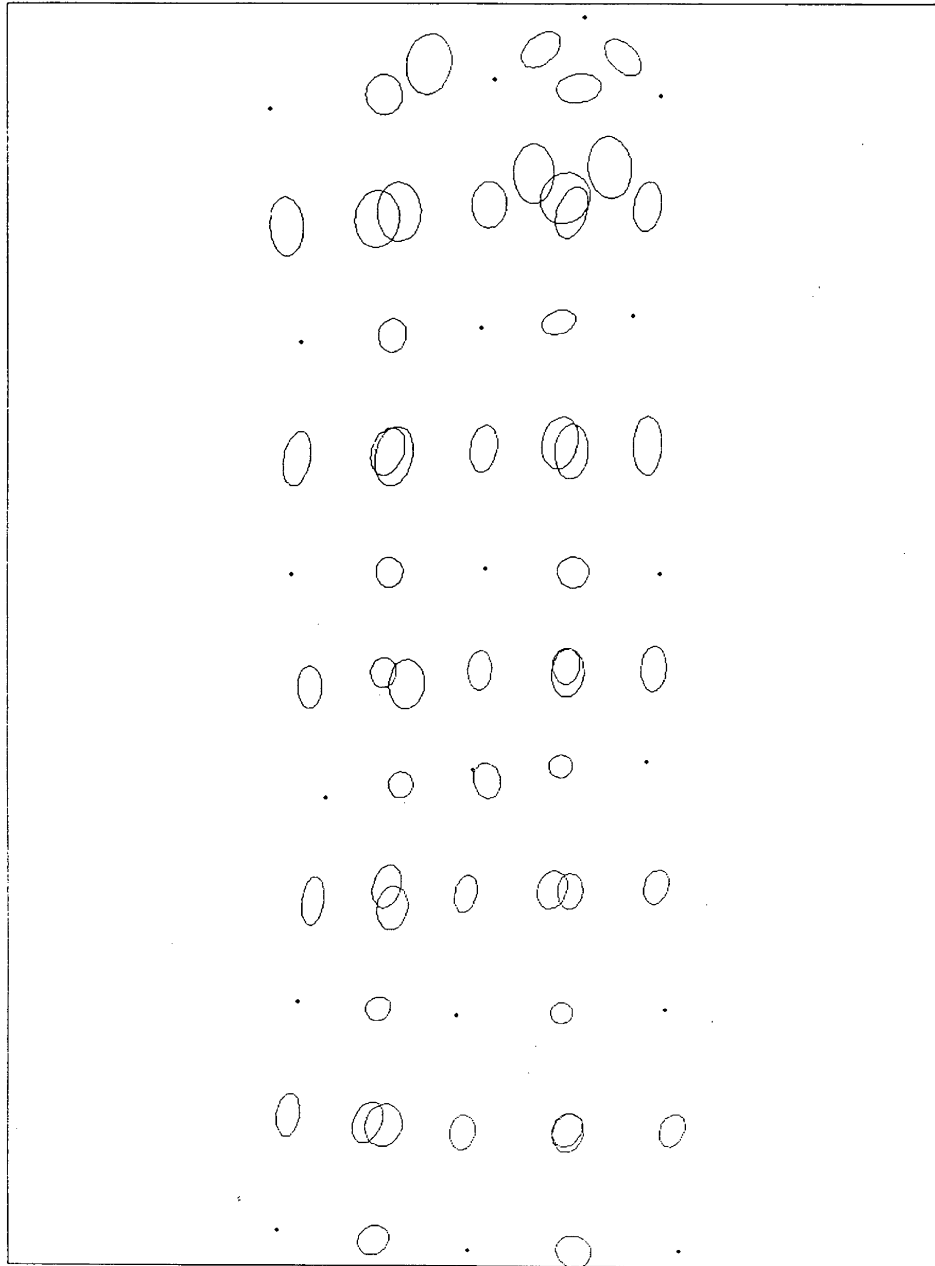


Figure 5.7 Relative confidence ellipses for the HOACS 3D network.

6. NETAN ENHANCEMENTS

6.1 Introduction

In this chapter, we discuss the incorporation of robustness analysis into the original NETAN software developed by Craymer et al. [1988; 1989]. Only a general description of the changes will be given. More details can be found in the source code.

The first modification was to replace the use of total strain with dilation to represent strength in scale. Total strain is computed from the square root of the sum of squares of the principal strains (eigenvalues) of the symmetric strain tensor. This quantity is a geometric mean and reflects only the absolute values of the principal strains. Negative changes in scale (i.e., contractions) can never be represented by this quantity. Dilation, on the other hand, is simply the sum of the principal strains (or the diagonal elements of the symmetric strain tensor) which accounts for the sign of the principal strains. The strength in scale based on this quantity can therefore represent both extension in scale (positive dilation) as well as contraction in scale (negative dilation).

The selection of the largest strain primitives to represent the strength parameters at each point in the network has also been changed. In the former version, the sign of the strain primitive was taken into account when searching for the largest value at each station. This resulted in large negative values being ignored in favour of small positive values. In the current version, this problem has been corrected by selecting the largest absolute value of the strain primitives representing the strength at each point.

The most significant change to NETAN involved the incorporation of robustness analysis. This necessitated computing the standard deviations of all residuals within NETAN since the GHOST software uses only Pope's approximation. Because these approximate values are identical for observations with the same standard deviation, they were of no use for determining the internal reliability; the redundancy numbers would (incorrectly) be the same for

all observations with the same a priori standard deviation. Although the internal reliability results (i.e., the maximum undetectable error for each observation) are not presently included in the strength output, primarily because of the volume of information, this can be added in a later version if deemed necessary.

The practical implementation of robustness analysis required us to identify observations which are used to uniquely determine points in the network. For example, two intersecting directions to a point, two intersecting distances, or a distance and direction all provide only a unique determination of the relative position of a point. There is zero redundancy in these cases, and the maximum undetectable error is in theory infinite. Such observations are currently identified in the output listing and omitted from the strength computations for the purposes of this report. It is recommended, however, that this be changed in the next version of NETAN by assigning a specific value representing a very large number (say, $0.33E33$) to the strength parameters at these stations. These points would then show up as very large peaks in the contour plots. Currently, these points are assigned zero strains and omitted from the plots.

A similar problem can also arise when a single observation is used to define the network datum. Examples are a single azimuth observation defining the network orientation or a single distance defining the network scale. A single position difference observation without any azimuths or distances defines both azimuth and scale. Large maximum undetectable errors result in these cases, which would overwhelm the strength results. Therefore these observations have also been omitted from the strength analysis for the purposes of this report. Currently, a tolerance limit of 0.001 for the redundancy number is used to detect such cases. Observations with redundancy numbers smaller than this will be identified in the output listing and omitted from the strength analysis. We recommend, however, that the software be changed to use the actual (large) maximum undetectable errors in the strength computations so that these points will show up as very large peaks in the contour plots of the strength parameters.

A more fundamental problem with the strength (and strain) computation occurs when there is only one unique observation tie to a station. For example, a direction and distance both along the same line. Such cases represent geometric singularities in the determination of strain since it will not be possible to fit a plane surface to just two points and no strain can therefore be computed. These strength and robustness parameters at points with such geometric singularities are currently assigned zero values. It is recommended instead to flag these points using a specific value representing an undefined quantity (say, 0.33E33) in the next version of NETAN.

Geometric ill-conditioning or near-singularities can also arise when the observation ties to a station are near collinear. The fitting of a plane to nearly collinear lines will be very ill-conditioned and may result in spuriously large strain elements. An example of this is shown for the real network analysed in Chapter 7. Presently NETAN does not identify such geometric ill-conditioning. One possibility may be to simply check the determinant of the normal equation matrix for the surface fitting solution. Small values would indicate geometric ill-conditioning. An alternative and more general approach may be to estimate standard deviations for the strain elements and strength parameters and to perform some elementary statistical tests for significance. It is strongly recommended to investigate these and other methods of identifying and dealing with such geometric ill-conditioning.

External reliability is not computed since the robustness analysis of the internal reliability provides a better and more detailed picture of the strength (deformation) of the network. Although this could be incorporated if desired, it would be very time consuming (of the same order as the robustness analysis). Nevertheless, external reliability may provide a means of providing strength estimates at points where there are geometric singularities or ill-conditioning.

6.2 Update to User's Guide

The incorporation of robustness analysis into the NETAN software resulted in a new “Strength Analysis Option” menu for selecting the type of strength analysis to be performed; either geometrical strength or robustness analysis (see Figure 6.1). The geometrical strength analysis uses the observation standard deviations to perturb the network as in the original version of NETAN. The robustness analysis perturbs the network using the internal reliability measure, i.e., the maximum undetectable error for each observation. This menu is presented immediately after selecting the “Strength Analysis” option from the main menu.

```

Strength Analysis Options
-----
0) Robustness analysis
1) Geometrical strength analysis

Select option [0]:

```

Figure 6.1 “Strength Analysis Options” menu.

In addition to the prompts already described in Craymer et al. [1988], selection of the “robustness analysis” option also presents an additional prompt to enter the non-centrality parameter for the internal reliability computations. The following prompt is used to list the acceptable non-centrality values together with their associated levels of significance and power of the test:

```

Non-centrality parameters:
-----

```

Significance Level (%)	Power of the Test (%)				
	99.0	95.0	90.0	85.0	80.0
0.1	5.60	4.94	4.58	4.34	4.14
1.0	4.90	4.22	3.86	3.62	3.42
5.0	4.29	3.61	3.24	3.00	2.80

```

Enter non-centrality parameter:

```

Finally, the output listing for the strength analysis has also been augmented with additional information pertinent to the robustness analysis. Added to the original strength output listing is a list of the omitted observations which uniquely determine points or uniquely define the network datum.

7. NUMERICAL EXAMPLES

7.1 Introduction

In this chapter, examples of robustness analysis are given for both simulated and real three-dimensional (3D) networks, each with a variety of different types of geodetic observations including azimuths, directions, distances, 3D position observations, and 3D position difference observations.

The plots of the robustness results presented here have been generated in two ways. The plots of observation ties were created using NETAN. Hard copies were made from screen dumps to a Tektronix 4693D Color Image Printer using a thermal wax printing process. Plots of the robustness in rotation, shear, and scale were generated using the CARIS software system only for the purposes of this report. A temporary data file containing the information to be plotted was generated by NETAN for input to CARIS. CARIS allowed us to include on the contour plots the robustness values at each point in the network. NETAN does not display this information on the plot but instead lists station and observation information interactively when the user graphically selects a point or observation tie.

7.2 Simulated Network HOACS

A simulated network, called HOACS, was obtained from the Canadian Geodetic Survey. This test network was originally created by the U.S. National Geodetic Survey for testing their own network adjustment software and is also used by the Canadian Geodetic Survey to test their 3D adjustment software GHOST. The network consists of a variety of geodetic observations including:

- 11 free stations (none explicitly fixed)
- 3 azimuth observations with 1 second standard deviations
- 77 direction observations with 0.7 second standard deviations

- 6 distance observations with 2 ppm standard deviations
- 8 three-dimensional position observations with 10 cm standard deviations (i.e., 24 coordinate observations)
- 3 three-dimensional position difference observations with 5 mm standard deviations (i.e., 9 coordinate difference observations)
- 3 three-dimensional position difference observations with 1 cm standard deviations (i.e., 9 coordinate difference observations)

Figures 7.1 to 7.5 illustrate the locations of the stations and the different types of observations. Table 7.2 gives a listing of the input GHOST data file for this network.

The results from the NETAN robustness analysis are displayed in terms of robustness in rotation (local twisting), robustness in shear (local changes in configuration or shape), and robustness in scale in Figures 7.6, 7.7, and 7.8, respectively. The NETAN output listing for this analysis is given in Table 7.3. These robustness results are all based on $\alpha_0=5\%$ and $\beta_0=5\%$ which gives a non-centrality parameter of $\sqrt{\lambda_0}=3.61$ (the standardized value of maximum undetectable error). Different α_0 and β_0 result in a different $\sqrt{\lambda_0}$ which only scales the magnitude of the strength parameters by the ratio of the non-centrality parameters. The plots are otherwise identical.

The results indicate that the perimeter of the network is relatively weaker than the middle since the largest values for rotation, shear, and scale are all located on the edges of the network. No points uniquely determined by a minimum number of observations are present. The datum orientation and scale are defined by a multitude of observations. Because of the ideal geometry of this network, all strain determinations were well conditioned. Table 7.1 summarizes the range of values, the largest and smallest (absolute) values in magnitude, and the average and standard deviation (dispersion about the mean) for each robustness parameter. Note that the averages and standard deviations of these parameters are all of the same magnitude as the relative accuracy of the observations. Individual values less than about 10 ppm may therefore not be very statistically significant (this should be investigated more

rigorously by developing and implementing algorithms for determining the standard deviations of the strength parameters).

Table 7.1 Summary of robustness results for the HOACS network.

	Robustness in rotation (μrad)	Robustness in shear (ppm)	Robustness in scale (ppm)
Maximum	-1.6	10.9	10.4
Minimum	-9.1	2.1	-7.7
Largest absolute	-9.1	10.9	10.4
Smallest absolute	-1.6	2.1	3.4
Mean	-5.3	5.1	2.4
Standard deviation	2.2	2.6	5.9

The robustness in rotation results are illustrated in Figure 7.6 and listed in Table 7.3. These results describe the ability of the network to resist local changes in orientation (twisting). The largest values are obtained for station 1017 ($-9.1 \mu\text{rad}$ due to position observation #117), station 1015 ($-8.4 \mu\text{rad}$ due to position observation #117), station 1016 ($-8.0 \mu\text{rad}$ due to position observation #117), and station NO SUCH MOUNTAIN ($-8.0 \mu\text{rad}$ due to direction observation #8). All of these weak points are located on the perimeter of the network where there are fewer observations tying these stations to the rest of the network. Even the largest of these values, however, is well within first-order accuracy standards (20 ppm). The best (smallest absolute value) robustness in rotation is obtained for station 1007 ($-1.6 \mu\text{rad}$) which, although located at the bottom edge of the network, has many observations tying this point to the rest of the network. The average of the differential rotations is only $-5.3 \mu\text{rad}$ and the standard deviation (dispersion about the mean) only $2.2 \mu\text{rad}$.

The robustness in shear results are given in Figure 7.7 and Table 7.3. These results describe the ability of the network to resist local deformations in configuration or shape. The largest values are obtained for station NO SUCH MOUNTAIN (10.9 ppm due to direction observation #8) and station 1016 (10.6 ppm due to position observation #123), both of which are on the perimeter of the network and have fewer observation ties. These values are also well

within first-order accuracy limits. The best (smallest absolute value) robustness in shear is obtained for station 1008 (2.1 ppm) which is in the middle of the network and has many observation ties connecting it to the rest of the network. The average shear is only 5.1 ppm and the standard deviation is 2.6 ppm.

The robustness in scale results are given in Figure 7.8 and Table 7.3. These results describe the ability of the network to resist local deformations in scale (dilation). The largest values are obtained for station 1003 (10.4 ppm due to position difference observation #90), station 1002 (9.6 ppm due to position difference observation #90), station NO SUCH MOUNTAIN (9.2 ppm due to position observation #114), and station 1016 (-7.7 ppm due to position difference observation #105). All of these stations are on the perimeter of the network and have fewer observation ties to the rest of the network. These values are again well within first-order accuracy limits. The best (smallest absolute value) robustness in scale is obtained for station 1001 (3.4 ppm) which, although at the edge of the network, has many observation ties (especially 3D position differences) to the rest of the network. The average dilation is only 2.4 ppm and the standard deviation is 5.9 ppm.

Other than the number of observations to and from the points of interest, there does not seem to be much indication of the cause of the weaknesses. Although different observations seem to affect different robustness parameters in some cases, there are other cases where these trends breaks down. We therefore have to rely on an analytical approach to learn about the weaknesses. More experience and experiments will be required to gain a better understanding of how the robustness parameters are affected by the different types of observations.

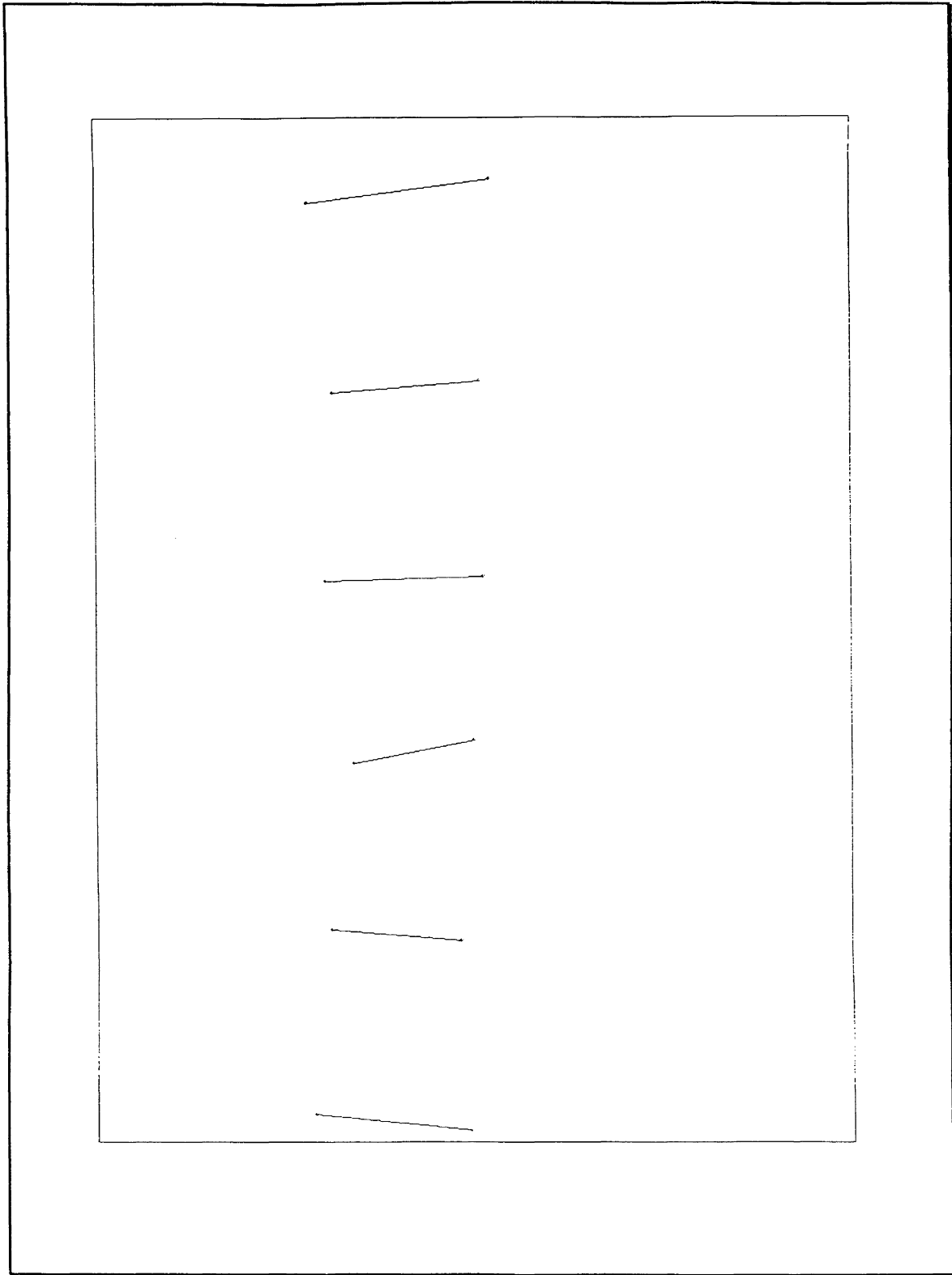


Figure 7.1 Distance observations for simulated 3D HOACS network.

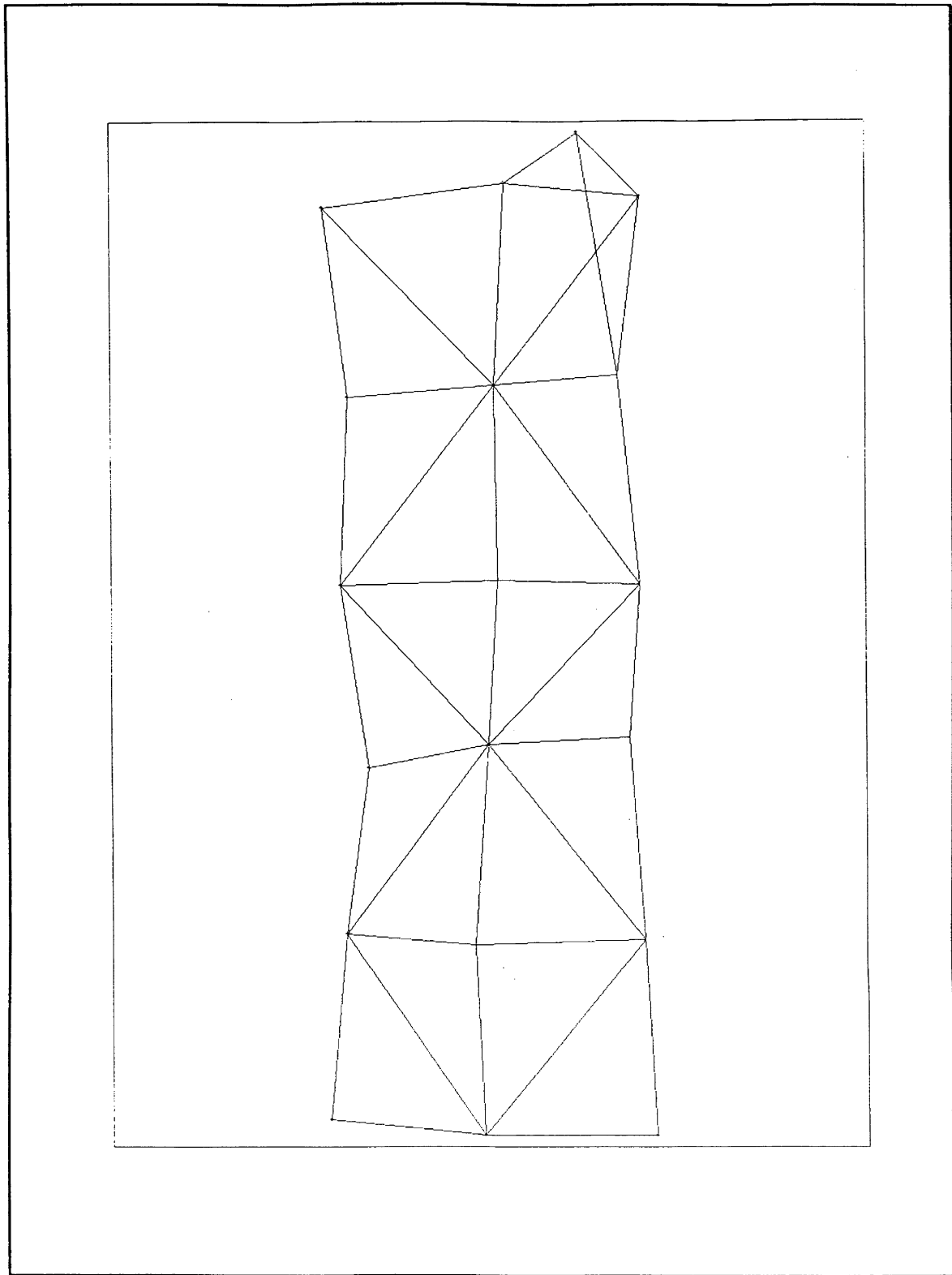


Figure 7.2 Direction observations for simulated 3D HOACS network.

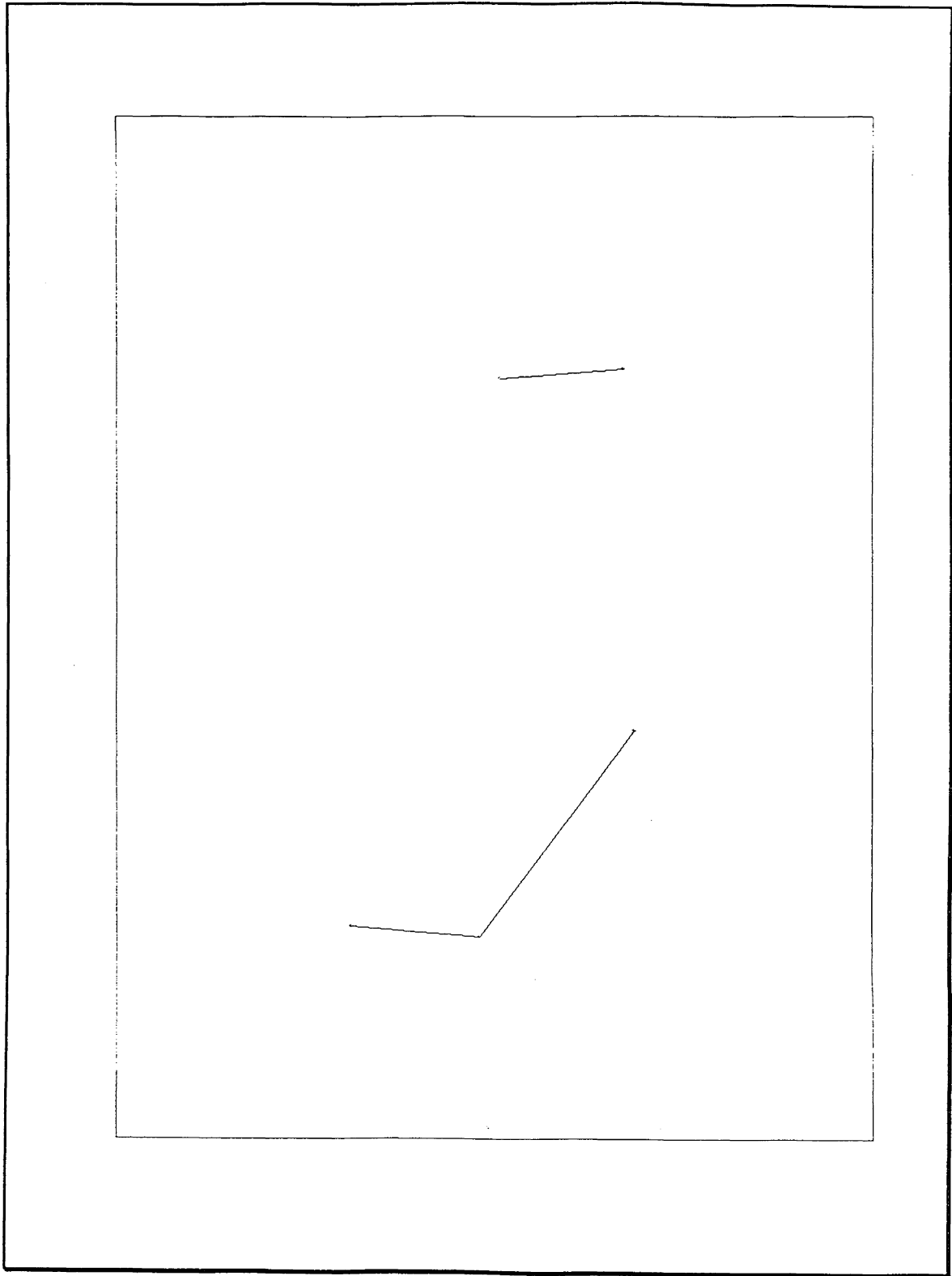


Figure 7.3 Azimuth observations for simulated 3D HOACS network.

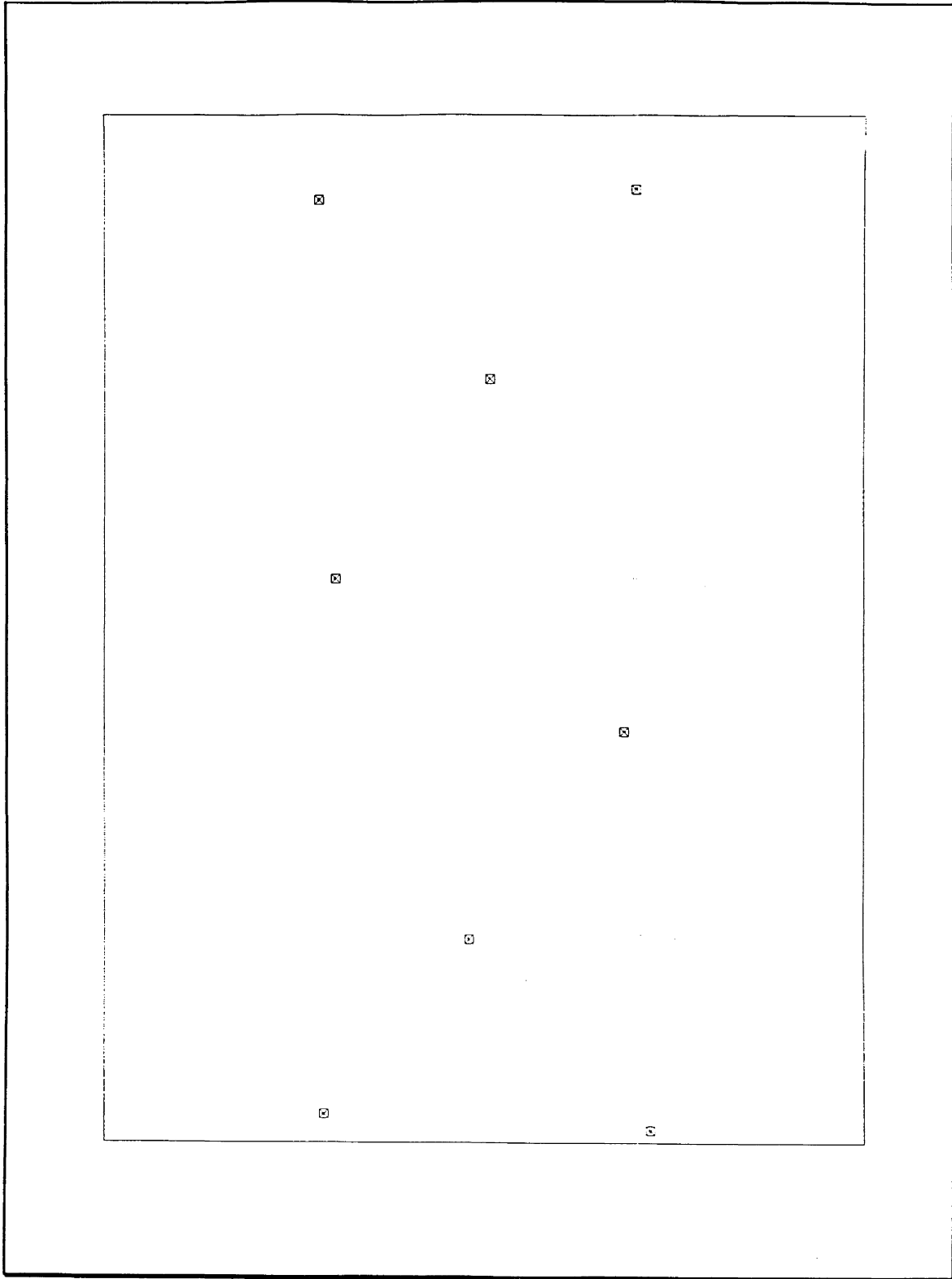


Figure 7.4 3D position observations for simulated 3D HOACS network.

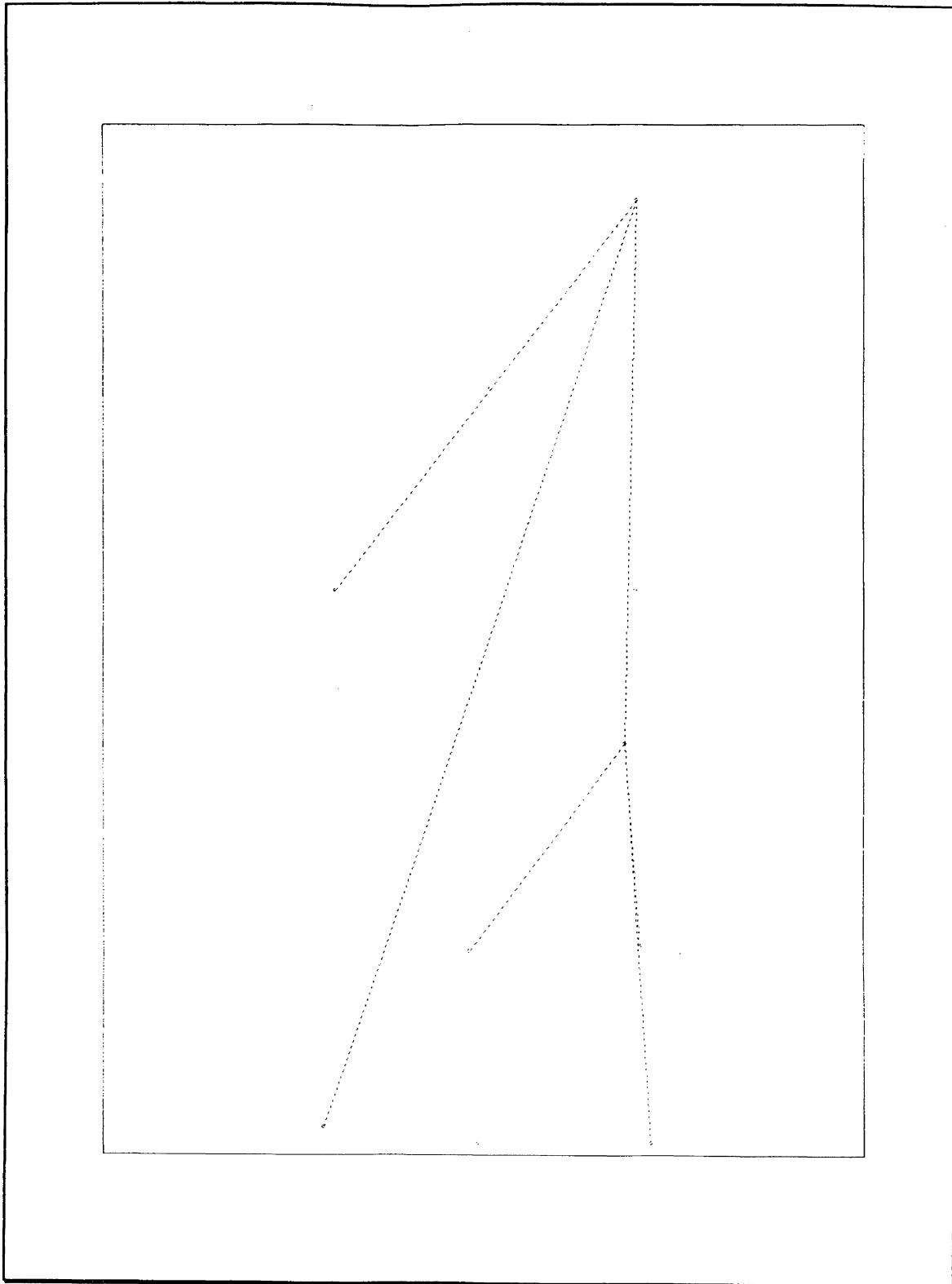


Figure 7.5 3D position difference observations for simulated 3D HOACS network.

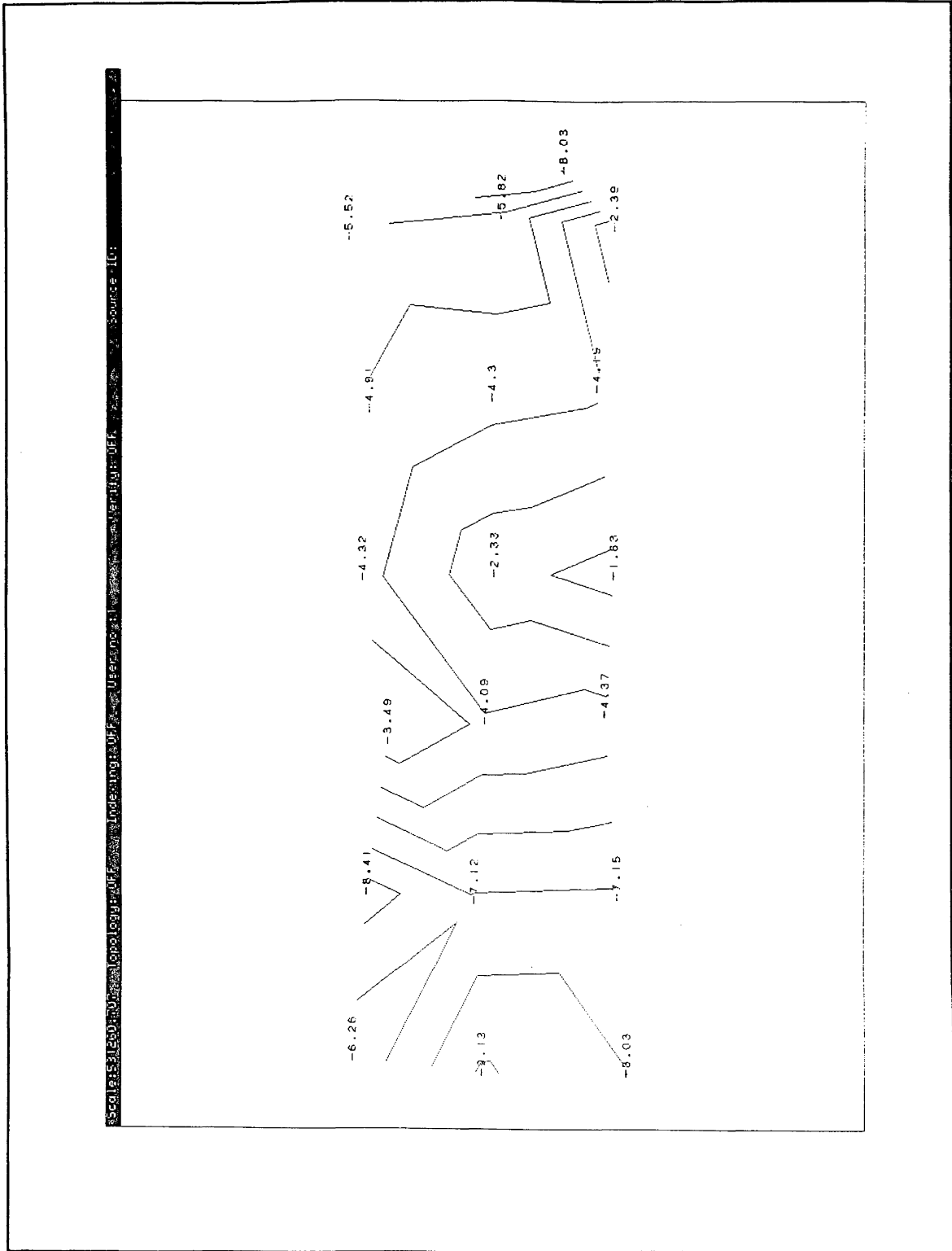


Figure 7.6 Robustness in rotation for simulated 3D HOACS network.

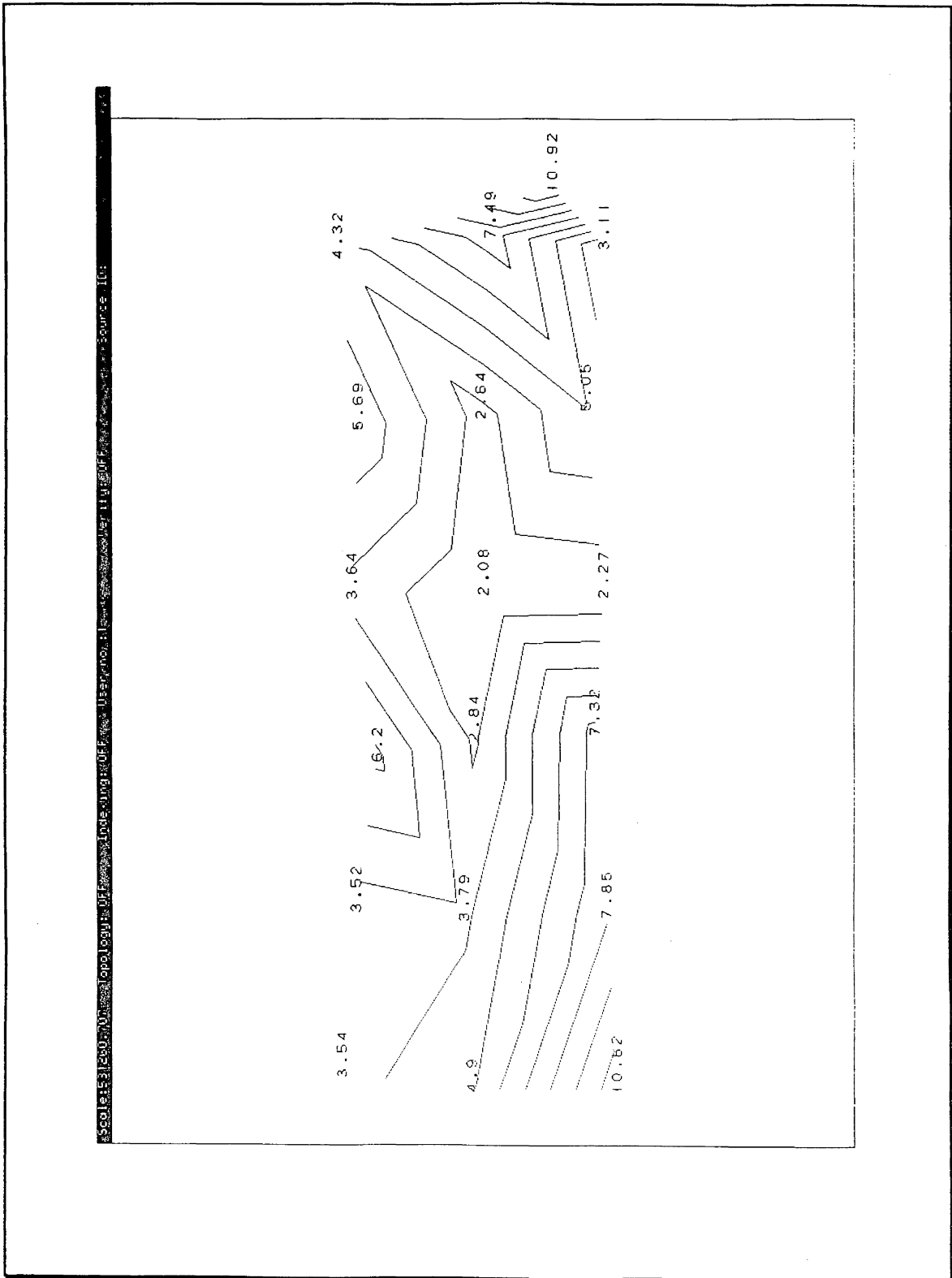


Figure 7.7 Robustness in shear for simulated 3D HOACS network.

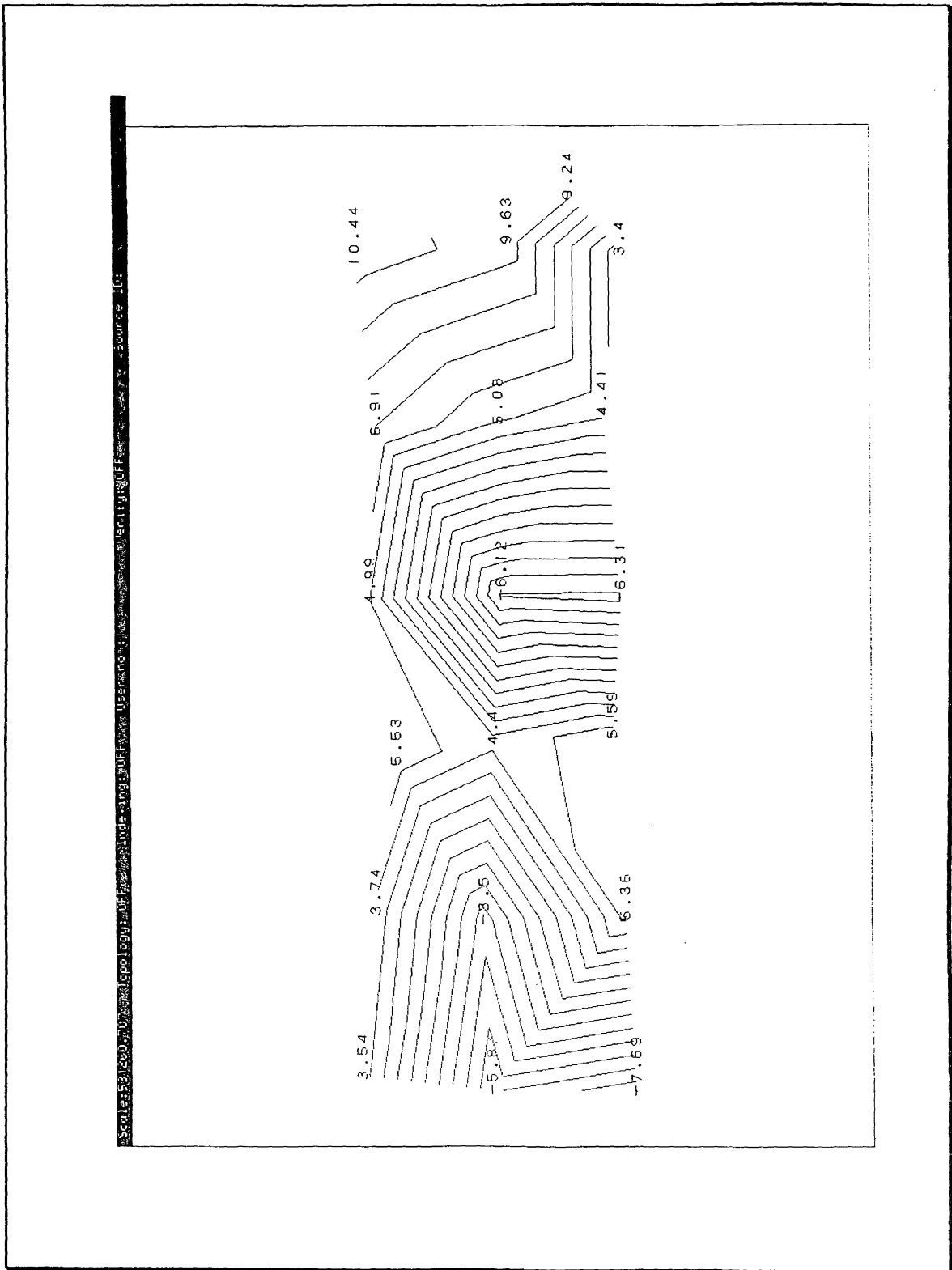


Figure 7.8 Robustness in scale for simulated 3D HOACS network.

Table 7.2 GHOST input data file for simulated 3D HOACS network.

```

HOACS TERRESTRIAL TEST DATA
  1 3 1 1 1 1 1
*
* STATION INFORMATION SECTION
*
10
4300ND SUCH MOUNTAIN          30 5 0.00000w 89 55 0.00000 3500.000
43001001 STATION              30 0 0.00000w 90 0 0.00000 1955.800
43001002 STATION              30 10 54.03925w 89 58 58.98067 2164.320
43001003 STATION              30 25 40.03862w 90 0 54.04869 1996.800
43001004 STATION              30 1 46.97851w 90 14 9.01720 2015.190
43001005 STATION              30 11 47.98894w 90 14 58.98289 1914.260
43001006 STATION              30 23 40.99617w 90 15 57.95561 2203.180
43001007 STATION              30 0 1.94870w 90 30 52.04613 1937.020
43001008 STATION              30 11 35.94621w 90 30 33.01558 2075.930
43001009 STATION              30 24 16.94934w 90 30 56.02636 2042.170
43001010 STATION              30 0 57.03795w 90 43 .04138 1987.610
43001011 STATION              30 12 20.95802w 90 43 35.04939 1954.820
43001012 STATION              30 22 1.99561w 90 45 25.95232 1874.160
43001013 STATION              29 59 43.97387w 90 59 10.05335 1819.660
43001014 STATION              30 13 29.02889w 90 59 34.00567 2006.180
43001015 STATION              30 23 53.99599w 90 58 39.97635 1950.240
43001016 STATION              29 58 51.95506w 91 15 3.97056 2150.690
43001017 STATION              30 12 46.02388w 91 15 1.05684 2071.250
43001018 STATION              30 25 15.02776w 91 13 42.95407 1990.500
*
* ASTRONOMIC DATA RECORDS
*
7 1001 STATION                30 1.08 w 90 1.94000
7 1002 STATION                30 10 56.48 w 89 59 01.10000
7 1003 STATION                30 25 37.30 w 90 00 54.33000
7 1004 STATION                30 01 45.69 w 90 14 15.54000
7 1005 STATION                30 11 49.69 w 90 15 01.50000
7 1006 STATION                30 23 38.59 w 90 16 02.12000
7 1007 STATION                30 3.51 w 90 30 49.12000
7 1008 STATION                30 11 36.81 w 90 30 36.41000
7 1009 STATION                30 24 16.69 w 90 30 59.39000
7 1010 STATION                30 55.32 w 90 43 01.90000
7 1011 STATION                30 12 30.51 w 90 43 37.08000
7 1012 STATION                30 21 49.15 w 90 45 23.98000
7 1013 STATION                29 59 45.81 w 90 59 14.06000
7 1014 STATION                30 13 29.75 w 90 59 33.45000
7 1015 STATION                30 23 53.10 w 90 58 47.00000
7 1016 STATION                29 58 50.08 w 91 15 6.39000
7 1017 STATION                30 12 45.48 w 91 15 2.23000
*
* GEODIAL DATA RECORDS
*
9300ND SUCH MOUNTAIN          0 0 .00010 0 0 .00010 0.000
93001001 STATION              0 0 .00010 0 0 .00010 10.200
93001002 STATION              0 0 .00010 0 0 .00010 10.100

```

93001003 STATION	0 0	.00010	0 0	.00010	10.000
93001004 STATION	0 0	.00010	0 0	.00010	9.800
93001005 STATION	0 0	.00010	0 0	.00010	9.800
93001006 STATION	0 0	.00010	0 0	.00010	9.800
93001007 STATION	0 0	.00010	0 0	.00010	9.600
93001008 STATION	0 0	.00010	0 0	.00010	9.500
93001009 STATION	0 0	.00010	0 0	.00010	9.400
93001010 STATION	0 0	.00010	0 0	.00010	9.600
93001011 STATION	0 0	.00010	0 0	.00010	9.200
93001012 STATION	0 0	.00010	0 0	.00010	9.400
93001013 STATION	0 0	.00010	0 0	.00010	9.300
93001014 STATION	0 0	.00010	0 0	.00010	9.100
93001015 STATION	0 0	.00010	0 0	.00010	9.000
93001016 STATION	0 0	.00010	0 0	.00010	8.900
93001017 STATION	0 0	.00010	0 0	.00010	9.100
93001018 STATION	0 0	.00010	0 0	.00010	9.000

*

* AUXILIARY PARAMETER DECLARATIONS

*

94disDISSCAL	SCAL
943dcDOPXF	ROTX ROTY ROTZ SCAL
943ddGPSXF	ROTX ROTY ROTZ SCAL

*

* DIRECTION OBSERVATIONS

*

10

512 0.7

12 1001 STATION	1002 STATION	0 0 0.00000	.70000
12 1001 STATION	NO SUCH MOUNTAIN	36 22 19.00000	.70000
12 1001 STATION	1004 STATION	273 39 55.81000	.70000
12 1001 STATION	1005 STATION	307 35 44.15000	.70000
12 1002 STATION	1001 STATION	0 0 0.00000	.70000
12 1002 STATION	1005 STATION	89 7 46.95000	.70000
12 1002 STATION	1003 STATION	168 56 24.90000	.70000
12 1002 STATION	NO SUCH MOUNTAIN	324 56 2.00000	.70000
12 1003 STATION	1002 STATION	0 0 0.00000	.70000
12 1003 STATION	1005 STATION	47 52 52.20000	.70000
12 1003 STATION	1006 STATION	87 51 43.81000	.70000
12 1004 STATION	1001 STATION	0 0 0.00000	.70000
12 1004 STATION	1007 STATION	165 1 48.21000	.70000
12 1004 STATION	1005 STATION	257 41 6.38000	.70000
12 1004 STATION	NO SUCH MOUNTAIN	340 48 40.00000	.70000
12 1005 STATION	1001 STATION	0 0 0.00000	.70000
12 1005 STATION	1004 STATION	43 45 22.67000	.70000
12 1005 STATION	1007 STATION	97 32 3.44000	.70000
12 1005 STATION	1008 STATION	137 6 52.31000	.70000
12 1005 STATION	1009 STATION	180 0 39.45000	.70000
12 1005 STATION	1006 STATION	223 47 36.15000	.70000
12 1005 STATION	1003 STATION	269 13 30.41000	.70000
12 1005 STATION	1002 STATION	321 32 4.11000	.70000
12 1006 STATION	1003 STATION	0 0 0.00000	.70000
12 1006 STATION	1005 STATION	94 35 13.50000	.70000
12 1006 STATION	1009 STATION	191 24 35.41000	.70000
12 1007 STATION	1004 STATION	0 0 0.00000	.70000

12 1007 STATION	1010 STATION	191 56 23.05000	.70000
12 1007 STATION	1011 STATION	235 3 54.67000	.70000
12 1007 STATION	1008 STATION	278 17 28.81000	.70000
12 1007 STATION	1005 STATION	326 26 1.39000	.70000
12 1008 STATION	1005 STATION	0 0 0.00000	.70000
12 1008 STATION	1007 STATION	92 16 37.74000	.70000
12 1008 STATION	1011 STATION	184 45 23.59000	.70000
12 1008 STATION	1009 STATION	269 24 40.25000	.70000
12 1009 STATION	1005 STATION	0 0 0.00000	.70000
12 1009 STATION	1008 STATION	46 30 55.20000	.70000
12 1009 STATION	1011 STATION	90 40 53.58000	.70000
12 1009 STATION	1012 STATION	127 56 .10000	.70000
12 1009 STATION	1006 STATION	320 36 12.55000	.70000
12 1010 STATION	1007 STATION	0 0 0.00000	.70000
12 1010 STATION	1013 STATION	170 12 55.49000	.70000
12 1010 STATION	1011 STATION	262 32 42.46000	.70000
12 1011 STATION	1007 STATION	0 0 0.00000	.70000
12 1011 STATION	1010 STATION	39 25 12.88000	.70000
12 1011 STATION	1013 STATION	89 4 44.90000	.70000
12 1011 STATION	1014 STATION	136 42 14.89000	.70000
12 1011 STATION	1015 STATION	173 27 34.71000	.70000
12 1011 STATION	1012 STATION	212 33 47.39000	.70000
12 1011 STATION	1009 STATION	264 31 31.23000	.70000
12 1011 STATION	1008 STATION	315 42 19.42000	.70000
12 1012 STATION	1009 STATION	0 0 0.00000	.70000
12 1012 STATION	1011 STATION	90 47 7.63000	.70000
12 1012 STATION	1015 STATION	199 30 15.18000	.70000
12 1013 STATION	1010 STATION	0 0 0.00000	.70000
12 1013 STATION	1016 STATION	181 29 32.08000	.70000
12 1013 STATION	1017 STATION	228 28 33.78000	.70000
12 1013 STATION	1014 STATION	273 33 42.81000	.70000
12 1013 STATION	1011 STATION	321 59 17.07000	.70000
12 1014 STATION	1011 STATION	0 0 0.00000	.70000
12 1014 STATION	1013 STATION	83 56 57.60000	.70000
12 1014 STATION	1017 STATION	172 24 26.66000	.70000
12 1014 STATION	1015 STATION	269 40 59.47000	.70000
12 1015 STATION	1011 STATION	0 0 0.00000	.70000
12 1015 STATION	1014 STATION	52 55 42.06000	.70000
12 1015 STATION	1017 STATION	100 35 .28000	.70000
12 1015 STATION	1018 STATION	144 36 30.28000	.70000
12 1015 STATION	1012 STATION	327 49 16.76000	.70000
12 1016 STATION	1013 STATION	0 0 0.00000	.70000
12 1016 STATION	1017 STATION	273 49 41.47000	.70000
12 1017 STATION	1013 STATION	0 0 0.00000	.70000
12 1017 STATION	1016 STATION	46 50 42.45000	.70000
12 1017 STATION	1018 STATION	231 49 22.16000	.70000
12 1017 STATION	1015 STATION	278 28 27.94000	.70000
12 1017 STATION	1014 STATION	313 32 37.58000	.70000
12 1018 STATION	1015 STATION	0 0 0.00000	.70000
12 1018 STATION	1017 STATION	89 19 25.16000	.70000

*

* DISTANCE OBSERVATIONS

*

```

52Y  0.0 2.0      .0 .0          DISSCAL
2Y 1003 STATION      1002 STATION      27464.39500 5.492879
2Y 1006 STATION      1005 STATION      22020.80400 4.404168
2Y 1009 STATION      1008 STATION      23448.91400 4.689782
2Y 1012 STATION      1011 STATION      18140.43400 3.628086
2Y 1015 STATION      1014 STATION      19305.54400 3.861108
2Y 1018 STATION      1017 STATION      23165.24100 4.633048
*
* AZIMUTH OBSERVATIONS
*
53B 1.0
3B 1005 STATION      1004 STATION      175 51 33.33000 1.00000
3B 1010 STATION      1014 STATION      311 5 55.59000 1.00000
3B 1015 STATION      1014 STATION      184 17 23.14000 1.00000
*
* DOPPLER POSITION OBSERVATIONS
*
953dcDOPPLER POSITION OBSERVATIONS
92 1001 STATION      -55.64 -5530068.70 3171200.3400
92 1003 STATION      -1497.17 -5506232.99 3212211.510
92 1005 STATION      -24110.43 -5519043.83 3190045.920
92 1009 STATION      -49612.74 -5507343.03 3210029.190
92 1010 STATION      -69214.24 -5528784.75 3172735.750
92 1014 STATION      -95655.96 -5516780.82 3192779.730
92 1016 STATION      -120827.22 -5529963.78 3169482.250
92 1018 STATION      -118126.76 -5505349.97 3211543.350
943dcDOPXF
97POVDIAGONAL
98 0.01      0.01      0.01
98 0.01      0.01      0.01
98 0.01      0.01      0.01
98 0.01      0.01      0.01
98 0.01      0.01      0.01
98 0.01      0.01      0.01
98 0.01      0.01      0.01
98 0.01      0.01      0.01
98 0.01      0.01      0.01
*
* VLBI POSITION DIFFERENCE OBSERVATIONS
*
913ddVLBI POSITION DIFFERENCE OBSERVATIONS
92 1001 STATION      0.00 -5530065.28 3171180.470
92 1009 STATION      -49557.16 -5507340.00 3210009.750
92 1010 STATION      -69158.69 -5528781.74 3172716.390
92 1018 STATION      -118070.97 -5505347.69 3211524.130
97PDVUPPER
98 0.25E-4      0.20E-5      0.0
98 0.0      -0.40E-5      0.0
98 0.0      0.0      0.0
98 0.16E-4      0.0      -0.12E-5
98 -0.16E-5      0.0      0.0
98 0.0      -0.40E-5
98 0.90E-5      0.0      0.0
98 0.0      0.15E-5      0.15E-5
98 0.0

```

```

98 0.90E-5      0.0      0.0
98 0.15E-5      0.0      0.0
98 0.16E-4     -0.20E-5    -0.40E-5
98 0.0          0.0
98 0.25E-4      0.0      0.0
98 0.0
98 0.25E-4      0.0      0.0
98 0.25E-4      0.25E-5
98 0.25E-4
*
* GPS POSITION DIFFERENCE OBSERVATIONS
*
913ddGPS POSITION DIFFERENCE OBSERVATIONS
92 1010 STATION      -69251.20   -5528758.12  3172774.76
92 1013 STATION      -95267.38   -5529349.94  3170743.46
92 1014 STATION      -95692.56   -5516753.96  3192818.800
92 1016 STATION      -120864.08  -5529936.89  3169521.400
943ddGPSXF
97PDVDIAGONAL
98 1.0E-4          1.E-4      2.25E-4
98 1.0E-4          0.64E-4    1.0E-4
98 1.0E-4          1.0E-4     1.0E-4
99

```

Table 7.3 NETAN listing of reliability analysis results for simulated 3D HOACS network.

```

-----
NETAN: Network Analysis (Version 21 Nov 90)
Network Strength Analysis
-----

Piece-Wise Linear Approximation -- Connected Stations

Input network data file : []
(NETAN) TEST HOACS GHOST TERRESTRIAL DATA

Station   Name
          Lat (DMS), Long (DMS), Ht (m)
          Strength in Rotation: Lat/Lon, Lat/Ht, Lon/Ht (rad)
          Obs # and Type
          Strength in Shear: Lat/Lon, Lat/Ht, Lon/Ht (strain)
          Obs # and Type
          Strength in Scale: (strain)
          Obs # and Type

1  NO SUCH M   MOUNTAIN
   30 4 59.849800 -89 54 59.736034      3500.000000
   -0.8026581412E-05 0.0000000000E+00 0.0000000000E+00
     8 dir      0      0
   0.1091513284E-04 0.0000000000E+00 0.0000000000E+00
     8 dir      0      0
   0.9239484003E-05
     114 pos

2  1001 STAT   TION
   29 59 59.851957 -89 59 59.734301      1966.254360
   -0.2388609726E-05 0.0000000000E+00 0.0000000000E+00
     111 pos    0      0
   0.3112551925E-05 0.0000000000E+00 0.0000000000E+00
     114 pos    0      0
   0.3395127742E-05
     90 dpos

3  1002 STAT   TION
   30 10 53.849676 -89 58 58.732088      2174.420000
   -0.5816950042E-05 0.0000000000E+00 0.0000000000E+00
     8 dir      0      0
   0.7489362239E-05 0.0000000000E+00 0.0000000000E+00
     8 dir      0      0
   0.9625842198E-05
     90 dpos

4  1003 STAT   TION
   30 25 39.851202 -90 0 53.729260      2006.840615
   -0.5517790657E-05 0.0000000000E+00 0.0000000000E+00

```



```

    111 pos      0      0
0.4320969610E-05 0.0000000000E+00 0.0000000000E+00
    90 dpos      0      0
0.1044322603E-04
    90 dpos

5 1004 STAT TION
    30 1 46.853908 -90 14 8.733804 2024.990000
-0.4193263814E-05 0.0000000000E+00 0.0000000000E+00
    111 pos      0      0
0.5046679535E-05 0.0000000000E+00 0.0000000000E+00
    8 dir      0      0
0.4409285201E-05
    90 dpos

6 1005 STAT TION
    30 11 47.852079 -90 14 58.732385 1924.276268
-0.4299814151E-05 0.0000000000E+00 0.0000000000E+00
    111 pos      0      0
0.2644233588E-05 0.0000000000E+00 0.0000000000E+00
    111 pos      0      0
0.5075764374E-05
    90 dpos

7 1006 STAT TION
    30 23 40.852787 -90 15 57.734057 2212.980000
-0.4911522032E-05 0.0000000000E+00 0.0000000000E+00
    111 pos      0      0
0.5689289749E-05 0.0000000000E+00 0.0000000000E+00
    90 dpos      0      0
0.6913426577E-05
    90 dpos

8 1007 STAT TION
    30 0 1.854932 -90 30 51.730790 1946.620000
-0.1625908368E-05 0.0000000000E+00 0.0000000000E+00
    44 dir      0      0
0.2272408046E-05 0.0000000000E+00 0.0000000000E+00
    31 dir      0      0
-0.6314001371E-05
    114 pos

9 1008 STAT TION
    30 11 35.852757 -90 30 32.729836 2085.430000
-0.2329687269E-05 0.0000000000E+00 0.0000000000E+00
    44 dir      0      0
0.2080895605E-05 0.0000000000E+00 0.0000000000E+00
    96 dpos      0      0
-0.6123746780E-05
    114 pos

10 1009 STAT TION
    30 24 16.851410 -90 30 55.730357 2051.734562
-0.4319115962E-05 0.0000000000E+00 0.0000000000E+00

```

	111 pos	0	0	
	0.3635786501E-05	0.0000000000E+00	0.0000000000E+00	
	114 pos	0	0	
	0.4993779365E-05			
	111 pos			
11	1010 STAT TION			
	30 0 56.853268	-90 42 59.731058	1997.382402	
	-0.4370081402E-05	0.0000000000E+00	0.0000000000E+00	
	117 pos	0	0	
	0.7321804042E-05	0.0000000000E+00	0.0000000000E+00	
	123 pos	0	0	
	0.5585010897E-05			
	123 pos			
12	1011 STAT TION			
	30 12 20.852495	-90 43 34.725644	1964.020000	
	-0.4090951484E-05	0.0000000000E+00	0.0000000000E+00	
	117 pos	0	0	
	0.2837360333E-05	0.0000000000E+00	0.0000000000E+00	
	123 pos	0	0	
	0.4395271148E-05			
	111 pos			
13	1012 STAT TION			
	30 22 1.852968	-90 45 25.723984	1883.560000	
	-0.3485735196E-05	0.0000000000E+00	0.0000000000E+00	
	117 pos	0	0	
	0.6204770709E-05	0.0000000000E+00	0.0000000000E+00	
	111 pos	0	0	
	0.5532237335E-05			
	111 pos			
14	1013 STAT TION			
	29 59 43.854453	-90 59 9.729649	1829.087482	
	-0.7154654314E-05	0.0000000000E+00	0.0000000000E+00	
	117 pos	0	0	
	0.7849933001E-05	0.0000000000E+00	0.0000000000E+00	
	123 pos	0	0	
	0.5357576345E-05			
	123 pos			
15	1014 STAT TION			
	30 13 28.853227	-90 59 33.729039	2015.332708	
	-0.7117499833E-05	0.0000000000E+00	0.0000000000E+00	
	117 pos	0	0	
	0.3786634816E-05	0.0000000000E+00	0.0000000000E+00	
	123 pos	0	0	
	-0.3498957363E-05			
	105 dpos			
16	1015 STAT TION			
	30 23 53.852800	-90 58 39.727600	1959.240000	
	-0.8411430126E-05	0.0000000000E+00	0.0000000000E+00	

	117 pos	0	0	
	0.3517979138E-05	0.0000000000E+00	0.0000000000E+00	
	114 pos	0	0	
	0.3743625715E-05			
	90 dpos			
17	1016 STAT TION			
	29 58 51.854512	-91 15 3.728499	2159.675769	
	-0.8032074231E-05	0.0000000000E+00	0.0000000000E+00	
	117 pos	0	0	
	0.1062148367E-04	0.0000000000E+00	0.0000000000E+00	
	123 pos	0	0	
	-0.7689695578E-05			
	105 dpos			
18	1017 STAT TION			
	30 12 45.855024	-91 15 0.725979	2080.350000	
	-0.9132876044E-05	0.0000000000E+00	0.0000000000E+00	
	117 pos	0	0	
	0.4900893724E-05	0.0000000000E+00	0.0000000000E+00	
	126 pos	0	0	
	-0.5868983027E-05			
	126 pos			
19	1018 STAT TION			
	30 25 14.852635	-91 13 42.726788	1999.590054	
	-0.6260417822E-05	0.0000000000E+00	0.0000000000E+00	
	117 pos	0	0	
	0.3538720212E-05	0.0000000000E+00	0.0000000000E+00	
	126 pos	0	0	
	0.3535383204E-05			
	90 dpos			

7.3 Real 2D Network

A real 2D network was obtained from the Canadian Geodetic Survey for an area in Québec along the south shore of the St. Lawrence River. The network consists of a total of 58 stations. Only one point is fixed and a single azimuth observation is used to control the datum orientation. The network consists of the following observations:

- 125 distance observations with standard deviations ranging from 1 cm + 2 ppm to 6 cm + 6 ppm (most around 3 cm + 3 ppm)
- 307 direction observations with standard deviations ranging from 0.6 to 2.0 seconds (most around 0.7 seconds)
- 1 azimuth observation with a standard deviation of 0.8 seconds.

Figures 7.9 to 7.11 illustrate the locations of the stations and the different types of observations. Table 7.5 gives a listing of the input GHOST data file for this network.

The results from the NETAN robustness analysis are displayed in terms of robustness in rotation (local twisting), robustness in shear (local changes in configuration or shape), and robustness in scale in Figures 7.12, 7.13, and 7.14, respectively. The NETAN output listing for this analysis is given in Table 7.6. These robustness results are all based on $\alpha_0=5\%$ and $\beta_0=5\%$ which gives a non-centrality parameter of $\sqrt{\lambda_0}=3.61$ (the standardized value of maximum undetectable error). Different α_0 and β_0 result in a different $\sqrt{\lambda_0}$ which only scales the magnitude of the strength parameters by the ratio of the non-centrality parameters. The plots are otherwise identical.

The results indicate that the weakest point in the network is at station HEMMING where the differential rotation is 33 μ rad, shear is 39 ppm, and dilation is 21 ppm. These relatively large deformations, however, are actually a result of a weakness in the determination of the strain primitives rather than a weakness in the network itself. The points connected to this station are nearly collinear which makes the fitting of a plane surface to these points ill-conditioned for the determination of the strain elements. This problem with the determination of strain has already been pointed out by Craymer et al. [1989]. It may be possible to detect

such ill-conditioning by computing the determinant of the matrix of normal equations for the determination of the strain elements. On the other hand, it would be more useful in general to compute standard deviations for the strain primitives and test them for statistical significance. Station HEMMING will therefore not be considered further in the following discussion of the results.

A number of points were found to be uniquely determined by a minimum number of observations. These observations were omitted from the robustness analysis since their redundancy numbers are zero resulting in infinitely large maximum undetectable errors. The robustness parameters for these points have been set to zero in the output listing. As discussed in the previous chapter, it is recommended to include these observations and points in the next version of NETAN by setting their maximum undetectable errors to a very large number (say, 0.33E33) so that they will show up as very large weaknesses in the contour plots of the robustness parameters.

The single azimuth controlling the datum orientation was also omitted from the analysis since its redundancy number was very small. This would give a very large maximum undetectable error that would overwhelm the robustness analysis. As discussed in the previous chapter, we also recommend that in a future version of NETAN these observations be included in the robustness analysis so that the weakness in datum definition would be evident as large robustness parameters in the contour plots.

The results indicate that the north part of the network is relatively weaker than the south part. Table 7.4 summarizes the range of values, the largest and smallest (absolute) values in magnitude, and the average and standard deviation for each robustness parameter. Note again that the average and standard deviations of these parameters are all of the same magnitude as the relative accuracy of the observations. Values less than about 10 ppm are therefore probably not very statistically significant. The only obviously common feature to most of these weak points is the lack of direction observations emanating from them. Although it seems reasonable

that this may have a detrimental effect on differential rotation and shear, it is not clear why this would also cause relatively large dilations.

Table 7.4 Summary of robustness results for the real network.

	Robustness in rotation (μrad)	Robustness in shear (ppm)	Robustness in scale (ppm)
Maximum	16.2	38.7	22.5
Minimum	-19.8	0.6	-4.2
Largest absolute	-19.8	38.7	22.5
Smallest absolute	1.8	0.6	0.7

The robustness in rotation results are illustrated in Figure 7.12 and listed in Table 7.6. These results describe the ability of the network to resist local changes in orientation (twisting). The largest values are obtained for station STRATFORD ($-19.8 \mu\text{rad}$ due to direction observation #228), station KINGSEY FALLS ($16.2 \mu\text{rad}$ due to distance observation #412), station ADSTOCK ($-12.3 \mu\text{rad}$ due to direction observation #151), station ARTHABASKA ($11.9 \mu\text{rad}$ due to distance observation #412), and station ST ZEPHIRIN ($-11.1 \mu\text{rad}$ due to distance observation #401). All these stations have relatively fewer observation ties connecting them to the rest of the network (generally only a few directions and distances at most). Note that these values are within first-order accuracy standards, however. The best (smallest absolute value) robustness in rotation is obtained for station ST ARMAND ($1.8 \mu\text{rad}$) which has many more observation ties (14 directions and 2 distances) than the weak points.

The robustness in shear results are given in Figure 7.13 and Table 7.6. These results describe the ability of the network to resist local deformations in configuration or shape. The largest values are obtained for station ST ZEPHIRIN (21.4 ppm due to distance observation #401), station STRATFORD (17.8 ppm due to direction observation #228), station ARTHABASKA (15.9 ppm due to distance observation #412), station VIANNEY (15.0 ppm due to distance observation #383), station KINGSEY FALLS (14.0 ppm due to distance observation #412), and station GILBERT (13.5 ppm due to position observation #123). All of

these points have relatively fewer observation ties connecting them to the rest of the network. With the exception of ST ZEPHIRIN, these values are also within first-order accuracy limits. The best (smallest absolute value) robustness in shear is obtained for station HEREFORD (0.6 ppm) which has many more observation ties (16 directions and 4 distances) than the weak points.

The robustness in scale results are given in Figure 7.14 and Table 7.6. These results describe the ability of the network to resist local deformations in scale (dilation). The largest values are obtained for station VIANNEY (22.5 ppm due to distance observation #383), station ARTHABASKA (18.0 ppm due to distance observation #412), station ST ZEPHIRIN (17.0 ppm due to distance observation #401), station STRATFORD (15.4 ppm due to distance observation #422), station ADSTOCK (12.9 ppm due to distance observation #395), and station KINGSEY FALLS (11.6 ppm due to direction observation #244). All of these points have relatively fewer observation ties connecting them to the rest of the network. With the exception of VIANNEY, these values are also within first-order accuracy limits. The best (smallest absolute value) robustness in scale is obtained for station SHERBROOKE (0.7 ppm) which has many more observation ties (18 directions and 9 distances) than the weak points.

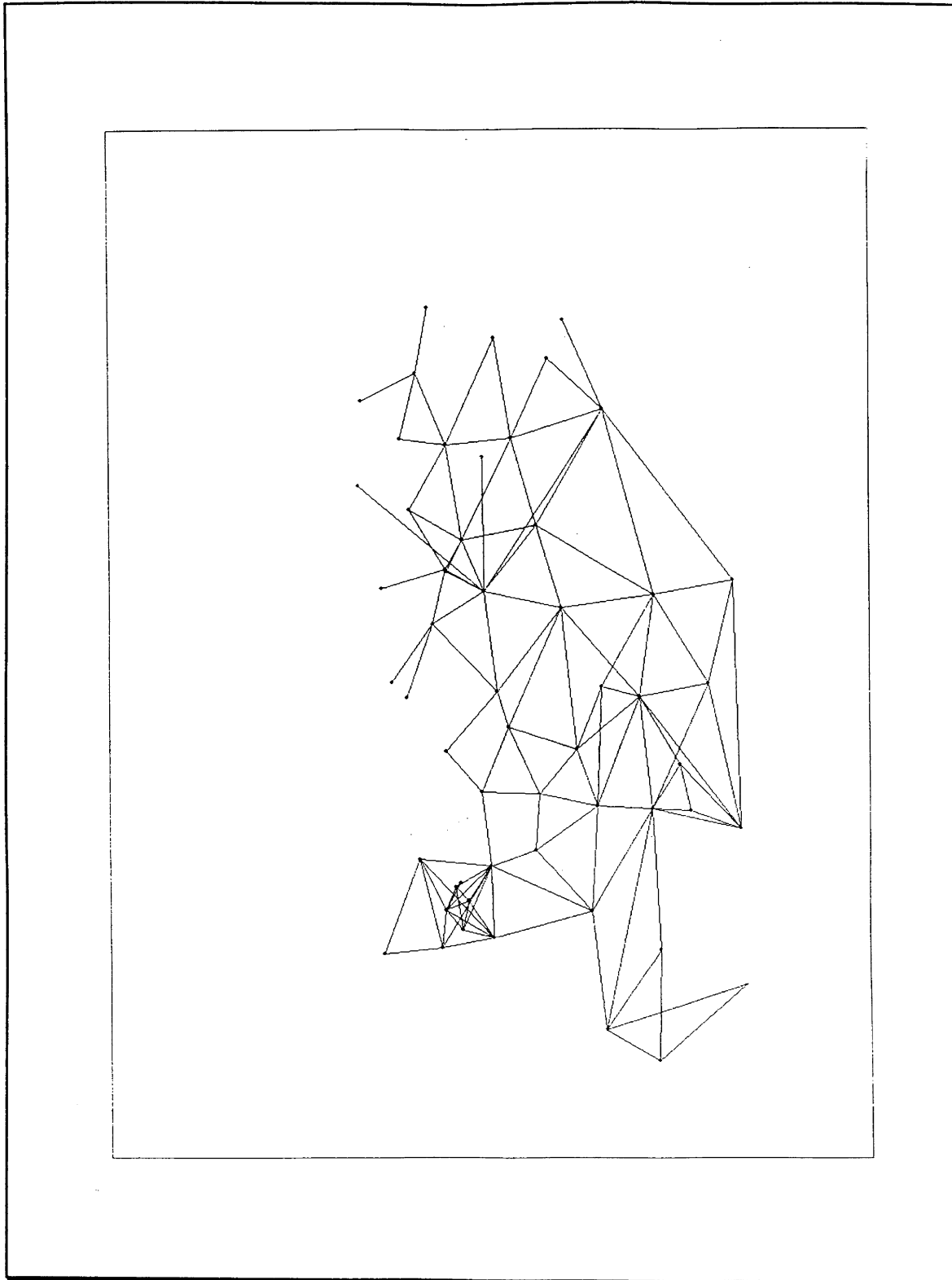


Figure 7.9 Distance observations for real 2D network.

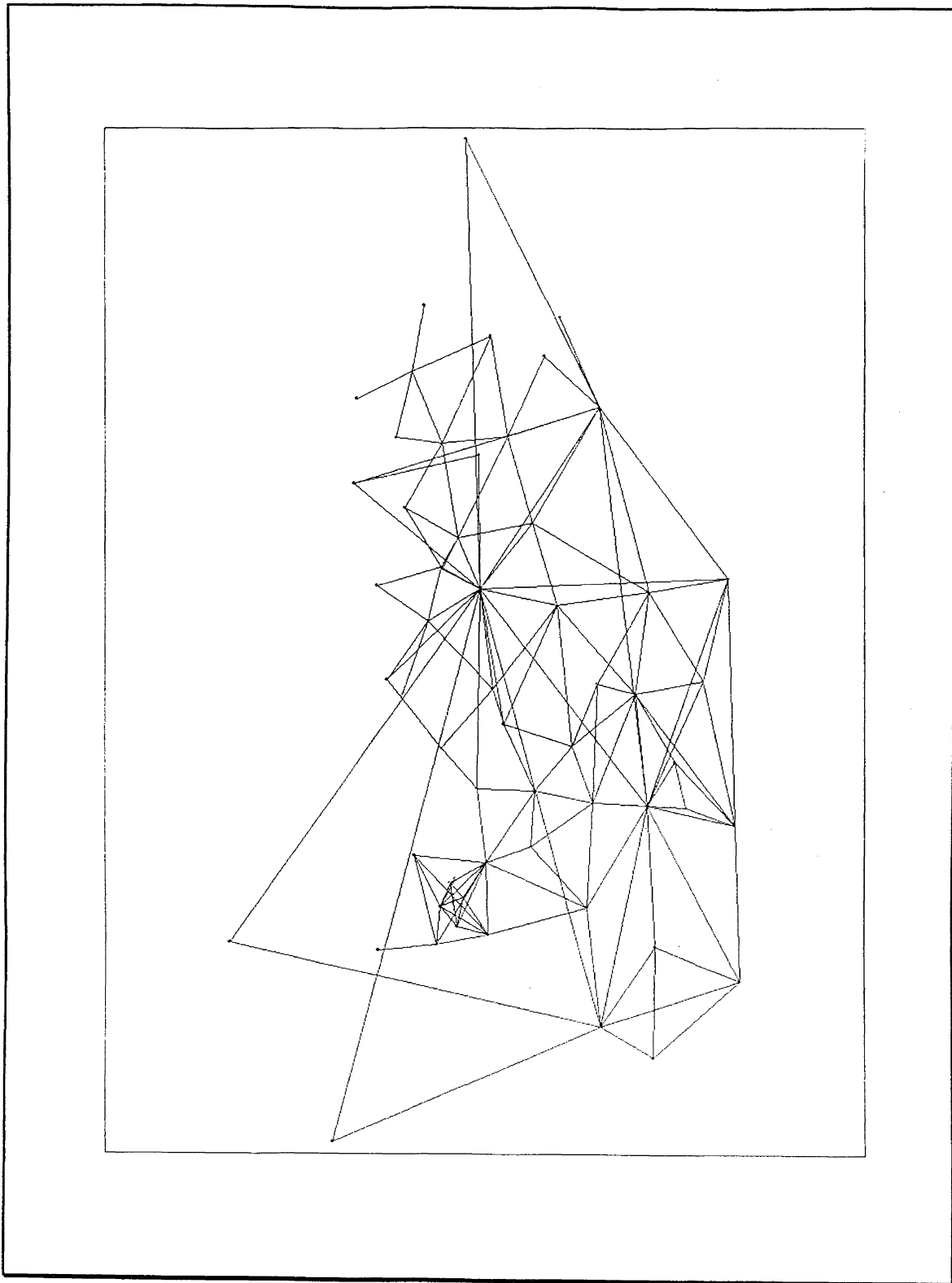


Figure 7.10 Direction observations for real 2D network.

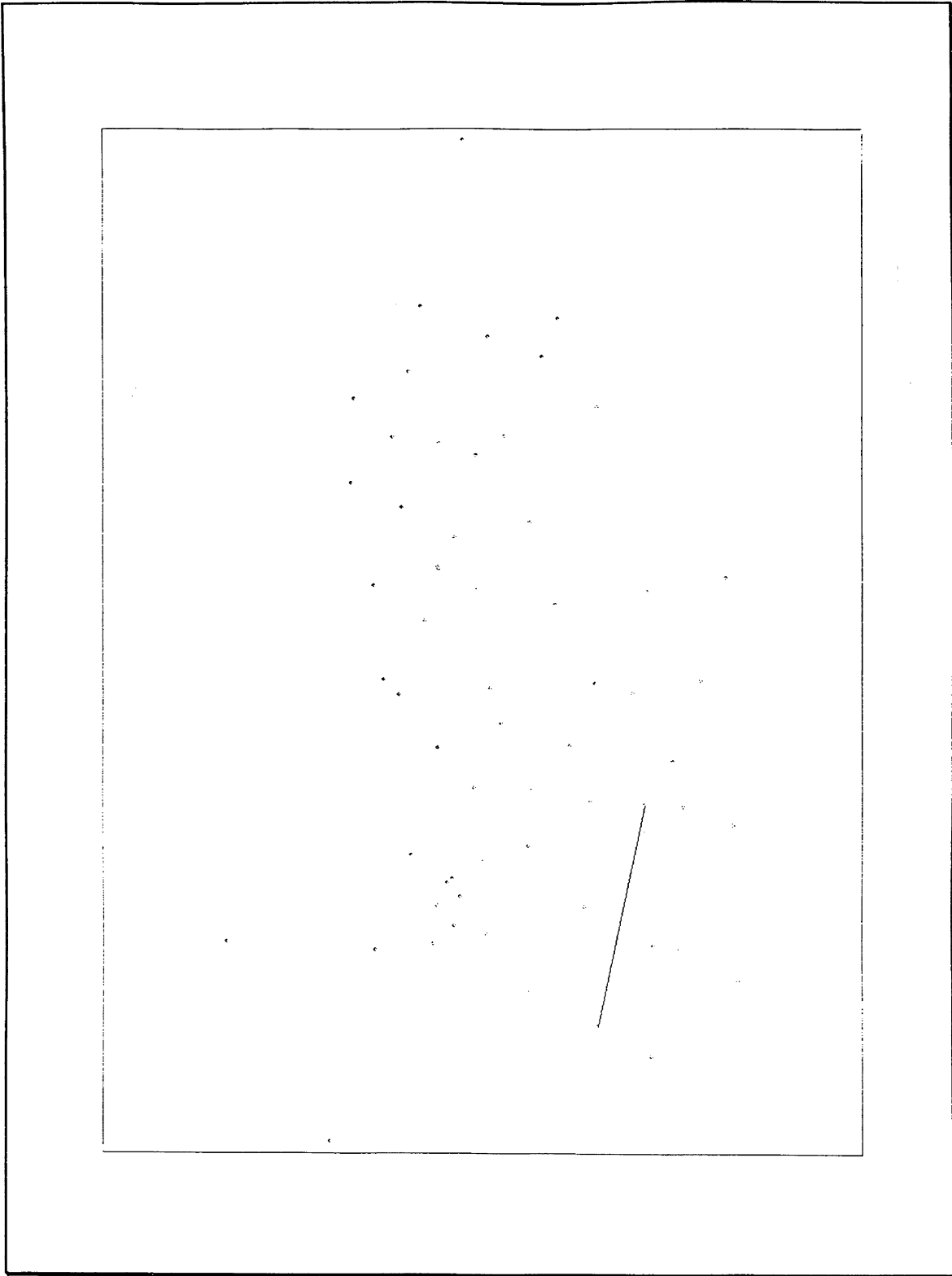


Figure 7.11 Azimuth observation for real 2D network.

Table 7.5 GHOST input data file for real 2D network.

Real 2D Network, Geodetic Survey of Canada. Sigma records commented out.

```

1 3 1 1 111
4 09206 ORFORD          N45 1843.080825W 72 1430.207541 851.9000
10
5 08200 ST ARMAND      N45 246.875283W 72 4420.977882 711.7200
5 09201 YAMASKA        N45 2645.375984W 72 52 8.649835 421.7800
4 652401 FARNHAM       N45 1743.910275W 72 5719.624866 77.9800
4 652402 BROMONT       N45 1721.079434W 72 3816.142978 552.8000
4 69K4238 DAIGLE       1 QLF N45 29 9.969288W 72 3138.846985 276.3000
5 712051 ST MAJORIQUE  1 QLF N45 5458.877438W 72 38 1.278776 82.9280
4 712056 WICKHAM       1 QLF N45 46 7.568544W 72 3621.113477 106.8230
4 08207 OWLS HEAD      N45 345.156706W 72 1752.895781 749.9000
5 09202 DUSABLE        1 274 N46 1237.122695W 73 1159.764446 135.9410
5 09204 CARMEL         1 173 N46 2958.646202W 72 3739.182006 188.6410
5 09205 HAM            N45 4728.148868W 71 38 .735368 711.7000
4 09207 HEREFORD       N45 457.209129W 71 36 3.594684 872.1000
4SBF 09208 MEGANTIC    N45 2651.257597W 71 713.0032151085.7875
5 09209 THETFORD       N46 848.515359W 71 2011.406728 694.0700
5 09210 LINIERE        N45 4945.092500W 70 2220.286423 776.0900
5 09216 ARTHABASKA    1 233 N46 314.110312W 71 5316.763943 350.2910
5 14200 STRATFORD     2 233 N45 4739.752238W 71 1520.012822 436.9000
5 65K0335 CROIX        N45 3346.481649W 70 5222.732410 490.8600
5 66KP115 CARIBOU E-15 1 164 N46 015.967744W 71 2410.058178 556.7000
4 68K2071 SHERBROOKE   N45 2046.261393W 71 5533.821339 440.3000
4 68K2073 BEAUVOIR    1 164 N45 2717.104197W 71 5353.741152 307.9000
5 692009 HONORE        N45 5653.160925W 70 5016.132369 474.3400
5 692010 GRELOTS       1 172 N45 59 2.193228W 71 121.630665 408.7890
5 692011 BROUGHTON    1 172 N46 817.581129W 71 549.572672 608.5880
5 692012 ADSTOCK       1 164 N46 146.972910W 71 1218.355831 713.1880
4 69K4239 DUSSAULT     1 164 N45 28 4.320930W 72 1351.756838 430.8000
4 69K4240 GALLUP HILL  1 164 N45 38 6.700659W 72 1157.248631 348.2000
4 69K4241 SOUTH DURHAM 1 164 N45 3848.371625W 72 2126.889288 208.8100
4 69K4242 PINNACLE    1 QLF N45 4321.445932W 72 041.591747 416.4000
4 69K4243 LAROCHELLE  1 164 N45 3143.227349W 72 423.551476 333.1000
4 69K4346 CHARLES     1 163 N45 5234.275759W 72 2739.825309 93.3900
4 69K4348 LEMAIRE     1 163 N45 5123.415278W 72 3452.384059 93.5300
4 69K4349 BREBOEUF    1 163 N45 5020.787836W 72 2959.667450 89.2000
4 69K4350 HEMMING     2 163 N45 5146.549886W 72 27 .762848 115.3700
4 70K4244 MAGOG        N45 1357.376894W 72 7 2.330626 345.0000
4 70K4245 AUSTIN       N45 12 7.761103W 72 1445.003137 318.3000
4 70K4631 HATLEY       N45 9 8.355020W 71 5318.368308 423.0000
4 70K4632 MARTIN       N45 1823.800369W 71 3831.348936 423.1000
4 70K4633 CHAPMAN     1 164 N45 3416.980871W 71 4044.156151 658.4000
4 70K4634 ASBESTOS    1 QLF N45 4516.870156W 71 5442.774960 338.1000
4 70K4635 WEEDON      N45 3832.841031W 71 2642.205826 413.6000
5 70K4637 GILBERT     N45 3621.022836W 70 5844.386984 570.8000
5 70K4638 COULOMBE    1 QLF N45 5112.412896W 71 2919.000750 465.8000
4 70K4639 MOISAN      4 164 N45 5356.869207W 71 3435.946548 597.5000
5 712050 BON CONSEIL  1 174 N45 5840.686135W 72 2258.068549 121.2210
5 712053 ST ZEPHIRIN  1 174 N46 447.587703W 72 39 2.801747 55.2430
4 712055 MALLARD      1 QLF N45 4628.674715W 72 24 5.669217 171.4480

```

4	712057	DRUMMOND	1	174 N45	5416.673859W	72	3135.417580	93.6700
5	71K6154	STORNOWAY		N45	4245.378012W	71	1213.496977	510.0000
5	71K6155	STE PRAXEDE	1	164 N45	5351.210905W	71	1323.129308	391.4000
5	71K6156	SEBASTIEN		N45	4536.557799W	70	5519.545890	825.7000
5	71K6159	LAPOINTE	1	QLF N45	54 6.371447W	71	3414.951193	627.8000
5	71K6165	VIANNEY	1	QLF N46	452.995542W	71	3730.212463	592.3000
5	72K7455	VICTORIAVILLE	1	QLF N46	041.609238W	71	5546.742907	274.7530
5	72K7457	SEVIGNY	1	QLF N45	5613.677425W	71	4317.715169	528.2000
5	72K7462	KINGSEY FALLS	1	QLF N45	54 5.083744W	72	440.296902	154.5000
5	72K7463	ST FELIX	1	QLF N45	4758.866518W	72	1128.912506	209.6000
7	36 09202	DUSABLE		274 N46	12 36.48	W 73	12 01.40	135.9
7	71 09206	ORFORD		233 N45	18 39.31	W 72	14 30.93	838.
7	72 09208	MEGANTIC		233 N45	26 52.92	W 71	07 14.60	1082.
7	38 09216	ARTHABASKA		233 N46	03 26.01	W 71	53 35.16	350.291
7	72 692009	HONORE		164 N45	56 57.00	W 70	50 18.42	474.3
7	72 69K4241	SOUTH DURHAM		163 N45	38 53.69	W 72	21 41.72	206.9
7	72 712057	DRUMMOND		174 N45	54 25.52	W 72	31 50.58	93.7
9	08200	ST ARMAND	MAIN1.3	4.33		-10.02		-28.38
9	08207	OWLS HEAD	MAIN1.3	-1.11		1.25		-27.64
9	09201	YAMASKA	MAIN1.3	2.30		-8.89		-29.49
9	09202	DUSABLE	GEM10B1	1.22		-4.18		-31.16
9	09204	CARMEL	GEM10B1	1.45		-4.06		-30.02
9	09205	HAM	MAIN1.3	-2.39		-2.41		-27.72
9	09206	ORFORD	MAIN1.4	-3.12		-.48		-27.99
9	09207	HEREFORD	MAIN1.3	-.74		-5.85		-26.57
9	09208	MEGANTIC	MAIN1.3	3.21		-3.41		-26.32
9	09209	THETFORD	MAIN1.3	4.08		-.49		-27.50
9	09210	LINIERE	MAIN1.3	5.49		-8.74		-25.80
9	09216	ARTHABASKA	GEM10B2	1.05		-3.77		-28.56
9	14200	STRATFORD	GEM10B2	.73		-3.46		-27.03
9	652401	FARNHAM	MAIN1.3	1.91		-6.72		-29.28
9	652402	BROMONT	MAIN1.3	1.22		-12.62		-28.71
9	65K0335	CROIX	MAIN1.3	2.05		-4.21		-26.14
9	66KP115	CARIBOU E-15	GEM10B2	.97		-3.56		-27.54
9	68K2073	BEAUVOIR	GEM10B2	.40		-3.67		-27.60
9	692009	HONORE	GEM10B2	.87		-3.28		-26.57
9	692010	GRELOTS	MAIN1.3	.98		.87		-26.88
9	692011	BROUGHTON	GEM10B2	1.09		-3.44		-27.09
9	692012	ADSTOCK	MAIN1.3	-1.44		3.70		-27.21
9	68K2071	SHERBROOKE	GEM10B2	.27		-3.65		-27.45
9	69K4238	DAIGLE	GEM10B2	.50		-3.90		-28.95
9	69K4239	DUSSAULT	MAIN1.3	-1.05		.29		-28.30
9	69K4240	GALLUP HILL	GEM10B1	.63		-3.82		-28.61
9	69K4241	SOUTH DURHAM	GEM10B2	.66		-3.88		-28.97
9	69K4242	PINNACLE	GEM10B2	.71		-3.77		-28.39
9	69K4243	LAROCHELLE	GEM10B2	.50		-3.75		-28.11
9	69K4346	CHARLES	GEM10B1	.90		-3.95		-29.62
9	69K4348	LEMAIRE	GEM10B0	.89		-3.99		-29.83
9	69K4349	BREBOEUF	GEM10B0	.87		-3.96		-29.64
9	69K4350	HEMMING	GEM10B1	.89		-3.95		-29.57
9	70K4244	MAGOG	MAIN1.4	-2.76		-.19		-27.60
9	70K4245	AUSTIN	MAIN1.4	-2.62		.52		-27.78
9	70K4631	HATLEY	GEM10B2	.04		-3.59		-27.06
9	70K4632	MARTIN	GEM10B2	.19		-3.52		-26.88

9	70K4633	CHAPMAN	MAIN1.3	-3.42	-1.45	-27.41
9	70K4634	ASBESTOS	GEM10B2	.74	-3.74	-28.23
9	70K4635	WEEDON	GEM10B2	.57	-3.51	-27.12
9	70K4637	GILBERT	MAIN1.3	1.97	-2.60	-26.34
9	70K4638	COULOMBE	MAIN1.3	-3.47	.35	-27.53
9	70K4639	MOISAN	MAIN1.4	-3.03	-1.74	-27.76
9	712050	BON CONSEIL	GEM10B0	1.00	-3.94	-29.59
9	712051	ST MAJORIQUE	GEM10B0	.95	-4.01	-30.02
9	712053	ST ZEPHIRIN	GEM10B0	1.10	-4.04	-30.22
9	712055	MALLARD	GEM10B0	.80	-3.92	-29.32
9	712056	WICKHAM	GEM10B0	.80	-3.98	-29.72
9	712057	DRUMMOND	GEM10B0	.93	-3.98	-29.79
9	71K6154	STORNOWAY	GEM10B2	.63	-3.42	-26.83
9	71K6155	STE PRAEDE	MAIN1.3	-1.41	1.24	-27.11
9	71K6156	SEBASTIEN	MAIN1.3	2.48	-2.42	-26.47
9	71K6159	LAPOINTE	MAIN1.4	-2.99	-1.67	-27.76
9	71K6165	VIANNEY	MAIN1.3	5.99	-4.28	-28.02
9	72K7455	VICTORIAVILLE	GEM10B1	1.01	-3.79	-28.62
9	72K7457	SEVIGNY	GEM10B2	.92	-3.69	-28.10
9	72K7462	KINGSEY FALLS	GEM10B1	.90	-3.83	-28.83
9	72K7463	ST FELIX	GEM10B1	.81	-3.85	-28.92

*

* Observations

*

40

* 51F16 0.85 0.0 0.01969 .20 .20G-213 QLF

1	69K4238	DAIGLE	712056	WICKHAM	0 0 0.00000	.850
1	69K4238	DAIGLE	712055	MALLARD	27 57 34.93000	.850
1	69K4238	DAIGLE	69K4241	SOUTH DURHAM	47 32 33.13000	.850
1	69K4241	SOUTH DURHAM	69K4238	DAIGLE	0 0 0.00000	.850
1	69K4241	SOUTH DURHAM	712055	MALLARD	129 45 4.61000	.851
1	712056	WICKHAM	69K4348	LEMAIRE	0 0 0.00000	.852
1	712056	WICKHAM	69K4349	BREBOEUF	35 21 4.54000	.852
1	712056	WICKHAM	712055	MALLARD	76 28 25.74000	.851
1	712056	WICKHAM	69K4238	DAIGLE	157 51 13.81000	.850
1	712055	MALLARD	69K4241	SOUTH DURHAM	0 0 0.00000	.851
1	712055	MALLARD	69K4238	DAIGLE	30 39 56.09000	.850
1	712055	MALLARD	712056	WICKHAM	101 19 33.90000	.851
1	712055	MALLARD	69K4348	LEMAIRE	136 45 37.08000	.851
1	712055	MALLARD	69K4349	BREBOEUF	146 47 25.39000	.852
1	712055	MALLARD	69K4346	CHARLES	171 21 7.70000	.851
1	69K4350	HEMMING	69K4346	CHARLES	0 0 0.00000	.917
1	69K4350	HEMMING	712057	DRUMMOND	337 49 51.27000	.854
1	712057	DRUMMOND	69K4346	CHARLES	0 0 0.00000	.856
1	712057	DRUMMOND	69K4350	HEMMING	6 8 43.91000	.854
1	712057	DRUMMOND	69K4349	BREBOEUF	42 17 1.97000	.853
1	712057	DRUMMOND	69K4348	LEMAIRE	96 35 36.40000	.854
1	69K4348	LEMAIRE	712057	DRUMMOND	0 0 0.00000	.854
1	69K4348	LEMAIRE	69K4346	CHARLES	38 19 48.12000	.852
1	69K4348	LEMAIRE	69K4349	BREBOEUF	68 33 46.39000	.855
1	69K4348	LEMAIRE	712055	MALLARD	84 36 03.20000	.851
1	69K4348	LEMAIRE	712056	WICKHAM	152 41 34.08000	.852
1	69K4349	BREBOEUF	712055	MALLARD	0 0 0.00000	.852
1	69K4349	BREBOEUF	69K4348	LEMAIRE	153 55 56.77000	.855

1	69K4349 BREBOEUF	712057 DRUMMOND	211 3 36.34000	.853
1	69K4349 BREBOEUF	69K4346 CHARLES	263 4 13.69000	.858
1	69K4346 CHARLES	69K4349 BREBOEUF	0 0 0.00000	.858
1	69K4346 CHARLES	69K4348 LEMAIRE	40 37 44.90000	.852
1	69K4346 CHARLES	712057 DRUMMOND	85 42 19.22000	.856
1	69K4346 CHARLES	69K4350 HEMMING	294 1 10.24000	.917
1	69K4346 CHARLES	712055 MALLARD	301 29 29.62000	.851
*	51F17 .70 0.0 0.01971	.20 .20FORGUESRL GEOD		
1	712057 DRUMMOND	712055 MALLARD	0 0 0.00000	.701
1	712057 DRUMMOND	712056 WICKHAM	56 10 20.86000	.701
1	712055 MALLARD	712056 WICKHAM	0 0 0.00000	.701
1	712055 MALLARD	712057 DRUMMOND	58 25 52.51000	.701
1	712056 WICKHAM	712055 MALLARD	0 0 0.00000	.701
1	712056 WICKHAM	712057 DRUMMOND	294 36 9.46000	.701
*	51F18 .70 0.0 0.06971	.20 .20G-252 QLF		
1	09201 YAMASKA	69K4238 DAIGLE	0 0 0.00000	.700
1	09201 YAMASKA	09206 ORFORD	26 14 32.07000	.700
1	69K4238 DAIGLE	69K4241 SOUTH DURHAM	0 0 0.00000	.700
1	69K4238 DAIGLE	69K4239 DUSSAULT	58 20 6.87000	.700
1	69K4238 DAIGLE	09206 ORFORD	94 12 10.59000	.700
1	69K4238 DAIGLE	09201 YAMASKA	224 4 44.22000	.700
1	09206 ORFORD	09201 YAMASKA	0 0 0.00000	.700
1	09206 ORFORD	69K4238 DAIGLE	23 52 57.48000	.700
1	09206 ORFORD	69K4239 DUSSAULT	75 40 44.35000	.701
1	09206 ORFORD	68K2071 SHERBROOKE	154 4 12.77000	.700
1	09206 ORFORD	70K4631 HATLEY	195 23 38.11000	.700
1	09206 ORFORD	70K4244 MAGOG	204 58 14.12000	.701
1	09206 ORFORD	70K4245 AUSTIN	254 26 4.14000	.702
1	09206 ORFORD	08207 OWLS HEAD	262 0 29.83000	.700
1	69K4241 SOUTH DURHAM	69K4240 GALLUP HILL	0 0 0.00000	.702
1	69K4241 SOUTH DURHAM	69K4239 DUSSAULT	57 39 21.24000	.700
1	69K4241 SOUTH DURHAM	69K4238 DAIGLE	120 46 53.20000	.700
1	69K4239 DUSSAULT	68K2071 SHERBROOKE	0 0 0.00000	.700
1	69K4239 DUSSAULT	09206 ORFORD	63 20 52.66000	.701
1	69K4239 DUSSAULT	69K4238 DAIGLE	155 41 2.20000	.700
1	69K4239 DUSSAULT	69K4241 SOUTH DURHAM	214 13 25.92000	.700
1	69K4239 DUSSAULT	69K4240 GALLUP HILL	248 10 34.54000	.701
1	69K4239 DUSSAULT	69K4243 LAROCHELLE	301 48 33.39000	.701
1	69K4239 DUSSAULT	68K2073 BEAUVOIR	333 40 3.05000	.700
1	69K4240 GALLUP HILL	69K4242 PINNACLE	0 0 0.00000	.701
1	69K4240 GALLUP HILL	69K4243 LAROCHELLE	83 54 31.06000	.701
1	69K4240 GALLUP HILL	69K4239 DUSSAULT	131 17 30.49000	.701
1	69K4240 GALLUP HILL	69K4241 SOUTH DURHAM	219 41 1.14000	.702
1	69K4242 PINNACLE	70K4634 ASBESTOS	0 0 0.00000	.703
1	69K4242 PINNACLE	70K4633 CHAPMAN	57 32 43.37000	.700
1	69K4242 PINNACLE	69K4243 LAROCHELLE	127 18 20.41000	.700
1	69K4242 PINNACLE	69K4240 GALLUP HILL	171 10 14.78000	.701
1	69K4243 LAROCHELLE	69K4242 PINNACLE	0 0 0.00000	.700
1	69K4243 LAROCHELLE	70K4633 CHAPMAN	68 32 34.91000	.700
1	69K4243 LAROCHELLE	68K2073 BEAUVOIR	108 22 53.91000	.701
1	69K4243 LAROCHELLE	68K2071 SHERBROOKE	137 48 47.34000	.700
1	69K4243 LAROCHELLE	69K4239 DUSSAULT	228 47 21.19000	.701
1	69K4243 LAROCHELLE	69K4240 GALLUP HILL	307 46 24.87000	.701
1	68K2073 BEAUVOIR	68K2071 SHERBROOKE	0 0 0.00000	.702

1	68K2073	BEAUVOIR	69K4239	DUSSAULT	83	5	20.51000	.700
1	68K2073	BEAUVOIR	69K4243	LAROCHELLE	110	49	24.26000	.701
1	68K2073	BEAUVOIR	70K4632	MARTIN	299	2	22.45000	.700
1	68K2071	SHERBROOKE	69K4243	LAROCHELLE	0	0	0.00000	.700
1	68K2071	SHERBROOKE	68K2073	BEAUVOIR	39	44	44.10000	.702
1	68K2071	SHERBROOKE	70K4633	CHAPMAN	67	7	11.58000	.700
1	68K2071	SHERBROOKE	70K4632	MARTIN	130	36	5.77000	.700
1	68K2071	SHERBROOKE	70K4631	HATLEY	201	42	34.67000	.701
1	68K2071	SHERBROOKE	08207	OWLS HEAD	252	29	39.97000	.700
1	68K2071	SHERBROOKE	70K4244	MAGOG	259	31	22.71000	.701
1	68K2071	SHERBROOKE	09206	ORFORD	290	54	20.21000	.700
1	68K2071	SHERBROOKE	69K4239	DUSSAULT	329	9	59.13000	.700
1	70K4244	MAGOG	08207	OWLS HEAD	0	0	0.00000	.700
1	70K4244	MAGOG	70K4245	AUSTIN	34	30	27.98000	.702
1	70K4244	MAGOG	09206	ORFORD	95	8	2.19000	.701
1	70K4244	MAGOG	68K2071	SHERBROOKE	192	51	3.39000	.701
1	70K4245	AUSTIN	08207	OWLS HEAD	0	0	0.00000	.701
1	70K4245	AUSTIN	09206	ORFORD	166	40	21.85000	.702
1	70K4245	AUSTIN	70K4244	MAGOG	236	34	57.11000	.702
1	70K4633	CHAPMAN	68K2071	SHERBROOKE	0	0	0.00000	.700
1	70K4633	CHAPMAN	69K4243	LAROCHELLE	43	36	38.24000	.700
1	70K4633	CHAPMAN	69K4242	PINNACLE	85	18	27.31000	.700
1	70K4633	CHAPMAN	70K4634	ASBESTOS	100	36	48.69000	.700
1	70K4633	CHAPMAN	09205	HAM	150	27	22.68000	.700
1	70K4633	CHAPMAN	70K4635	WEEDON	208	44	22.87000	.701
1	70K4633	CHAPMAN	70K4632	MARTIN	316	37	6.26000	.700
1	70K4632	MARTIN	70K4635	WEEDON	0	0	0.00000	.700
1	70K4632	MARTIN	09208	MEGANTIC	46	29	13.96000	.700
1	70K4632	MARTIN	09207	HEREFORD	150	15	5.41000	.700
1	70K4632	MARTIN	70K4631	HATLEY	206	11	12.76000	.700
1	70K4632	MARTIN	68K2071	SHERBROOKE	258	55	12.17000	.700
1	70K4632	MARTIN	70K4633	CHAPMAN	332	3	25.58000	.700
1	70K4631	HATLEY	68K2071	SHERBROOKE	0	0	0.00000	.701
1	70K4631	HATLEY	70K4632	MARTIN	56	9	32.26000	.700
1	70K4631	HATLEY	09207	HEREFORD	116	36	44.09000	.700
1	70K4631	HATLEY	08207	OWLS HEAD	260	44	22.26000	.700
1	70K4631	HATLEY	09206	ORFORD	310	31	6.17000	.700
1	70K4634	ASBESTOS	09205	HAM	0	0	0.00000	.701
1	70K4634	ASBESTOS	70K4633	CHAPMAN	58	54	59.51000	.700
1	70K4634	ASBESTOS	69K4242	PINNACLE	166	3	56.41000	.703
1	09205	HAM	70K4639	MOISAN	0	0	0.00000	.701
1	09205	HAM	70K4638	COULOMBE	38	10	20.70000	.701
1	09205	HAM	09208	MEGANTIC	113	16	24.69000	.700
1	09205	HAM	70K4635	WEEDON	118	8	13.44000	.700
1	09205	HAM	70K4633	CHAPMAN	168	3	43.54000	.700
1	09205	HAM	70K4634	ASBESTOS	239	18	10.09000	.701
1	70K4635	WEEDON	09205	HAM	0	0	0.00000	.700
1	70K4635	WEEDON	70K4638	COULOMBE	33	19	38.48000	.700
1	70K4635	WEEDON	71K6154	STORNOWAY	108	55	30.15000	.701
1	70K4635	WEEDON	09208	MEGANTIC	171	54	56.82000	.700
1	70K4635	WEEDON	70K4632	MARTIN	244	1	45.40000	.700
1	70K4635	WEEDON	70K4633	CHAPMAN	288	12	29.60000	.701
1	70K4639	MOISAN	70K4638	COULOMBE	0	0	0.00000	.703
1	70K4639	MOISAN	09205	HAM	73	39	27.26000	.701

1	70K4638 COULOMBE	71K6159 LAPOINTE	0 0 0.00000	.703
1	70K4638 COULOMBE	66KP115 CARIBOU E-15	71 29 28.41000	.701
1	70K4638 COULOMBE	71K6155 STE PRAXEDE	126 24 50.10000	.701
1	70K4638 COULOMBE	71K6154 STORNOWAY	175 1 59.09000	.700
1	70K4638 COULOMBE	70K4635 WEEDON	221 38 54.81000	.700
1	70K4638 COULOMBE	09205 HAM	288 21 25.12000	.701
1	70K4638 COULOMBE	70K4639 MOISAN	356 31 35.59000	.703
1	71K6159 LAPOINTE	71K6165 VIANNEY	0 0 0.00000	.701
1	71K6159 LAPOINTE	66KP115 CARIBOU E-15	60 35 18.24000	.701
1	71K6159 LAPOINTE	70K4638 COULOMBE	141 55 10.70000	.703
1	71K6154 STORNOWAY	71K6155 STE PRAXEDE	0 0 0.00000	.701
1	71K6154 STORNOWAY	71K6156 SEBASTIEN	80 31 13.62000	.700
1	71K6154 STORNOWAY	70K4637 GILBERT	128 12 39.02000	.701
1	71K6154 STORNOWAY	09208 MEGANTIC	171 40 32.86000	.700
1	71K6154 STORNOWAY	70K4635 WEEDON	251 44 19.65000	.701
1	71K6154 STORNOWAY	70K4638 COULOMBE	309 31 32.90000	.700
1	71K6155 STE PRAXEDE	692012 ADSTOCK	0 0 0.00000	.701
1	71K6155 STE PRAXEDE	692010 GRELOTS	52 48 9.24000	.701
1	71K6155 STE PRAXEDE	71K6156 SEBASTIEN	117 37 8.74000	.700
1	71K6155 STE PRAXEDE	71K6154 STORNOWAY	170 23 33.07000	.701
1	71K6155 STE PRAXEDE	70K4638 COULOMBE	251 17 57.87000	.701
1	71K6155 STE PRAXEDE	66KP115 CARIBOU E-15	305 5 56.85000	.701
1	692010 GRELOTS	692009 HONORE	0 0 0.00000	.701
1	692010 GRELOTS	71K6156 SEBASTIEN	57 3 46.11000	.700
1	692010 GRELOTS	71K6155 STE PRAXEDE	132 53 33.64000	.701
1	692010 GRELOTS	692012 ADSTOCK	184 23 49.21000	.701
* 51F20	.70 0.0 0.01971	.20 .20FORGUESRL GEOD		
1	712050 BON CONSEIL	712055 MALLARD	0 0 0.00000	.700
1	712050 BON CONSEIL	712056 WICKHAM	33 3 44.15000	.700
1	712050 BON CONSEIL	712057 DRUMMOND	50 10 11.76000	.701
1	712050 BON CONSEIL	712051 ST MAJORIQUE	66 59 55.20000	.701
1	712051 ST MAJORIQUE	712050 BON CONSEIL	0 0 0.00000	.701
1	712051 ST MAJORIQUE	712057 DRUMMOND	28 21 2.07000	.703
1	712051 ST MAJORIQUE	712055 MALLARD	60 32 35.67000	.700
1	712051 ST MAJORIQUE	712056 WICKHAM	101 58 5.17000	.701
1	712050 BON CONSEIL	712057 DRUMMOND	0 0 0.00000	.701
1	712050 BON CONSEIL	712051 ST MAJORIQUE	16 49 43.04000	.701
1	712050 BON CONSEIL	712055 MALLARD	309 49 48.11000	.700
1	712050 BON CONSEIL	712056 WICKHAM	342 53 33.11000	.700
1	712057 DRUMMOND	712050 BON CONSEIL	0 0 0.00000	.701
1	712057 DRUMMOND	712055 MALLARD	92 18 10.08000	.701
1	712057 DRUMMOND	712056 WICKHAM	148 28 26.40000	.701
1	712051 ST MAJORIQUE	712053 ST ZEPHIRIN	0 0 0.00000	.701
1	712051 ST MAJORIQUE	712050 BON CONSEIL	74 40 32.39000	.701
1	712057 DRUMMOND	712055 MALLARD	0 0 0.00000	.701
1	712057 DRUMMOND	712050 BON CONSEIL	267 41 50.59000	.701
1	712055 MALLARD	712056 WICKHAM	0 0 0.00000	.701
1	712055 MALLARD	712050 BON CONSEIL	95 57 33.41000	.700
1	712057 DRUMMOND	712056 WICKHAM	0 0 0.00000	.701
1	712057 DRUMMOND	712051 ST MAJORIQUE	76 42 19.21000	.703
1	712057 DRUMMOND	712050 BON CONSEIL	211 31 33.55000	.701
1	712056 WICKHAM	712051 ST MAJORIQUE	0 0 0.00000	.701
1	712056 WICKHAM	712050 BON CONSEIL	44 5 44.55000	.700
1	712056 WICKHAM	712055 MALLARD	95 4 29.34000	.701

1	712055	MALLARD	712051	ST MAJORIQUE	0 0 0.00000	.700
1	712055	mallard	712050	bon conseil	52 27 30.03000	.700
1	712056	WICKHAM	712055	MALLARD	0 0 0.00000	.701
1	712056	WICKHAM	712050	BON CONSEIL	309 1 15.17000	.700
1	712055	MALLARD	712057	DRUMMOND	0 0 0.00000	.701
1	712055	MALLARD	712050	BON CONSEIL	37 31 41.70000	.700
1	712055	MALLARD	712056	WICKHAM	301 34 9.60000	.701
1	712056	WICKHAM	712057	DRUMMOND	0 0 0.00000	.701
1	712056	WICKHAM	712050	BON CONSEIL	14 25 4.78000	.700
1	712056	WICKHAM	712055	MALLARD	65 23 48.98000	.701
* 51F19 .70 0.0 0.01969 .20 .20SELLEYAD GEOD						
1	692010	GRELOTS	692012	ADSTOCK	0 0 0.00000	.701
1	692010	GRELOTS	692011	BROUGHTON	51 35 38.80000	.701
1	692010	GRELOTS	692009	HONORE	175 36 10.89000	.701
* 51F21 .70 0.0 0.01965 .20 .20G-22 QLF						
1	652402	BROMONT	08200	ST ARMAND	0 0 0.00000	.700
1	652402	BROMONT	652401	FARNHAM	75 14 59.77000	.700
1	652402	BROMONT	09201	YAMASKA	117 28 38.98000	.700
1	652402	BROMONT	09206	ORFORD	248 43 2.52000	.700
1	09206	ORFORD	652402	BROMONT	0 0 0.00000	.700
1	09206	ORFORD	09201	YAMASKA	21 35 53.30000	.700
1	09206	ORFORD	08200	ST ARMAND	327 38 30.11000	.700
1	652401	FARNHAM	09201	YAMASKA	0 0 0.00000	.701
1	652401	FARNHAM	652402	BROMONT	69 29 59.23000	.700
1	652401	FARNHAM	08200	ST ARMAND	126 21 55.30000	.700
1	09201	YAMASKA	09206	ORFORD	0 0 0.00000	.700
1	09201	YAMASKA	652402	BROMONT	27 9 43.36000	.700
1	09201	YAMASKA	08200	ST ARMAND	60 23 6.94000	.700
1	09201	YAMASKA	652401	FARNHAM	95 26 7.78000	.701
* 51F22 .60 0.0 0.00917 .20 .20BIGGERCA GEOD						
1	09206	ORFORD	08200	ST ARMAND	0 0 0.00000	.600
1	09206	ORFORD	09201	YAMASKA	53 57 23.47000	.600
1	09206	ORFORD	09205	HAM	168 22 58.78000	.600
1	09206	ORFORD	09208	MEGANTIC	206 44 27.02000	.600
1	09206	ORFORD	09207	HEREFORD	243 30 22.34000	.600
1	09206	ORFORD	08207	OWLS HEAD	315 57 53.29000	.600
1	09201	YAMASKA	08200	ST ARMAND	0 0 0.00000	.600
1	09201	YAMASKA	09202	DUSABLE	176 15 45.12000	.600
1	09201	YAMASKA	09204	CARMEL	201 58 27.05000	.600
1	09201	YAMASKA	09205	HAM	260 49 45.47000	.600
1	09201	YAMASKA	09206	ORFORD	299 36 53.83000	.600
1	09205	HAM	09209	THETFORD	0 0 0.00000	.600
1	09205	HAM	09210	LINIERE	56 58 9.61000	.600
1	09205	HAM	14200	STRATFORD	59 3 26.46000	.600
1	09205	HAM	09208	MEGANTIC	103 21 26.36000	.600
1	09205	HAM	09207	HEREFORD	148 1 39.92000	.600
1	09205	HAM	09206	ORFORD	191 49 56.63000	.600
1	09205	HAM	09201	YAMASKA	218 37 20.09000	.600
1	09205	HAM	09202	DUSABLE	261 27 29.72000	.600
1	09205	HAM	09204	CARMEL	285 58 2.16000	.600
* 51F12 .70 0.0 0.01914 .20 .20BIGGERCA GEOD						
1	14200	STRATFORD	09205	HAM	0 0 0.00000	.700
1	14200	STRATFORD	09209	THETFORD	81 29 40.13000	.700
* 51F04 1.20 0.0 0.01909 .20 .20BIGGERCA GEOD						

1	09205	HAM	09209	THETFORD	0	0	0.00000	1.200
1	09205	HAM	09216	ARTHABASKA	295	55	51.30000	1.200
* 51F23 .85 0.0 0.01974 .20 .20G-272 QLF								
1	71K6159	LAPOINTE	70K4638	COULOMBE	0	0	0.00000	.853
1	71K6159	LAPOINTE	09205	HAM	71	35	7.76000	.851
1	71K6159	LAPOINTE	72K7457	SEVIGNY	158	34	38.99000	.851
1	71K6159	LAPOINTE	71K6165	VIANNEY	218	4	52.37000	.850
1	72K7457	SEVIGNY	72K7455	VICTORIAVILLE	0	0	0.00000	.851
1	72K7457	SEVIGNY	09216	ARTHABASKA	18	1	30.66000	.851
1	72K7457	SEVIGNY	71K6165	VIANNEY	87	43	47.83000	.851
1	72K7457	SEVIGNY	71K6159	LAPOINTE	171	17	16.76000	.851
1	72K7457	SEVIGNY	09205	HAM	219	53	4.95000	.851
1	72K7457	SEVIGNY	70K4634	ASBESTOS	278	55	28.28000	.850
1	70K4638	COULOMBE	09205	HAM	0	0	0.00000	.851
1	70K4638	COULOMBE	71K6159	LAPOINTE	71	38	33.63000	.853
1	09205	HAM	70K4634	ASBESTOS	0	0	0.00000	.850
1	09205	HAM	72K7457	SEVIGNY	77	41	6.70000	.851
1	09205	HAM	71K6159	LAPOINTE	122	5	47.43000	.851
1	09205	HAM	70K4638	COULOMBE	158	52	6.90000	.851
1	70K4634	ASBESTOS	72K7457	SEVIGNY	0	0	0.00000	.850
1	70K4634	ASBESTOS	09205	HAM	43	16	30.97000	.850
* 51F24 2.00 0.0 0.01974 .20 .20G-333-1 QLF								
1	72K7462	KINGSEY FALLS	72K7463	ST FELIX	0	0	0.00000	2.000
1	72K7462	KINGSEY FALLS	09216	ARTHABASKA	182	54	18.41000	2.000
1	72K7462	KINGSEY FALLS	70K4634	ASBESTOS	283	37	1.02000	2.000
1	70K4634	ASBESTOS	69K4242	PINNACLE	0	0	0.00000	2.001
1	70K4634	ASBESTOS	72K7462	KINGSEY FALLS	76	21	35.35000	2.000
1	70K4634	ASBESTOS	09205	HAM	193	56	4.07000	2.000
1	09205	HAM	69K4242	PINNACLE	0	0	0.00000	2.000
1	09205	HAM	72K7463	ST FELIX	15	50	11.28000	2.000
1	09205	HAM	09216	ARTHABASKA	70	25	24.97000	2.000
1	72K7463	ST FELIX	72K7462	KINGSEY FALLS	0	0	0.00000	2.000
1	72K7463	ST FELIX	69K4240	GALLUP HILL	144	1	10.17000	2.000
1	72K7463	ST FELIX	712055	MALLARD	222	30	17.05000	2.000
1	69K4240	GALLUP HILL	72K7463	ST FELIX	0	0	0.00000	2.000
1	69K4240	GALLUP HILL	69K4242	PINNACLE	54	24	31.70000	2.000
1	69K4240	GALLUP HILL	712055	MALLARD	312	40	43.99000	2.000
* 52T33 5.00 5.0 0.01969 .20 .20G-213 QLF								
2	69K4238	DAIGLE	69K4241	SOUTH DURHAM	4	22248.805	12.199	
2	69K4238	DAIGLE	712055	MALLARD	4	33538.096	17.500	
2	69K4241	SOUTH DURHAM	712055	MALLARD	4	14620.739	8.861	
2	69K4348	LEMAIRE	712056	WICKHAM	4	9938.004	7.055	
2	712056	WICKHAM	69K4349	BREBOEUF	4	11356.349	7.571	
2	712055	MALLARD	69K4348	LEMAIRE	4	16666.069	9.722	
2	712055	MALLARD	69K4349	BREBOEUF	4	10478.186	7.247	
2	69K4238	DAIGLE	712056	WICKHAM	4	32007.383	16.768	
2	712056	WICKHAM	712055	MALLARD	4	15903.665	9.397	
* 52G66 1.00 1.2 0.01969 .20 .20G-213 QLF								
2	712055	MALLARD	69K4346	CHARLES	4	12198.025	1.795	
2	69K4348	LEMAIRE	712057	DRUMMOND	4	6830.520	1.324	
2	69K4348	LEMAIRE	69K4346	CHARLES	4	9583.193	1.550	
2	69K4348	LEMAIRE	69K4349	BREBOEUF	4	6605.216	1.307	
2	69K4349	BREBOEUF	69K4346	CHARLES	4	5107.571	1.207	
2	69K4349	BREBOEUF	712057	DRUMMOND	4	7570.098	1.380	

2	69K4346 CHARLES	69K4350 HEMMING	4	1697.535	1.059
2	69K4346 CHARLES	712057 DRUMMOND	4	5982.974	1.263
2	69K4350 HEMMING	712057 DRUMMOND	4	7520.554	1.376
* 52T34 3.00 3.0 0.01971 .20 .20FORGUESRL GEOD					
2	712056 WICKHAM	712057 DRUMMOND	1	16311.219	5.747
2	712056 WICKHAM	712055 MALLARD	1	15903.735	5.643
2	712055 MALLARD	712057 DRUMMOND	1	17406.470	6.029
* 52T03 5.00 5.0 0.06971 .20 .20G-252 QLF					
2	68K2073 BEAUVOIR	70K4632 MARTIN	4	25958.954	13.911
2	70K4632 MARTIN	09207 HEREFORD	4	25114.522	13.516
2	70K4632 MARTIN	70K4631 HATLEY	4	25855.606	13.863
2	70K4631 HATLEY	09207 HEREFORD	4	23915.600	12.961
2	09201 YAMASKA	09206 ORFORD	4	51349.497	26.155
2	09201 YAMASKA	69K4238 DAIGLE	4	27087.768	14.439
2	69K4238 DAIGLE	69K4241 SOUTH DURHAM	4	22248.919	12.199
2	69K4238 DAIGLE	69K4239 DUSSAULT	4	23266.547	12.665
2	69K4238 DAIGLE	09206 ORFORD	4	29589.185	15.615
2	09206 ORFORD	69K4239 DUSSAULT	4	17353.488	10.015
2	09206 ORFORD	68K2071 SHERBROOKE	4	25042.285	13.483
2	09206 ORFORD	70K4631 HATLEY	4	32937.049	17.210
2	09206 ORFORD	70K4244 MAGOG	4	13167.713	8.268
2	09206 ORFORD	70K4245 AUSTIN	4	12221.058	7.896
2	09206 ORFORD	08207 OWLS HEAD	4	28074.228	14.902
2	69K4241 SOUTH DURHAM	69K4240 GALLUP HILL	4	12404.558	7.971
2	69K4241 SOUTH DURHAM	69K4239 DUSSAULT	4	22201.299	12.177
2	69K4239 DUSSAULT	68K2071 SHERBROOKE	4	27441.676	14.605
2	69K4239 DUSSAULT	69K4240 GALLUP HILL	4	18763.557	10.634
2	69K4239 DUSSAULT	69K4243 LAROCHELLE	4	14067.426	8.634
2	69K4239 DUSSAULT	68K2073 BEAUVOIR	4	26069.828	13.963
2	69K4240 GALLUP HILL	69K4242 PINNACLE	4	17557.730	10.106
2	69K4240 GALLUP HILL	69K4243 LAROCHELLE	4	15392.461	9.182
2	69K4242 PINNACLE	70K4634 ASBESTOS	4	8537.313	6.580
2	69K4242 PINNACLE	70K4633 CHAPMAN	4	30904.295	16.242
2	69K4242 PINNACLE	69K4243 LAROCHELLE	4	22087.271	12.125
2	69K4243 LAROCHELLE	70K4633 CHAPMAN	4	31156.248	16.361
2	69K4243 LAROCHELLE	68K2073 BEAUVOIR	4	15954.418	9.419
2	69K4243 LAROCHELLE	68K2071 SHERBROOKE	4	23323.516	12.691
2	68K2073 BEAUVOIR	68K2071 SHERBROOKE	4	12262.201	7.916
2	68K2071 SHERBROOKE	70K4633 CHAPMAN	4	31626.690	16.586
2	68K2071 SHERBROOKE	70K4632 MARTIN	4	22698.097	12.404
2	68K2071 SHERBROOKE	70K4631 HATLEY	4	21747.938	11.971
2	68K2071 SHERBROOKE	08207 OWLS HEAD	4	42989.262	22.068
2	68K2071 SHERBROOKE	70K4244 MAGOG	4	19608.686	11.009
2	70K4244 MAGOG	08207 OWLS HEAD	4	23652.302	12.840
2	70K4244 MAGOG	70K4245 AUSTIN	4	10647.587	7.309
2	70K4245 AUSTIN	08207 OWLS HEAD	4	16056.795	9.459
2	70K4633 CHAPMAN	70K4634 ASBESTOS	4	27291.916	14.534
2	70K4633 CHAPMAN	09205 HAM	4	24683.525	13.318
2	70K4633 CHAPMAN	70K4632 MARTIN	4	29571.329	15.609
2	70K4632 MARTIN	70K4635 WEEDON	4	40381.821	20.802
2	70K4634 ASBESTOS	09205 HAM	4	22030.464	12.098
2	09205 HAM	70K4639 MOISAN	4	12790.996	8.122
2	09205 HAM	70K4638 COULOMBE	4	13223.970	8.293
2	09205 HAM	70K4635 WEEDON	4	22105.434	12.133

2	09205	HAM	09209	THETFORD	4	45751.072	23.415
2	70K4635	WEEDON	70K4638	COULOMBE	4	23696.215	12.862
2	70K4635	WEEDON	71K6154	STORNOWAY	4	20354.838	11.342
2	70K4639	MOISAN	70K4638	COULOMBE	4	8516.299	6.573
2	70K4638	COULOMBE	71K6159	LAPOINTE	4	8343.637	6.517
2	70K4638	COULOMBE	66KP115	CARIBOU E-15	4	18055.555	10.323
2	70K4638	COULOMBE	71K6155	STE PRAXEDE	4	21190.456	11.718
2	70K4638	COULOMBE	71K6154	STORNOWAY	4	27127.252	14.458
2	71K6159	LAPOINTE	71K6165	VIANNEY	4	20404.081	11.364
2	71K6159	LAPOINTE	66KP115	CARIBOU E-15	4	17319.615	10.003
2	71K6154	STORNOWAY	71K6155	STE PRAXEDE	4	20613.706	11.458
2	71K6154	STORNOWAY	71K6156	SEBASTIEN	4	22553.585	12.337
2	71K6154	STORNOWAY	70K4637	GILBERT	4	21159.368	11.704
2	71K6155	STE PRAXEDE	692012	ADSTOCK	4	14759.889	8.917
2	71K6155	STE PRAXEDE	692010	GRELOTS	4	18269.250	10.417
2	71K6155	STE PRAXEDE	71K6156	SEBASTIEN	4	27938.314	14.837
2	71K6155	STE PRAXEDE	66KP115	CARIBOU E-15	4	18311.539	10.435
*	52T02	6.12	6.1	0.06971	.20	.20G-252	QLF
2	692010	GRELOTS	692009	HONORE	4	14873.258	10.947
*	52G83	1.40	1.7	0.06971	.20	.20G-252	QLF
2	70K4635	WEEDON	70K4633	CHAPMAN	4	19884.200	3.669
*	52T43	1.50	3.0	0.01969	.20	.20SELLEYAD	GEOD
2	692010	GRELOTS	692011	BROUGHTON	1	18091.670	5.637
2	692010	GRELOTS	692012	ADSTOCK	1	15021.754	4.757
*	52T35	3.00	3.0	0.01971	.20	.20FORGUESRL	GEOD
2	712050	BON CONSEIL	712053	ST ZEPHIRIN	1	23639.304	7.705
2	712050	BON CONSEIL	712051	ST MAJORIQUE	1	20623.942	6.882
2	712050	BON CONSEIL	712057	DRUMMOND	1	13807.056	5.122
2	712050	BON CONSEIL	712056	WICKHAM	2	28993.797	9.205
2	712051	ST MAJORIQUE	712057	DRUMMOND	1	8417.650	3.932
2	712051	ST MAJORIQUE	712053	ST ZEPHIRIN	1	18224.873	6.243
2	712056	WICKHAM	712051	ST MAJORIQUE	1	16545.896	5.807
2	712055	MALLARD	712051	ST MAJORIQUE	1	23942.647	7.789
*	52T36	6.00	3.0	0.01971	.20	.20FORGUESRL	GEOD
2	712055	MALLARD	712050	BON CONSEIL	1	22647.652	9.069
*	52T32	3.70	3.7	0.01965	.20	.20G-22	QLF
2	09201	YAMASKA	08200	ST ARMAND	4	45568.921	17.262
2	09201	YAMASKA	652401	FARNHAM	4	18037.649	7.635
2	09201	YAMASKA	652402	BROMONT	4	25135.574	10.012
2	652402	BROMONT	09206	ORFORD	4	31174.455	12.115
2	652402	BROMONT	652401	FARNHAM	4	24932.164	9.941
*	52T01	5.00	5.0	0.01972	.20	.20G-272	QLF
2	71K6159	LAPOINTE	09205	HAM	4	13226.475	8.295
2	72K7457	SEVIGNY	72K7455	VICTORIAVILLE	4	18125.702	10.353
2	72K7457	SEVIGNY	09216	ARTHABASKA	4	18296.441	10.428
2	72K7457	SEVIGNY	09205	HAM	4	17609.832	10.128
2	72K7457	SEVIGNY	70K4634	ASBESTOS	4	25096.466	13.510
2	71K6159	LAPOINTE	72K7457	SEVIGNY	4	12340.221	7.946
*	52G84	1.40	1.7	0.01974	.20	.20G-333-1	QLF
2	72K7463	ST FELIX	69K4240	GALLUP HILL	4	18293.961	3.422
2	72K7463	ST FELIX	712055	MALLARD	4	16581.838	3.160
*	52T04	5.00	5.0	0.01974	.20	.20G-333-1	QLF
2	72K7462	KINGSEY FALLS	72K7463	ST FELIX	4	14338.006	8.745
2	72K7462	KINGSEY FALLS	70K4634	ASBESTOS	4	20793.098	11.539

2	72K7463 ST FELIX	69K4242 PINNACLE	4	16404.403	9.609
2	72K7463 ST FELIX	69K4240 GALLUP HILL	4	18293.913	10.428
* 52T05	5.20 5.2 0.0	.20 .20G-257 SGQ			
2	09205 HAM	14200 STRATFORD	4	29394.835	16.146
* 53???	.80 .2 1.0	.20 .20 GEOD			
3	09206 ORFORD	09201 YAMASKA	287	4 48.92700	1.089
* 51F25	.70 0.0 0.06971	.20 .20G-252 QLF			
1	09208 MEGANTIC	09207 HEREFORD	0	0 0.00000	.700
1	09208 MEGANTIC	70K4632 MARTIN	26	7 1.87000	.700
1	09208 MEGANTIC	70K4635 WEEDON	87	31 3.38000	.700
1	09208 MEGANTIC	09205 HAM	90	44 18.88000	.700
1	09208 MEGANTIC	71K6154 STORNOWAY	124	27 51.03000	.700
1	09208 MEGANTIC	70K4637 GILBERT	168	57 40.27000	.701
1	09208 MEGANTIC	65K0335 CROIX	193	15 38.35000	.700
1	08207 OWLS HEAD	09206 ORFORD	0	0 0.00000	.700
1	08207 OWLS HEAD	70K4245 AUSTIN	5	45 13.57000	.701
1	08207 OWLS HEAD	70K4244 MAGOG	27	49 43.37000	.700
1	08207 OWLS HEAD	68K2071 SHERBROOKE	33	39 5.61000	.700
1	08207 OWLS HEAD	70K4631 HATLEY	63	36 25.33000	.700
1	08207 OWLS HEAD	09207 HEREFORD	78	22 59.22000	.700
1	09207 HEREFORD	08207 OWLS HEAD	0	0 0.00000	.700
1	09207 HEREFORD	70K4631 HATLEY	21	5 48.54000	.700
1	09207 HEREFORD	70K4632 MARTIN	84	42 29.48000	.700
1	09207 HEREFORD	09208 MEGANTIC	134	49 36.75000	.700
* 51F26	.70 0.0 0.01965	.20 .20G-22 QLF			
1	08200 ST ARMAND	09201 YAMASKA	0	0 0.00000	.700
1	08200 ST ARMAND	652402 BROMONT	29	18 .75000	.700
1	08200 ST ARMAND	09206 ORFORD	65	39 36.76000	.700
1	08200 ST ARMAND	652401 FARNHAM	341	24 53.93000	.700
* 51F27	.60 0.0 0.00917	.20 .20BIGGERCA GEOD			
1	08200 ST ARMAND	09201 YAMASKA	0	0 0.00000	.600
1	08200 ST ARMAND	09206 ORFORD	65	39 37.18000	.600
1	08200 ST ARMAND	08207 OWLS HEAD	99	46 8.20000	.600
1	08207 OWLS HEAD	08200 ST ARMAND	0	0 0.00000	.600
1	08207 OWLS HEAD	09206 ORFORD	101	51 26.66000	.600
1	08207 OWLS HEAD	09207 HEREFORD	180	14 25.69000	.600
1	09207 HEREFORD	08207 OWLS HEAD	0	0 0.00000	.600
1	09207 HEREFORD	09206 ORFORD	29	9 31.30000	.600
1	09207 HEREFORD	09205 HAM	90	13 59.17000	.600
1	09207 HEREFORD	09208 MEGANTIC	134	49 35.51000	.600
1	09208 MEGANTIC	09205 HAM	0	0 0.00000	.600
1	09208 MEGANTIC	09209 THETFORD	34	2 22.24000	.600
1	09208 MEGANTIC	09210 LINIERE	99	52 16.74000	.600
1	09208 MEGANTIC	09207 HEREFORD	269	15 43.17000	.600
1	09208 MEGANTIC	09206 ORFORD	306	49 50.20000	.600
* 52T00	5.00 5.0 0.06971	.20 .20G-252 QLF			
2	08207 OWLS HEAD	70K4631 HATLEY	4	33747.646	17.599
2	08207 OWLS HEAD	09207 HEREFORD	4	54940.557	27.920
2	09208 MEGANTIC	65K0335 CROIX	4	23201.228	12.631
2	09208 MEGANTIC	70K4637 GILBERT	4	20774.777	11.528
2	09208 MEGANTIC	71K6154 STORNOWAY	4	30177.294	15.894
2	09208 MEGANTIC	09205 HAM	4	55331.838	28.111
2	09208 MEGANTIC	70K4635 WEEDON	4	33363.916	17.413
2	09208 MEGANTIC	70K4632 MARTIN	4	43778.057	22.450


```
* 52T06 6.12 6.1 0.06971 .20 .20G-252 QLF
2 09208 MEGANTIC 09207 HEREFORD 4 55407.113 34.344
* 52T37 3.70 3.7 0.01965 .20 .20G-22 QLF
2 08200 ST ARMAND 652401 FARNHAM 4 32503.501 12.583
```

Table 7.6 NETAN listing of reliability analysis results for real 2D network.

NETAN: Network Analysis (Version 21 Nov 90)
Network Strength Analysis

Piece-Wise Linear Approximation -- Connected Stations

Input network data file : [ong.work.gsc]
Real 2D Network. Sigma record commented out. November 16, 1990.

Station	Name	Lat (DMS), Long (DMS), Ht (m)	Strength in Rotation: Lat/Lon, Lat/Ht, Lon/Ht (rad)	Obs # and Type
			Strength in Shear: Lat/Lon, Lat/Ht, Lon/Ht (strain)	Obs # and Type
			Strength in Scale: (strain)	Obs # and Type
1	09206	ORFORD		
		45 18 43.080825 -72 14 30.207541 823.910000		
		0.2291992303E-05 0.0000000000E+00 0.0000000000E+00		
		216 dir 0 0		
		0.6780170129E-06 0.0000000000E+00 0.0000000000E+00		
		408 dis 0 0		
		0.1048841776E-05		
		408 dis		
2	08200	ST ARMAND		
		45 2 46.871261 -72 44 20.953894 683.340000		
		0.1787265735E-05 0.0000000000E+00 0.0000000000E+00		
		406 dis 0 0		
		0.1887607108E-05 0.0000000000E+00 0.0000000000E+00		
		408 dis 0 0		
		0.2712184001E-05		
		408 dis		
3	09201	YAMASKA		
		45 26 45.361290 -72 52 8.645262 392.290000		
		0.2439381765E-05 0.0000000000E+00 0.0000000000E+00		
		225 dir 0 0		
		0.3127375182E-05 0.0000000000E+00 0.0000000000E+00		
		224 dir 0 0		
		0.3791708636E-05		
		224 dir		
4	652401	FARNHAM		
		45 17 43.897511 -72 57 19.611919 48.700000		

	0.5001618512E-05	0.0000000000E+00	0.0000000000E+00
	204 dir	0	0
	0.3307516240E-05	0.0000000000E+00	0.0000000000E+00
	202 dir	0	0
	0.3517456435E-05		
	409 dis		
5	652402 BROMONT		
	45 17 21.072496	-72 38 16.135074	524.090000
	-0.1843621826E-05	0.0000000000E+00	0.0000000000E+00
	221 dir	0	0
	0.1889051795E-05	0.0000000000E+00	0.0000000000E+00
	293 dir	0	0
	0.2437763748E-05		
	408 dis		
6	69K4238 DAIGLE		
	45 29 9.961951	-72 31 38.850628	247.350000
	0.2953850819E-05	0.0000000000E+00	0.0000000000E+00
	417 dis	0	0
	0.2575428970E-05	0.0000000000E+00	0.0000000000E+00
	310 dis	0	0
	0.2161766696E-05		
	310 dis		
7	712051 ST MAJORIQUE		
	45 54 58.861380	-72 38 1.304256	52.908000
	0.7749727553E-05	0.0000000000E+00	0.0000000000E+00
	417 dis	0	0
	0.9316988431E-05	0.0000000000E+00	0.0000000000E+00
	401 dis	0	0
	0.5348008518E-05		
	401 dis		
8	712056 WICKHAM		
	45 46 7.554535	-72 36 21.129165	77.103000
	0.7476142592E-05	0.0000000000E+00	0.0000000000E+00
	417 dis	0	0
	0.2536399125E-05	0.0000000000E+00	0.0000000000E+00
	9 dir	0	0
	0.1995342595E-05		
	310 dis		
9	08207 OWLS HEAD		
	45 3 45.158627	-72 17 52.885732	722.260000
	0.2594546255E-05	0.0000000000E+00	0.0000000000E+00
	216 dir	0	0
	0.1615778936E-05	0.0000000000E+00	0.0000000000E+00
	215 dir	0	0
	0.1226679828E-05		
	408 dis		
10	09202 DUSABLE		
	46 12 37.072604	-73 11 59.806107	104.781000

	0.3101339429E-05	0.0000000000E+00	0.0000000000E+00
	225 dir	0	0
	0.3994191380E-05	0.0000000000E+00	0.0000000000E+00
	224 dir	0	0
	-0.4188316514E-05		
	232 dir		
11	09204 CARMEL		
	46 29 58.619050	-72 37 39.231578	158.621000
	0.2303922089E-05	0.0000000000E+00	0.0000000000E+00
	225 dir	0	0
	0.4533089469E-05	0.0000000000E+00	0.0000000000E+00
	224 dir	0	0
	0.4979524888E-05		
	224 dir		
12	09205 HAM		
	45 47 28.152005	-71 38 0.762182	683.980000
	0.2419608259E-05	0.0000000000E+00	0.0000000000E+00
	216 dir	0	0
	0.2157032141E-05	0.0000000000E+00	0.0000000000E+00
	224 dir	0	0
	0.2422139615E-05		
	224 dir		
13	09207 HEREFORD		
	45 4 57.225000	-71 36 3.592868	845.530000
	0.2897477348E-05	0.0000000000E+00	0.0000000000E+00
	216 dir	0	0
	0.6010754979E-06	0.0000000000E+00	0.0000000000E+00
	109 dir	0	0
	0.7700208902E-06		
	393 dis		
14	09208 MEGANTIC		
	45 26 51.274493	-71 7 13.028206	1059.467500
	0.2854532175E-05	0.0000000000E+00	0.0000000000E+00
	216 dir	0	0
	0.3987041417E-05	0.0000000000E+00	0.0000000000E+00
	226 dir	0	0
	0.3929598540E-05		
	375 dis		
15	09209 THETFORD		
	46 8 48.515181	-71 20 11.437419	666.570000
	-0.8307484869E-05	0.0000000000E+00	0.0000000000E+00
	226 dir	0	0
	0.9124208779E-05	0.0000000000E+00	0.0000000000E+00
	226 dir	0	0
	0.1011247600E-04		
	375 dis		
16	09210 LINIERE		
	45 49 45.115005	-70 22 20.319318	750.290000

	0.2999085842E-05	0.0000000000E+00	0.0000000000E+00
	216 dir	0	0
	0.5236910186E-05	0.0000000000E+00	0.0000000000E+00
	229 dir	0	0
	0.5514152198E-05		
	229 dir		
17	09216	ARTHABASKA	
	46 3 14.104500	-71 53 16.799699	321.731000
	0.1191938293E-04	0.0000000000E+00	0.0000000000E+00
	412 dis	0	0
	0.1587670111E-04	0.0000000000E+00	0.0000000000E+00
	412 dis	0	0
	0.1798636910E-04		
	412 dis		
18	14200	STRATFORD	
	45 47 39.761115	-71 15 20.039726	409.870000
	-0.1980789843E-04	0.0000000000E+00	0.0000000000E+00
	228 dir	0	0
	0.1777116246E-04	0.0000000000E+00	0.0000000000E+00
	228 dir	0	0
	0.1534542300E-04		
	422 dis		
19	65K0335	CROIX	
	45 33 46.497791	-70 52 22.787639	464.720000
	0.0000000000E+00	0.0000000000E+00	0.0000000000E+00
	0	0	0
	0.0000000000E+00	0.0000000000E+00	0.0000000000E+00
	0	0	0
	0.0000000000E+00		
	0		
20	66KP115	CARIBOU E-15	
	46 0 15.971155	-71 24 10.097848	529.160000
	-0.5562603072E-05	0.0000000000E+00	0.0000000000E+00
	136 dir	0	0
	0.7851738514E-05	0.0000000000E+00	0.0000000000E+00
	156 dir	0	0
	0.5604775540E-05		
	391 dis		
21	68K2071	SHERBROOKE	
	45 20 46.266313	-71 55 33.826884	412.850000
	0.2689331661E-05	0.0000000000E+00	0.0000000000E+00
	216 dir	0	0
	0.8202859858E-06	0.0000000000E+00	0.0000000000E+00
	88 dir	0	0
	0.7052087482E-06		
	338 dis		
22	68K2073	BEAUVOIR	
	45 27 17.108246	-71 53 53.751099	280.300000

	0.3135858519E-05	0.0000000000E+00	0.0000000000E+00
	47 dir	0	0
	0.2486786173E-05	0.0000000000E+00	0.0000000000E+00
	83 dir	0	0
	0.2375535604E-05		
	358 dis		
23	692009 HONORE		
	45 56 53.174517	-70 50 16.176131	447.770000
	0.0000000000E+00	0.0000000000E+00	0.0000000000E+00
	0	0	0
	0.0000000000E+00	0.0000000000E+00	0.0000000000E+00
	0	0	0
	0.0000000000E+00		
	0		
24	692010 GRELOTS		
	45 59 2.203154	-71 1 21.673533	381.909000
	-0.7953237833E-05	0.0000000000E+00	0.0000000000E+00
	152 dir	0	0
	0.5792329569E-05	0.0000000000E+00	0.0000000000E+00
	158 dir	0	0
	0.3850007066E-05		
	158 dir		
25	692011 BROUGHTON		
	46 8 17.589232	-71 5 49.617509	581.498000
	0.0000000000E+00	0.0000000000E+00	0.0000000000E+00
	0	0	0
	0.0000000000E+00	0.0000000000E+00	0.0000000000E+00
	0	0	0
	0.0000000000E+00		
	0		
26	692012 ADSTOCK		
	46 1 46.979836	-71 12 18.397682	685.978000
	-0.1230437573E-04	0.0000000000E+00	0.0000000000E+00
	151 dir	0	0
	0.9751390846E-05	0.0000000000E+00	0.0000000000E+00
	151 dir	0	0
	0.1287876464E-04		
	395 dis		
27	69K4239 DUSSAULT		
	45 28 4.318988	-72 13 51.763295	402.500000
	0.4064810816E-05	0.0000000000E+00	0.0000000000E+00
	47 dir	0	0
	0.1295113346E-05	0.0000000000E+00	0.0000000000E+00
	58 dir	0	0
	0.1122547988E-05		
	308 dis		
28	69K4240 GALLUP HILL		
	45 38 6.697228	-72 11 57.261594	319.590000

	0.4348054981E-05	0.0000000000E+00	0.0000000000E+00
	47 dir	0	0
	0.4027722157E-05	0.0000000000E+00	0.0000000000E+00
	417 dis	0	0
	0.4826614114E-05		
	417 dis		
29	69K4241 SOUTH DURHAM		
	45 38 48.365666	-72 21 26.900929	179.840000
	0.5526232020E-05	0.0000000000E+00	0.0000000000E+00
	47 dir	0	0
	0.4290238242E-05	0.0000000000E+00	0.0000000000E+00
	310 dis	0	0
	0.3002360240E-05		
	310 dis		
30	69K4242 PINNACLE		
	45 43 21.443910	-72 0 41.610936	388.010000
	0.3371893597E-05	0.0000000000E+00	0.0000000000E+00
	47 dir	0	0
	0.2236453538E-05	0.0000000000E+00	0.0000000000E+00
	416 dis	0	0
	0.1793648331E-05		
	416 dis		
31	69K4243 LAROCHELLE		
	45 31 43.227302	-72 4 23.562369	304.990000
	0.3266237003E-05	0.0000000000E+00	0.0000000000E+00
	47 dir	0	0
	0.1435730976E-05	0.0000000000E+00	0.0000000000E+00
	75 dir	0	0
	0.1486183689E-05		
	350 dis		
32	69K4346 CHARLES		
	45 52 34.266330	-72 27 39.849084	63.770000
	0.7867890981E-05	0.0000000000E+00	0.0000000000E+00
	11 dir	0	0
	0.2237129517E-05	0.0000000000E+00	0.0000000000E+00
	317 dis	0	0
	0.2443078905E-05		
	317 dis		
33	69K4348 LEMAIRE		
	45 51 23.401352	-72 34 52.406629	63.700000
	0.7749620783E-05	0.0000000000E+00	0.0000000000E+00
	417 dis	0	0
	0.1378370310E-05	0.0000000000E+00	0.0000000000E+00
	317 dis	0	0
	0.2543066967E-05		
	317 dis		
34	69K4349 BREBOEUF		
	45 50 20.776812	-72 29 59.688552	59.560000

	0.7749624063E-05	0.0000000000E+00	0.0000000000E+00
	417 dis	0	0
	0.1378626132E-05	0.0000000000E+00	0.0000000000E+00
	317 dis	0	0
	0.2543066967E-05		
	317 dis		
35	69K4350 HEMMING		
	45 51 46.540782	-72 27 0.785585	85.800000
	0.3299870489E-04	0.0000000000E+00	0.0000000000E+00
	323 dis	0	0
	0.3869778647E-04	0.0000000000E+00	0.0000000000E+00
	323 dis	0	0
	0.2082584995E-04		
	34 dir		
36	70K4244 MAGOG		
	45 13 57.380010	-72 7 2.328885	317.400000
	0.3125550595E-05	0.0000000000E+00	0.0000000000E+00
	48 dir	0	0
	0.1775246505E-05	0.0000000000E+00	0.0000000000E+00
	366 dis	0	0
	0.1629930264E-05		
	296 dir		
37	70K4245 AUSTIN		
	45 12 7.762168	-72 14 44.998966	290.520000
	-0.3892163923E-05	0.0000000000E+00	0.0000000000E+00
	53 dir	0	0
	0.3882404481E-05	0.0000000000E+00	0.0000000000E+00
	53 dir	0	0
	0.3175721289E-05		
	365 dis		
38	70K4631 HATLEY		
	45 9 8.363523	-71 53 18.366476	395.940000
	0.2849218070E-05	0.0000000000E+00	0.0000000000E+00
	216 dir	0	0
	0.1392014735E-05	0.0000000000E+00	0.0000000000E+00
	109 dir	0	0
	0.1255207336E-05		
	330 dis		
39	70K4632 MARTIN		
	45 18 23.810822	-71 38 31.356562	396.220000
	0.2907676552E-05	0.0000000000E+00	0.0000000000E+00
	216 dir	0	0
	0.1293804221E-05	0.0000000000E+00	0.0000000000E+00
	108 dir	0	0
	0.1238682002E-05		
	393 dis		
40	70K4633 CHAPMAN		
	45 34 16.985548	-71 40 44.175426	630.990000

	0.2809255876E-05	0.0000000000E+00	0.0000000000E+00
	47 dir	0	0
	0.1139954816E-05	0.0000000000E+00	0.0000000000E+00
	393 dis	0	0
	0.1463766489E-05		
	393 dis		
41	70K4634 ASBESTOS		
	45 45 16.869121	-71 54 42.797011	309.870000
	-0.6302590378E-05	0.0000000000E+00	0.0000000000E+00
	418 dis	0	0
	0.4380594903E-05	0.0000000000E+00	0.0000000000E+00
	418 dis	0	0
	0.2612630896E-05		
	412 dis		
42	70K4635 WEEDON		
	45 38 32.848965	-71 26 42.228373	386.480000
	0.2944282103E-05	0.0000000000E+00	0.0000000000E+00
	216 dir	0	0
	0.1462416377E-05	0.0000000000E+00	0.0000000000E+00
	393 dis	0	0
	0.1634337190E-05		
	393 dis		
43	70K4637 GILBERT		
	45 36 21.037028	-70 58 44.422322	544.460000
	-0.1065074819E-04	0.0000000000E+00	0.0000000000E+00
	277 dir	0	0
	0.1350012469E-04	0.0000000000E+00	0.0000000000E+00
	277 dir	0	0
	0.7872459230E-05		
	426 dis		
44	70K4638 COULOMBE		
	45 51 12.417696	-71 29 19.031780	438.270000
	0.2935917950E-05	0.0000000000E+00	0.0000000000E+00
	216 dir	0	0
	0.2318051541E-05	0.0000000000E+00	0.0000000000E+00
	136 dir	0	0
	0.2066990702E-05		
	384 dis		
45	70K4639 MOISAN		
	45 53 56.871982	-71 34 35.977949	569.740000
	-0.8540689454E-05	0.0000000000E+00	0.0000000000E+00
	141 dir	0	0
	0.8638607481E-05	0.0000000000E+00	0.0000000000E+00
	121 dir	0	0
	0.7271839907E-05		
	378 dis		
46	712050 BON CONSEIL		
	45 58 40.678773	-72 22 58.101451	91.631000

	0.7749729450E-05	0.0000000000E+00	0.0000000000E+00
	417 dis	0	0
	0.9320161087E-05	0.0000000000E+00	0.0000000000E+00
	401 dis	0	0
	0.5348008518E-05		
	401 dis		
47	712053 ST ZEPHIRIN		
	46 4 47.569228 -72 39 2.842686		25.023000
	-0.1111213491E-04	0.0000000000E+00	0.0000000000E+00
	401 dis	0	0
	0.2135469992E-04	0.0000000000E+00	0.0000000000E+00
	401 dis	0	0
	0.1695259473E-04		
	401 dis		
48	712055 MALLARD		
	45 46 28.667244 -72 24 5.686794		142.128000
	0.5503102695E-05	0.0000000000E+00	0.0000000000E+00
	47 dir	0	0
	0.4757724749E-05	0.0000000000E+00	0.0000000000E+00
	417 dis	0	0
	0.4607355053E-05		
	417 dis		
49	712057 DRUMMOND		
	45 54 16.662029 -72 31 35.443646		63.880000
	0.7752047465E-05	0.0000000000E+00	0.0000000000E+00
	417 dis	0	0
	0.1308349826E-05	0.0000000000E+00	0.0000000000E+00
	400 dis	0	0
	0.1457931203E-05		
	317 dis		
50	71K6154 STORNOWAY		
	45 42 45.387397 -71 12 13.529074		483.170000
	-0.4225622773E-05	0.0000000000E+00	0.0000000000E+00
	146 dir	0	0
	0.4797120232E-05	0.0000000000E+00	0.0000000000E+00
	146 dir	0	0
	0.2794709671E-05		
	386 dis		
51	71K6155 STE PRAXEDE		
	45 53 51.218892 -71 13 23.166549		364.290000
	-0.5422173217E-05	0.0000000000E+00	0.0000000000E+00
	146 dir	0	0
	0.3967224861E-05	0.0000000000E+00	0.0000000000E+00
	151 dir	0	0
	0.3178432040E-05		
	386 dis		
52	71K6156 SEBASTIEN		
	45 45 36.572370 -70 55 19.585027		799.230000

```

-0.9159936778E-05  0.0000000000E+00  0.0000000000E+00
  146 dir          0          0
0.8023707250E-05  0.0000000000E+00  0.0000000000E+00
  146 dir          0          0
0.6881894531E-05
  386 dis

53  71K6159  LAPOINTE
    45 54 6.374812 -71 34 14.982987    600.040000
-0.5360384814E-05  0.0000000000E+00  0.0000000000E+00
  383 dis          0          0
0.9092228940E-05  0.0000000000E+00  0.0000000000E+00
  383 dis          0          0
0.1107144575E-04
  383 dis

54  71K6165  VIANNEY
    46 452.998888 -71 37 30.248075    564.280000
-0.7362515097E-05  0.0000000000E+00  0.0000000000E+00
  245 dir          0          0
0.1502158604E-04  0.0000000000E+00  0.0000000000E+00
  383 dis          0          0
0.2253310123E-04
  383 dis

55  72K7455  VICTORIAVILLE
    46 0 41.601241 -71 55 46.779541    246.133000
0.0000000000E+00  0.0000000000E+00  0.0000000000E+00
  0          0          0
0.0000000000E+00  0.0000000000E+00  0.0000000000E+00
  0          0          0
0.0000000000E+00
  0

56  72K7457  SEVIGNY
    45 56 13.678515 -71 43 17.746867    500.100000
0.6385320893E-05  0.0000000000E+00  0.0000000000E+00
  383 dis          0          0
0.9078455909E-05  0.0000000000E+00  0.0000000000E+00
  412 dis          0          0
0.9200836578E-05
  412 dis

57  72K7462  KINGSEY FALLS
    45 54 5.080173 -72 4 40.320796    125.670000
0.1617695032E-04  0.0000000000E+00  0.0000000000E+00
  412 dis          0          0
0.1396636558E-04  0.0000000000E+00  0.0000000000E+00
  412 dis          0          0
0.1159093134E-04
  244 dir

58  72K7463  ST FELIX
    45 47 58.863308 -72 11 28.930794    180.680000

```

-0.6568929503E-05	0.0000000000E+00	0.0000000000E+00
418 dis	0	0
0.8513433793E-05	0.0000000000E+00	0.0000000000E+00
418 dis	0	0
0.7365212531E-05		
418 dis		

99

8. PROPOSED SPECIFICATIONS FOR THE TOTAL ANALYSIS OF NETWORKS

8.1 Overall Scheme

Based upon the scientific analysis presented in the foregoing chapters, we are now in a position to propose a methodology to be used in the complete analysis of a 2D network (Table 8.1). The columns contain the various quantities to be assessed, while the rows contain the various measures and tests to be used. The proposal clearly integrates the standard assessment tools of random error analysis (covariance analysis — row 1), with that of the robustness (row 2), and external reliability (row 3) analyses. The quantities to be assessed consist of the estimated positions, model, observables, and functions of estimated positions. The observation and model measures are used in two modes: preanalysis and postanalysis.

8.2 Preanalysis

In standard statistical testing procedures, it is mandatory to predict beforehand the point and relative confidence regions of the coordinates. This yields a measure of how random errors will propagate from the observations into the estimated positions.

It is also mandatory to predict how the systematic blunders (if made) will propagate throughout the network and bias the estimated positions. These can be measured by internal reliability measures on the observables, i.e., the maximum undetectable errors, robustness, and external reliability measures on the estimated positions. Here, the robustness analysis gives us a measure of how strong the network is in resisting blunders or systematic errors in the observations. Recall, that the internal reliability measure is an estimate of how large a blunder can be before standard statistical testing can catch it, whereas robustness and the external reliability quantify the effect on the unknown parameters.

Table 8.1 Total analysis of a network.

Quantity Assessed Type of Measure	Observations and model		Positions pre- and postanalysis	Network as a whole	Functions of positions	Remarks
	Preanalysis	Postanalysis				
Accuracy (Type I error — random)	Given C_ρ and design matrices A and B , predict $C_{\hat{x}}$ $\Rightarrow (1-\alpha)$ confidence ellipses	Tests listed in Tables 13.2 to 13.5 in Vanicek and Krakiwsky [1986]	Point and relative $(1-\alpha)$ confidence ellipses	a) Test on σ_0 / σ_0^2 b) Test on distribution of residuals	a) Accuracy of position differences b) Accuracy of distances c) Accuracy of directions	These are all standard tests and measures
Internal Reliability, Robustness (Type II error — blunder)	a) Maximum undetectable errors $\nabla \ell_i$ b) Redundancy numbers r_i c) Predicted residuals $v_i = r_i \nabla \ell_i$	a) Max. undetectable errors $\hat{\nabla} \ell_i$ b) Redundancy numbers r_i c) Actual residuals $\hat{v}_i = r_i \hat{\nabla} \ell_i$	a) Robustness in scale σ b) Robustness in shear γ c) Robustness in twist ω	a) Average $ \sigma $ b) Average γ c) Average $ \omega $	a) Strain of a line b) Rotation of a line	Robustness of functions to be yet formulated
External Reliability (Type II error — blunder)			External reliability ∇x_i	a) Global external reliability $\nabla x^T C_{\hat{x}}^{-1} \nabla x$ b) Average ext. reliability ∇x_i		Only under exceptional circumstances

8.3 Postanalysis

Postanalysis, like preanalysis, is extended to take care of the Type II error, that is, the quantification of what happens when one considers the presence of blunders in the solution. The standard tests consisting of the null hypothesis H_0 (no blunders) must be amended to include the alternative hypothesis H_a (blunders). In this way, we are able to track down how our tests are affected by this new dimension.

The tests affected by the consideration of H_a are those listed in Vaníček and Krakiwsky [1986] as follows:

- (a) Univariate testing of an observational series as a unit (Table 13.2).
- (b) Univariate testing of individual observations (Table 13.3).
- (c) Multivariate testing of observables as model as a unit (Table 13.4).
- (d) Multivariate testing of individual observables (Table 13.5).

8.4 Other Considerations

The proposed total analysis scheme includes an extended preanalysis activity where both the Types I and II errors are modelled. We note that for reasons explained in Chapter 5, the external reliability measures should be used only when robustness cannot be computed because of some peculiar network configuration.

Robustness of functions of estimated positions, such as computed distances, angles, possibly coordinate differences, have not been formulated yet. It is clear from the theoretical viewpoint that such measures should exist, but mathematical expressions for these are yet to be derived.

We reiterate the point here that robustness of a network has to be measured by three independent primitives. It is not possible to combine these into a single measure. Tolerance limits and design criteria for robustness will have to be worked out on the basis of a 'reasonable' selection of β_0 -value (probability of Type II error). This selection requires further investigation.

9. CONCLUSIONS, RECOMMENDATIONS, AND ACKNOWLEDGEMENTS

The collaboration of UNB and U of C researchers on the comparison of reliability analysis with geometric strength analysis resulted in the conception of a new technique, robustness analysis, which is a natural merger of the two existing techniques. First experiences with robustness analysis show that it is a very powerful technique capable of providing a picture of the analysed network, which is complementary to the one furnished by the standard covariance analysis. ‘Network robustness’ (strength, as an ability to resist deformations induced by undetectable blunders, might be a term more readily understood) is invariant with respect to coordinate shifts and almost invariant with respect to orientation and scale changes.

Robustness is expressed in terms of three independent deformation primitives; namely, robustness in scale (strain), local configuration (shear), and twist (differential rotation). It thus makes no sense to talk about robustness in general but only about “robustness in scale,” “robustness in shear,” and “robustness in twist.” This will sound complicated to a surveyor uninitiated in the concepts of deformation analysis, where the three primitives are used routinely. Let us emphasize here that the full description of a deformation cannot be achieved with fewer than three primitives. If we wish to deal with network strength meaningfully, then we have to accept this fact and learn to live with it. It seems to us that the introduction of robustness analysis will require some educational effort aimed at the surveying community. Specifically, a guide/manual will have to be written with the aim to assist in the transfer of knowledge.

We recommend that robustness analysis be used side-by-side with the standard covariance analysis for a complete network analysis in the future. The Canadian federal specifications for horizontal control networks should be extended to include robustness analysis. It should be mentioned here that under special circumstances, the ‘external reliability’ measure discussed in

Chapter 3 would have to be used (in case of geometrical singularity encountered at a network point or set of points) and provisions should be made for this in the specifications.

As we have seen in Chapter 7, it is not always easy, or even possible, to guess at the reason behind a specific weakness in the network from the network configuration alone. More experiments should be conducted with robustness analysis, and more experience gained with practical application as well as the interpretation of robustness analysis results, particularly before specific values of robustness tolerance limits can be imposed through federal specifications. Some general criteria, however, can be formulated already, and these were spelled out in Chapter 8. A better graphical representation of robustness primitives is a must. Our investigations were definitely hindered by the unavailability of a decent graphics package on the UNB Vax computer system.

A strategy will have to be worked out on how to deal with the two kinds of singularities that may arise in robustness analysis. While the generic singularity associated with the extreme weakness of the network has so far been shown by 'large' values of the robustness primitives, geometrical singularities have been simply eliminated by leaving out the singular points. More worrisome is the case of geometrical near-singularities such as the one encountered at station HEMMING in the analysis of the real network in Chapter 7. A measure of ill-conditioning based either on confidence regions for strength primitives or the value of the determinant in the least-squares fitting of planes in the determination of strain matrices will have to be devised.

Some refinement of the reliability analysis as the first part of robustness analysis is called for in order to understand better the role of the probabilities (significance levels) used in the univariate and multivariate tests and their impact on the non-centrality parameter λ_0 . The total picture of how those probabilities work together should be assembled and illustrated on numerical examples to be shown in the guide/manual as mentioned above. Even though the appropriate selection of β_0 -probability was not necessary in our investigations — β_0 affects only the scale of the robustness primitive plots — it will become necessary for formulating the robustness tolerance limits. This point thus deserves further investigation.

We wish to express our gratitude to Mr. M. Pinch, the scientific authority for the contract, for his cooperation, and for assembling for us the observations of an actual two-dimensional network used in our investigations. Mr. D. Beattie kindly helped us with some problems we had with the GHOST program. Ms. M. Wilson's assistance with various pieces of software on the UNB Department of Surveying Engineering Vax computer system is gratefully acknowledged. Ms. W. Wells has done her usual flawless editing and word processing of several iterations of this report.

REFERENCES

- Baarda, W. (1968). "A testing procedure for use in geodetic networks." Netherlands Geodetic Commission, Publications on Geodesy, New Series, Vol. 2, No. 5, Delft, Netherlands.
- Baarda, W. (1976). "Reliability and precision of networks." *VII International Course for Engineering Surveys of High Precision*, Darmstadt, F.R.G., pp. 17-27..
- Baarda, W. (1979). "Measures for the accuracy of geodetic networks." In, *Optimization of Design and Computation of Control Networks*, lectures from the Symposium held in Sopron, 1977, Budapest, pp. 419-426.
- Chen, Y.Q., M. Kavouras, and A. Chrzanowski (1987). "A strategy for detection of outlying observations in measurements of high precision." *The Canadian Surveyor*, Vol. 41, No. 4, pp. 529-540.
- Craymer, M.R., A. Tarvydas, and P. Vaníček (1988). "NETAN: A program package for the interactive covariance, strain and strength analysis of networks." Canadian Geodetic Survey Contract Report, DSS #OSQ83-00102 prepared by Marshall Macklin Monaghan Ltd., Toronto, Ontario for the Canada Centre for Surveying, Ottawa, Ontario.
- Craymer, M.R., P. Vaníček, and A. Tarvydas (1989). "NETAN — A computer program for the interactive analysis of geodetic networks." *CISM Journal ACSGC*, Vol. 43, No. 1, pp. 25-37.
- Dare, P. (1983). Strength analysis of horizontal networks using strain." Survey Science Technical Report No. 2, University of Toronto, Erindale Campus, Mississauga, Ontario.
- Förstner, W. (1979). "On the internal and external reliability of photogrammetric coordinates." Presented at the ASP-ASCM Convention, Washington, D.C.
- Kavouras, M. (1982). "On the detection of outliers and the determination of reliability in geodetic networks." Department of Surveying Engineering Technical Report No. 87, University of New Brunswick, Fredericton, N.B., November.
- Kok, J.J. (1984). "On data snooping and multiple outlier testing." NOAA Technical Report NOS NGS 30, National Geodetic Information Center, NOAA, Rockville, Md.
- Mackenzie, A.P. (1985). "Design and assessment of horizontal survey networks." M.Sc.E. thesis, Division of Surveying Engineering, The University of Calgary, Calgary, Alberta, March.
- Mephram, M.P. and E.J. Krakiwsky (1984). "CANDSN: A computer aided network design and adjustment system." *The Canadian Surveyor*, Vol. 38, No. 2, pp. 99-114..
- Mikhail, E.M. (1976). *Observations and Least Squares*. IEP—A Dun-Donnelley Publisher, New York, N.Y.
- Rao, C.R. (1973). *Linear Statistical Inference and its Application*. 2nd ed., John Wiley and Sons, Inc.

- Schneider, D. (1982). "Complex crustal strain approximation." Department of Surveying Engineering Technical Report No. 91, University of New Brunswick, Fredericton, New Brunswick.
- Stefanovic, P. (1978). "Blunders and least squares." *ITC Journal*, Vol. 1, pp. 122-157.
- Steeves, R.R. and C.S. Fraser (1983). "Statistical post-analysis of least squares adjustment results." In, *Papers for the CIS Adjustment and Analysis Seminars*, Ed. E.J. Krakiwsky, Canadian Institute of Surveying, Ottawa, July, pp.182-210.
- Thapa, K. (1980). "Strain as a diagnostic tool to identify inconsistent observations and constraints in horizontal geodetic networks." Department of Surveying Engineering Technical Report No. 68, University of New Brunswick, Fredericton, New Brunswick.
- Uotila, A.U. (1976). "Statistical tests as guidelines in analysis of adjustment of control nets." Presented at the 14th Congress of FIG, Washington, D.C.
- Vaniček, P. and E.J. Krakiwsky (1986). *Geodesy: The Concepts*. 2nd ed., North-Holland, Amsterdam.
- Vaniček, P., K. Thapa, and D. Schneider (1981). "The use of strain to identify incompatible observations and constraints in horizontal geodetic networks." *Manuscripta Geodaetica*, 6, pp. 257-281.